Multidimensional separation approaches for complex sample analysis: two-dimensional ion chromatography × capillary electrophoresis

Leila Ranjbar Shourabi
(BSc, MSc)

A thesis submitted in fulfilment of the requirements for the degree of
Doctor of Philosophy

Australian Centre for Research on Separation Science
School of Physical Sciences

University of Tasmania
June 2017

Declaration

This thesis contains no material which has been accepted for a degree or diploma by the University or any other institution, except by way of background information and duly acknowledged in the thesis, and to the best of my knowledge and belief no material previously published or written by another person except where due acknowledgement is made in the text of the thesis, nor does the thesis contain any material that infringes copyright.

Leila Ranjbar Shourabi
March 2017

The publishers of the papers comprising Chapters 1 to 4 hold the copyright for that content, and access to the material should be sought from the respective journals. The remaining non-published content of the thesis may be made available for loan and limited copying and communication in accordance with the Copyright Act 1968.

Leila Ranjbar Shourabi
March 2017

To my beloved

Mom, Dad and Brother

تقدیم به مادر ، پدر و برادر عزیزتر از جانم

Acknowledgements

I remember it all very clearly; on a crisp summer morning in 2012 some time around sunrise in Tehran I spoke with Robert Shellie and Michael Breadmore for the first time in an interview to apply for a PhD position at the Australian Centre for Research on Separation Science (ACROSS). During our initial correspondence I had mentioned that I was interested in exploring the area of two-dimensional separations and when Michael mentioned that in his group they had built a capillary electrophoresis system which was able to sample from a flowing stream, I instantly knew that I was going to start a project on two-dimensional liquid chromatography - capillary electrophoresis. Here I am, four years later writing the preface to my thesis on two-dimensional ion chromatography × capillary electrophoresis in Hobart. It has been an amazing journey with lots of ups and downs, rights and lefts, twists and turns. I have come a long way from Tehran to Hobart and have learnt a lot not only about my project but also about life and myself. It has been an incredibly joyful experience to compile the results of all the work I have done with the assistance of an incredibly dedicated group of people in this thesis. I hope that the examiners as well as the future readers enjoy reading this collection as much as I enjoyed performing the experiments and preparing this thesis.

Finally the time has arrived to acknowledge the ones without whom all of this would have not been possible. My supervisors, Michael Breadmore and Robert Shellie, I would like to extend my gratitude to both of you for accepting me as your student and giving me the opportunity to work with a group of incredible researchers at ACROSS. Thank you for sharing your invaluable knowledge of capillary electrophoresis, ion chromatography and two-dimensional separations with me. Michael, thank you for accepting to become my primary supervisor in the second half of my candidature when Rob moved to a new position in Melbourne. I would like to express my thankfulness for all your support, advice and supervision. Thanks for having your office door open to me and all your students, it was and is an absolute pleasure to be a part of the Chippers and CEers.

I would also like to gratefully acknowledge Paul Haddad and Joe Foley who both graciously mentored me through the last year of my candidature. I do appreciate your

insightful discussions and comments and feel absolutely fortunate and thrilled to have collaborated with you both.

Through these four years I got to know an incredible group of people from all around the globe and not only have had the privilege of doing some great research and learning a lot from them but also have formed precious friendships. Mohammad, Mitra, Mari, Mathew, Joan Marc, Eli, Aliaa, Petr, Adam, Matt, Hong Heng, Min, Aemi, Eva and Soo Hyun, thank you for your friendship and help.

To my boyfriend, Jared: From the first time we met you have always been great! Thank you for all your love, patience, support and incredibly delicious food which made enduring the hard times easier. “Here is to feeling good together all the time!” Also, thanks to Jared’s family especially Patricia for all the encouragements and kindness during the last months of my PhD candidature.

Finally and most importantly, to my Mom, Dad and Brother: Sorry, I had to leave. I had to go and explore another corner of the world where they have wallabies and possums and eat vegemite on their toast for breakfast. I have missed you every single day but your love, support and inspirations have been and will always be with me. All I am and all I have, I owe it to you. Thank you!

Statement of co-authorship

The following people and institutions have contributed to the publication of work undertaken as a part of this thesis:

Leila Ranjbar Shourabi, ACROSS, School of Physical Sciences, UTAS: Candidate
Michael C Breadmore, ACROSS, School of Physical Sciences, UTAS
Robert A Shellie, Trajan Medical and Scientific and ACROSS, School of Physical Sciences, UTAS
Paul R Haddad, ACROSS, School of Physical Sciences, UTAS
Joe P Foley, department of Chemistry, Drexel University and ACROSS, School of Physical Sciences, UTAS
Adam J Gaudry, ACROSS, School of Physical Sciences, UTAS
Eva Tyteca, Department of Agronomy, Bio-engineering and Chemistry, University of Liège and ACROSS, School of Physical Sciences, UTAS
Joan Marc Cabot, ACES and ACROSS School of Physical Sciences, UTAS
Min Zhang, ACROSS, School of Physical Sciences, UTAS
Mohammad Talebi, ACROSS, School of Physical Sciences, UTAS
Soo Hyun Park, ACROSS, School of Physical Sciences, UTAS
Petr Smejkal, ACROSS, School of Physical Sciences, UTAS

Author contributions

1. **Multidimensional liquid-phase separations combining both chromatography and electrophoresis - a review**
   Presented in Chapter 1

Candidate was the primary author (70%) while MCB (20%) and JPF (10%) contributed to the idea, structure, refinement and presentation.

2. **Online comprehensive two-dimensional ion chromatography × capillary electrophoresis**
   Presented in Chapter 2

Candidate was the primary author and performed all the experiments (60%) while AJG performed all the engineering and programming (10%) and helped with refinement and,

MCB and RAS (15% each) contributed to the idea, presentation and refinement of the work.

3. **Effect of background electrolyte pH on sample dimensionality and peak capacity in ion chromatography × capillary electrophoresis separation of low-molecular-mass organic acids**

   Presented in Chapter 3

Candidate was the primary author and performed all the experiments (70%) while ET (10%), MCB (10%), JMC (5%), JPF (3%) and MZ (2%) helped with the formation of the idea, refinement and presentation. ET wrote the Matlab code and conducted the calculations. MZ improved the LabView programme.

4. ***In silico* screening of two-dimensional separation selectivity for ion chromatography × capillary electrophoresis separation of low-molecular-mass organic acids**

   Presented in Chapter 4

Candidate was the primary author and performed all the experiments (60%) while MT (10%), PRH (10%) and MCB (5%) helped with the formation of the idea, presentation and refinement. SHP performed the QSRR calculations (5%). PS and MZ helped with engineering and programming (total of 5%). JMC and JPF contributed to refinement and presentation of the published work (total of 5%).

Michael C Breadmore
Primary Supervisor
School of Physical Sciences
UTAS

Date: 21/3/2017

M Dickey
Head of School
School of Physical Sciences
UTAS

Date: 21/3/17

List of publications and presentations

1. L. Ranjbar, J.P. Foley, M.C. Breadmore, Multidimensional liquid-phase separations combining both chromatography and electrophoresis – A review, Anal. Chim. Acta, 950 (2017) 7-31 [Review Article]
2. L. Ranjbar, A.J. Gaudry, M.C. Breadmore, R.A. Shellie, Online comprehensive two-dimensional ion chromatography × capillary electrophoresis, Anal. Chem., 87 (2015) 8673–8678 [Research Article]
3. L. Ranjbar, E. Tyteca, J.M. Cabot, M. Zhang, M.C. Breadmore, Effect of background electrolyte pH on sample dimensionality and peak capacity in ion chromatography × capillary electrophoresis separation of low-molecular-mass organic acids [Submitted manuscript]
4. L. Ranjbar, M. Talebi, P.R. Haddad, S.H. Park, J.M. Cabot, M. Zhang, P. Smejkal, J.P. Foley, M.C. Breadmore, *In silico* screening of two-dimensional separation selectivity for ion chromatography × capillary electrophoresis separation of low-molecular-mass organic acids [Submitted manuscript]
5. L. Ranjbar, R.A. Shellie, M.C. Breadmore 'CAPILLARY ELECTROPHORESIS | Low Molecular Mass Ions' In: J. Reedijk (Ed.) Elsevier Reference Module in Chemistry, Molecular Sciences and Chemical Engineering. Waltham, MA: Elsevier. 29-Nov-2013. DOI: 10.1016/B978-0-12-409547-2.00048-2 [Book Chapter]
6. L. Ranjbar, M. Talebi, P.R. Haddad, S.H. Park, J.M. Cabot, M. Zhang, P. Smejkal, J.P. Foley, M.C. Breadmore, *In silico* screening of two-dimensional separation selectivity for ion chromatography × capillary electrophoresis separation of low-molecular-mass organic acids, *ACROSS International Symposium on Advances in Separation Science*, 30 Nov-2 Dec 2016, Hobart, Australia [Oral Presentation]
7. L. Ranjbar, M.C. Breadmore, R.A. Shellie, Online comprehensive ion chromatography × capillary electrophoresis, *Virtual Symposium on Applied Separation Science (VSASS)*, 25-29 May 2015 [Invited Oral Presentation]
8. R.A. Shellie, L. Ranjbar, M.C. Breadmore, Design and implementation of IC × CE for comprehensive two-dimensional analysis of ionic and ionogenic analytes, *39th International Symposium on Capillary Chromatography (ISCC)*

and 12th GC×GC Symposium, 16-21 May 2015, Fort Worth, Texas, USA [Oral Presentation]

9. L. Ranjbar, M.C. Breadmore, R.A. Shellie, Two-dimensional ion chromatography-capillary electrophoresis, *Royal Australian Chemical Institute (RACI) National Congress*, 7-12 Dec 2014, Adelaide Convention Centre, Adelaide, Australia [Oral Presentation]
10. L. Ranjbar, M.C. Breadmore, R.A. Shellie, Comprehensive two-dimensional ion chromatography-capillary electrophoresis for separation of disinfection byproducts, *21st International Symposium on Electro- and Liquid Phase-Separation Techniques and 20th Latin-American Symposium on Biotechnology, Biomedical, Biopharmaceutical, and Industrial Applications of Capillary Electrophoresis and Microchip Technology (ITP&LACE)*, 4-8 Oct 2014, SERHS Natal Grand Hotel, Natal, Brazil [Young Scientist Session Oral Presentation]
11. L. Ranjbar, R.A. Shellie, M.C. Breadmore, Two-dimensional ion chromatography-capillary electrophoresis, *5th Australia and New Zealand Micro/Nanofluidics Symposium (ANZNMF),* 14-16 Apr 2014, University of Tasmania, Hobart, Australia [Short Oral Presentation]
12. L. Ranjbar, R.A. Shellie, M.C. Breadmore, Two-dimensional liquid chromatography-capillary electrophoresis, *40th International Symposium on High Performance Liquid Phase Separations and Related Techniques*, 18-21 Nov 2013, The Hotel Grand Chancellor, Hobart, Australia [Poster Presentation]

Abstract

The work presented in this thesis describes development, evaluation and implementation of an online interfacing/modulation technique for comprehensive two-dimensional ion chromatography × capillary electrophoresis (IC × CE) separation of low-molecular-mass ionic or ionogenic compounds.

Chapter 1 provides an insight into the evolution of multidimensional liquid-phase separations combining both chromatography and electrophoresis from inception in 1948 to present. As noted in this chapter, column-based multidimensional electrophoretic and chromatographic separations have shown to be powerful complementary techniques to the traditional two-dimensional gel-electrophoresis approaches; especially for the analysis of lower molecular-mass-molecules in addition to proteins and peptides. However, complexities in instrumentation and online interfacing technologies are known to have hindered development of such techniques.

Chapter 2 introduces a non-focusing interfacing technology for online hyphenation of ion chromatography with capillary electrophoresis. The system compromised of an in-house sequential-injection capillary instrument which, through the use of a two-position six-port injection valve, allowed comprehensive sampling of the IC effluent for quantitative analysis of inorganic anions and haloacetic acids in water.

In addition to instrumental developments, the second section of this thesis focuses on alternative method development approaches for screening/optimisation of IC × CE separations:

Chapter 3 demonstrates the impact of background electrolyte pH on sample dimensionality and peak capacity for IC × CE separation of multi-valent low-molecular-mass organic acids. In this chapter, a simplified screening approach based on calculation and maximising of Euclidean distance between the two-dimensional peaks was used to predict the optimal background electrolyte pH in CE as well as the eluent profile in IC. However, due to lack of overall two-dimensional selectivity, further investigations were necessary to make full resolution of the analytes possible.

In **Chapter 4**, based on a ground set by the findings presented in Chapter 3, a universal framework is proposed for simultaneous screening of separation selectivity in both dimensions as a preceding step in method development/optimisation of two-dimensional separations. In this chapter, through the introduction of the concept of *two-dimensional selectivity mapping*, effect of stationary phase in IC and background electrolyte pH in CE on the overall two-dimensional separation selectivity was studied to enable full resolution of the organic acids.

Finally, **Chapter 5** of this thesis discusses the limitations of IC × CE and provides further insight and direction for future research.

Table of contents

List of Abbreviations

Acronym	Description
1D	One-dimensional
2D	Two-dimensional
^{1}D	First dimension
^{2}D	Second dimension
2D-GE	Two-dimensional gel electrophoresis
2D-PAGE	Two-dimensional polyacrylamide gel electrophoresis
APCE	Affinity probe capillary electrophoresis
BAC	Boronate affinity chromatography
CAE	Capillary array electrophoresis
CE	Capillary electrophoresis
CEC	Capillary electrochromatography
CEIA	Capillary electrophoresis immunoassay
CGE	Capillary gel electrophoresis
CIEF	Capillary isoelectric focusing
C^{4}D	Capacitively coupled contactless conductivity detection
E	Electromigration
ESI	Electrospray ionisation
FFE	Free flow electrophoresis
FLD	Fluorescence detection
FTICR-MS	Fourier transform ion cyclotron resonance mass spectrometry
GC	Gas chromatography
GFC	Gel filtration chromatography
GPC	Gel permeation chromatography
IC	Ion chromatography
IEC	Ion exchange chromatography
IEF	Isoelectric focusing
IPC	Ion pair chromatography
IT-MS	Ion trap mass spectrometry
LC	Liquid chromatography
LIF	Light induced fluorescence
MALDI-MS	Matrix assisted laser desorption ionization mass spectrometry
MD	Multidimensional
MEKC	Micellar electrokinetic chromatography
NPLC	Normal phase liquid chromatography
PEC	Planar electrochromatography
PPEC	Pressurised planar electrochromatography
RPLC	Reversed phase liquid chromatography
SCE	Simultaneous chromatography electrophoresis
SCX	Strong cation exchange chromatography
SEC	Size exclusion chromatography
SPE	Solid phase extraction
TLC	Thin layer chromatography
TLE,	Thin layer electrophoresis
TOF-MS	Time of flight mass spectrometry

Preface

One-dimensional analytical separation technologies often lack the peak capacity needed to adequately separate complex samples. This has led to increasing adoption of multi-dimensional approaches to address challenging analytical problems. Two-dimensional (2D) analytical separation technologies subject the eluate from a first separation dimension to further separation in a second separation dimension. Maximal benefit of multi-dimensional separations occurs when the separation dimensions rely on fundamentally different separation mechanisms [1, 2]. As a result, chromatographic × electrophoretic techniques are placed in Giddings' list of powerful 2D combinations [1].

The first comprehensively coupled multidimensional separation approach combining liquid chromatography (LC) and capillary electrophoresis (CE) (LC×CE) was described by Bushey and Jorgenson in 1990 [3]. This work offered remarkably enhanced resolving power compared to its mono-dimensional building blocks. The first interface for LC×CE was a computer-actuated six-port valve with a sample loop [3]. Later a transverse flow-gated interface [4], optical gating [5] and most recently adaptation of microfluidic devices [6-8] were introduced as coupling approaches. Notwithstanding the seemingly ideal mechanistic considerations, there are numerous practical constraints impeding LC×CE. With the typical peak volume in LC being substantially larger than the injection volume in CE as well as the hydrodynamic flow in LC affecting the electrophoretic separation, effective transfer of LC effluent to CE is the main challenge to address when coupling the two techniques [9]. As a result of complicated interfacing, LC×CE has not experienced the wide employment or development of GC×GC or LC×LC.

Ion chromatography (IC) and CE are the two major techniques utilised in analysis of ionic and ionogenic analytes. Two-dimensional separations using these building blocks are unquestionably superior to the individual techniques due to the genuine orthogonality of separation mechanisms. Suppressed IC uses a highly conducting eluent such as hydroxide, carbonate or sulfonate to elute the analytes from an ion-exchange resin stationary phase. When used with conductivity detection, the eluent is suppressed to a low conductivity medium allowing sensitive detection of analytes. In

the case of hydroxide eluent, analytes are left in water, which is a perfect matrix for injection into CE enabling sample concentration techniques such as stacking with minimum matrix effects.

The current thesis describes development and characterisation of an online comprehensive IC×CE system based on sequential sampling of the IC effluent (Part 1, presented in Chapter 2), introduces alternative method development strategies for IC×CE separation of low-molecular-mass compounds (Part 2, Chapters 3 and 4) and, finally concludes with a discussion on limitations, alternative coupling approaches and future directions.

References

[1] J.C. Giddings, Two-dimensional separations: concept and promise, Anal. Chem., 56 (1984) 1258A-1270A.

[2] J.C. Giddings, Concepts and comparisons in multidimensional separation, J. High. Resolut. Chromatogr., 10 (1987) 319-323.

[3] M.M. Bushey, J.W. Jorgenson, Automated instrumentation for comprehensive two-dimensional high-performance liquid chromatography/capillary zone electrophoresis, Anal. Chem., 62 (1990) 978-984.

[4] A.V. Lemmo, J.W. Jorgenson, Transverse flow gating interface for the coupling of microcolumn LC with CZE in a comprehensive two-dimensional system, Anal. Chem., 65 (1993) 1576-1581.

[5] A.W. Moore, J.W. Jorgenson, Rapid comprehensive two-dimensional separations of peptides via RPLC-optically gated capillary zone electrophoresis, Anal. Chem., 67 (1995) 3448-3455.

[6] A.G. Chambers, J.S. Mellors, W.H. Henley, J.M. Ramsey, Monolithic Integration of Two-Dimensional Liquid Chromatography−Capillary Electrophoresis and Electrospray Ionization on a Microfluidic Device, Anal. Chem., 83 (2011) 842-849.

[7] J.S. Mellors, W.A. Black, A.G. Chambers, J.A. Starkey, N.A. Lacher, J.M. Ramsey, Hybrid Capillary/Microfluidic System for Comprehensive Online Liquid Chromatography-Capillary Electrophoresis-Electrospray Ionization-Mass Spectrometry, Anal. Chem., 85 (2013) 4100-4106.

[8] M. Geiger, N.W. Frost, M.T. Bowser, Comprehensive Multidimensional Separations of Peptides Using Nano-Liquid Chromatography Coupled with Micro Free Flow Electrophoresis, Anal. Chem., 86 (2014) 5136-5142.

1 Multidimensional liquid-phase separations combining both chromatography and electrophoresis - literature review

"The union of opposites, in so far as they are really complementary, always results in the most perfect harmony; and the seemingly incongruous is often the most natural."
—Stefan Zweig

This chapter has been published as a review article in Anal. Chim. Acta, 950 (2017) 7-31.

1.1 Overview

Described as *intrinsically powerful building blocks* for two-dimensional separations by Giddings [1], the coupling of chromatography and electrophoresis has been proven to enhance the resolution of a wide array of molecules in complex biological, environmental and food samples. This chapter provides a comprehensive overview of multidimensional chromato-electrophoretic (LC-E) and electrophero-chromatographic (E-LC) separation systems from inception to the most recent published examples. LC separation modes include reversed phase, ion exchange, and size exclusion. Electromigration separation modes include capillary, microchip or free flow electrophoresis; micellar electrokinetic chromatography; electrochromatography; and isoelectric focusing. The advantages and disadvantages of various non-gel based off-line and on-line hyphenation technologies of LC-E and E-LC are discussed, with conditions and system characteristics also provided.

1.2 Introduction

The coupling of chromatography with electrophoresis has substantial history and dates back to 1948 [2] – not so long after two-dimensionality in separation was introduced in an experiment in which partition chromatography was carried out along the two axes of a paper sheet to separate a number of amino acids [3]. Despite its power when compared to one-dimensional (1D) paper chromatography, this method was shown to be insufficient when separating various acidic, basic and neutral amino acids with similar retention. To separate these an alternative additional separation was required whose *orthogonality* was beyond using different solvents along each axis. Utilising the fact that these are charged molecules possessing different structures, Haugaard *et al.* performed electrophoresis by passing an electric current through the paper (perpendicular to the concurrent chromatographic separation) to allow migration of acidic and basic amino acids in opposite directions while the neutral amino acids remained unaffected by the voltage (Figure 1-1) [2]. This simple and effective two-dimensional (2D) separation provides a great backdrop to discuss multidimensional separations for complex sample analysis as well as to briefly describe the fundamental concepts.

Multidimensional separations aim to adequately resolve complex samples by subjecting the eluate from a primary separation dimension (^{1}D) to further separation

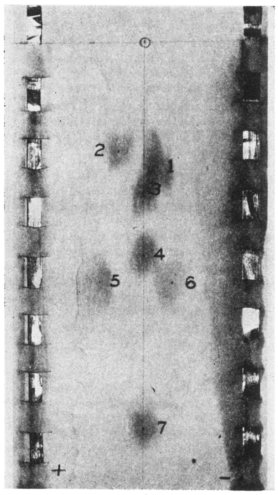

Figure 1-1*: First two-dimensional chromatographic × electrophoretic separation; partition chromatography of amino acids with applied voltage; 1: lysine; 2: aspartic acid; 3: serine; 4: glycine; 5: glutamic acid; 6: arginine and, 7: alanine. Platinum-ribbon electrodes on sides of paper; applied potential, 105 V. Phenol was used as the developing solvent. Reprinted with permission from [2].*

in subsequent separation dimension(s). To demonstrate maximal sample resolution, intrinsically different separative mechanisms are favoured so that the separation which cannot be achieved by one dimension can be reached in combination with the other due to their complementarity, as shown by Haugaard *et al*. [2] This explains why the coupling of chromatography and electrophoresis was described by Giddings as one of the most powerful 2D combinations [1].

Depending on how the eluate is transferred to subsequent separation dimension(s), multidimensional separations can be categorised as *offline* ($^1D/^2D$), where fractions of ^1D separation are collected and later subjected to ^2D separation, or *online* (^1D-^2D), when ^2D separation takes place in real-time with ^1D separation. Additionally, 2D approaches can be classified as *heart-cutting* or *comprehensive* ($^1D\times^2D$). In heart-cutting 2D techniques, only a targeted subsection of the first dimension is subjected to the second dimension separation, whereas in a comprehensive approach all sections of the first dimension are subjected to the second dimension.

The term *comprehensive* was initially introduced by Bushey and Jorgenson [4] and refers to an orthogonal 2D combination in which an equal percentage of sample components are subjected to each dimension and are equally detected. This criterion by itself is not enough to define a method as comprehensive and needs to be accompanied by preservation of ^1D resolution throughout the 2D separation [5]. To maintain the resolution obtained in ^1D, it is necessary to perform frequent sampling of ^1D by ^2D. Therefore, a method in which sampling frequency or modulation period is substantially greater than ^1D peak width, cannot be defined as comprehensive. Such an approach will demonstrate inferior resolving power (lower total peak capacity) when compared to its comprehensive counterparts due to loss of ^1D resolution. There have been a number of publications addressing the debate on what is sufficient sampling [6-8]. The latest publication on this topic takes both Gaussian and tailing peaks into account [8] and defines a modulation ratio of at least three for quantitative approaches while a ratio of 1.5 suffices for semi-quantitative separations . With modulation ratio being defined as 4 times the ^1D peak standard deviation ($4\ ^1\sigma$) divided by the modulation period. This requires the ^2D separation to be substantially fast, although modulation periods of 2.2 - 4 $^1\sigma$ have been defined as acceptable in order to maintain some useful capacity in the second dimension while avoiding excessively short ^2D separation times [9]. Being an inherently quicker technique

compared to chromatography, electrophoresis is an ideal candidate for ^{2}D separations in an online set-up from this perspective.

Up until the 80's, planar multidimensional separations were the only ones known, exemplified by 2D-GE which remains to this day one of the most well known and widely used of all 2D separation approaches. 2D-GE uses a gel-based media to spatially separate proteins and peptides according to their isoelectric point (p*I*) in ^{1}D and their size in ^{2}D [10]. Despite its impressive resolving power, which enables the separation of hundreds of proteins and peak capacities in order of thousands, as well as its wide acceptance through the last 4 decades, 2D-GE has a number of limitations [11]. 2D-GE is not suitable for separation of non-protein compounds or even the whole range of proteins in a sample, e.g., it is not capable of separating proteins with extreme p*I*, molecular mass, or hydrophobicity values. In addition, it cannot be easily coupled to mass spectrometry and has a limited linear dynamic range and difficulties with detection of low-abundant proteins when used for quantitative purposes. To overcome these shortcomings, coupled-column techniques which provide a temporal separation, are amenable to separation of a larger range of molecules as well as compatible with a wide variety of detection techniques, were introduced. First proposed by Guiochon [12], coupled-column techniques have received a great deal of attention in the past three decades.

As mentioned earlier, amongst all the possible combinations of coupled-column 2D separations, the combination of chromatography (LC) and electromigration (E), LC-E or E-LC, are considered to be the two most effective combinations. However, as pointed out in several review papers [13-18], they are also the most challenging combinations to achieve, especially when hyphenated in an online comprehensive manner. Substantially large elution and injection volumes in liquid chromatographic techniques compared to their electrophoretic counterparts, as well as presence of an electric field in the electrophoretic dimension and the necessity to isolate it from other system components, are the two main technical challenges to overcome when coupling chromatography and electrophoresis. As a result of all these complexities, LC×CE appeared many years later than the first paper-based chromatographic × electrophoretic separation and has not yet gained considerable ground compared to GC×GC or LC×LC. There have, however, been many approaches exploring the LC-E and E-LC, including use of lower flow rates in the liquid chromatographic dimension or splitting interfaces between the two dimensions, performing faster separations in

the electrophoretic dimension or alternatively, utilisation of chromatographic techniques which do not require fast ^{2}D separation techniques [19] and electrophoretic techniques of continuous nature which enable continuous analysis of the whole ^{1}D effluent [20]. It is also notable that the only online 3D separations utilise electrophoretic methods [21]. However, practical limitations have resulted in development of mainly two-dimensional approaches as the greater the number of dimensions, the greater the number of incompatibility-related complexities.

This chapter discusses and highlights the publications that have appeared in the field of hyphenated chromatographic and electrophoretic technologies and therefore excludes pure multidimensional LC and multidimensional CE, which have been covered elsewhere [16, 17, 22-24]. Approaches have been divided into offline and online categories with a special focus on online interfacing technologies in the following categories: valve-based, gating, microfluidic, droplet-based, membrane-based and planar techniques. Also, a detailed summary of all the discussed techniques is provided in Table 1-1. This literature review is not intended to be comprehensive, with articles selected to illustrate key concepts and advancements in the field and to highlight the most recent emerging contributions.

***Table 1-1**: Methods and conditions in multidimensional E-LC and LC-E publications.*

Hyphenation	^{1}D separation media and conditions	Interface	^{2}D separation media and conditions	Detector	Total analysis time *	Application	Peak capacity	Reference
Offline approaches								
Paper-chromatography × electrophoresis	paper strips (570 × 120 mm) dipped in M/15 phosphate buffer (pH 6.2), phenol as the developing solvent	-	Simultaneous with the ^{1}D, 100 V separation voltage applied through two nickel ribbon (6.35 × 0.025 mm)		18 hours	separation of aspartic acid, glutamic acid, lysine, arginine, serine, glycine, alanine, valine, leucine and proline	-	[2]
RPLC/CE	250 mm × 4.6 mm ODS C_{18} column, gradients of 0.1% TFA in water and 0.1% TFA in acetonitrile at 1 mL/min	-	310 mm × 0.050 mm ID fused-silica capillary, 50 mM phosphoric acid (pH 2.1)	UV	9 h	proteolytic digest of cytochrome c and myoglobin	-	[25]
RPLC/ACE	250 mm × 4.6 mm ODS C_{18} column, gradients of 0.1% TFA in water and 0.1% TFA in acetonitrile at 1 mL/min	-	8 × 12-array capillaries (520 mm × 0.050 mm ID), 20 mM borate (pH 9.0)	LIF	< 1 h	proteolytic digest of cytochrome c and myoglobin	-	[26]
RPLC/ACE	250 × 4.6 mm Vydac C4 column, gradients of 0.1% TFA in water and 0.1% TFA in acetonitrile at 1 mL/min	-	12-array capillary (550 mm × 0.075 mm ID), 23 mM borate buffer pH 9.2 12 kV	UV	1.5 h	mapping of ovarian cancer cell extracts	-	[27]
RPLC/CE	0.250 mm ID Vydac C_{18} column gradients of 5 mM ammonium formate at and 20% water-80% acetonitrile-5 mM ammonium formate at pH 6.88 at a flow rate of 0.003 mL/min	-	574 mm × 0.075 mm ID fused-silica capillary 20 mM phosphate-20 mM borate-50 mM SDS (pH 8.5); applied voltage, 15 kV.	UV and LIF	Over 2 h	mapping of enzymatic digests of the monoclonal antibody BR96 and its immunoconjugate	-	[28]
RPLC/CE	250 × 4.6 mm Vydac C4 column, gradients of 0.1% TFA in water and 0.1% TFA in acetonitrile at 1 mL/min	-	310 mm × 0.050 mm ID fused-silica capillary, 50 mM phosphoric acid (pH 2.1)	UV	-	a mixture of cytochrome C and myoglobin digests	-	[29]
RPLC/CE	250 mm × 4.6 mm Vydac C_{18} column, gradients of acetonitrile-water both conataing 0.1% TFA at 1 mL/min	-	600 mm × 0.030 mm ID fused-silica capillary, 10% isopropanol in 200 mM acetic acid, 15 kV	Sheathless *n*ESI-IT-MS	32 h	tryptic digested human serum proteins	-	[30]
Heart-cutting RPLC/CE	YMC ODS-AQ 3-mm particle reversed phase column, gradients of water and acetonitrile both with 0.09% TFA at 0.0002 mL/min	-	bovine serum albumin (BSA)-treated fused-silica capillaries (560 mm L_{eff} × 0.075 mm ID), 25 mM ammonium phosphate buffer (pH 3.00) 500 V/cm	MALDI-TOF-MS	Over 1.5 h for separation of 3 RPLC fractions	characterization of posttranslational modifications in glycoproteins	-	[31]

Hyphenation	^{1}D separation media and conditions	Interface	^{2}D separation media and conditions	Detector	Total analysis time *	Application	Peak capacity	Reference
RPLC/CE or MEKC	250 × 0.2 mm ID monolithic silica-ODS column gradients of methanol-30 mM phosphate buffer (pH 3.0) at a flow rate of 0.002 mL/min	-	605 mm × 0.050 (CE) or 0.075 (MEKC) mm ID fused-silica capillary 160 mM borate pH 9.4 (CE) 50 mM SDS-50 mM H_3PO_4-20% acetonitrile pH 2.0 (MEKC) at 18 kV for CE and -25 kV for MEKC	UV	Over 10 hours	Bacillus subtilis cell extracts	-	[32]
RPLC/CE	500 × 0.2 mm ID monolithic silica-ODS column gradients of 95:5 and 2:98 methanol and 30mM ammonium acetate (pH 4.0) at a flow rate of 0.002 mL/min	-	605 mm × 0.075 mm ID fused-silica capillary 100mM ammonium carbonate (pH 9.6) at 18 kV	UV	Over 10 hours	E. Coli cell extract	-	[33]
RPLC/CE	EC 250/4.6 Nucleosil 120-3 μm C18 column, gradient of water and 85% acetonitrile (both containing 0.1% TFA) at 0.500 mL/min	-	1000 mm × 0.030 mm ID neutral fused-silica capillary 10% (v/v) acetic acid as BGE at +30 kV with a BGE flow rate of 10 nL/min	LTQ-orbitrap MS	About 8 days	Yeast proteome digest	28 538 quantified peptides	[34]
Heart-cutting RPLC/CE	220 × 2.1 mm ABI Aquapore OD-300 C_{18} column, gradients of 5% acetonitrile/95% water and 40% acetonitrile /60 % water (both containing 0.1 % TFA) at 0.2 mL/min	-	540 mm × 0.100 mm ID bare-fused silica capillary, 50 mM phosphate (pH 2.5), 20 kV	UV	4.4 h for separation of 5 LC fractions	tryptic peptides of bovine serum albumin (BSA)	-	[35]
RPLC/CIEF	300 mm × 0.250 mm ID home-packed C_8 column, gradients of 0.1% TFA in methanol and 0.1% TFA in water at 0.002 mL/min	-	350 mm × 0.075 mm ID HPC-coated capillary, NaOH (20 mM) and H_3PO_4 (10 mM) were used as catholyte and anolyte 21 kV	LIF	9.5 h (BSA digest) 15.4 h (yeast sample)	protein/peptide samples, such as yeast cytosol and a BSA tryptic digest	10 000	[36]
RPLC/MEKC	50 mm × 2.1 mm Discovery HS PEG, gradients of 10 mM ammonium acetate in water (pH 3.0) and acetonitrile at 0.4 mL/min	-	480 mm × 0.025 mm ID fused-silica capillary, 25 mM borate buffer (pH 9.05) with addition of 10 g/L SDS and 1.85 g/L heptakis (6-*O*-sulfo)-β-CD, 20 kV	UV	10.5 h	phenolic acids and flavone natural antioxidants in green tea[37] and red wine[38]	450	[37, 38]
IEF/RPLC	preparative-scale Rotofor using 0.1% *n*-octyl beta-D-galactopyranoside (OG) and 8 M urea and 2.5% Biolyte ampholytes, pH 3.5-10	-	4.6 × 14 mm nanoporous RP C_{18}(ODSI) column, gradients of water/acetonitrile (0.1% TFA, 0.05% OG at 1.0 mL/min	MALDI-TOF MS	10 h	mapping of cellular proteins of human erythroleukemia cell	ca 700 peaks observed	[39]

Hyphenation	^{1}D separation media and conditions	Interface	^{2}D separation media and conditions	Detector	Total analysis time *	Application	Peak capacity	Reference
OFFGEL-IEF /RPLC	In OFFGEL Fractionator containing am mixture of 8 M urea, 2.5 M thiourea,0.08 M DTT, 12% glycerol, and 1.2% of the appropriate ampholytes At 2 kV	-	100 mm × 2.1 mm Ascentis Express Fused-Core peptide ES-C18 column gradients of 0.3% (v/v) acetic acid in water and acetonitrile at 0.4 mL/min	ESI-QTOF MS	About 2 hours	bioactive peptide lunasin in soybeans	-	[40]
OFFGEL-IEF /RPLC	In OFFGEL Fractionator containing IPG strips and 0.2% ampholytes pH 3−10 At 2 kV	-	0.075 × 150 mm C18 analytical column gradients of 2% acetonitrile in 0.1%formic acid in water and 0.1% formic acid in 98% acetonitrile at a flow rate of 250 nL/min	SRM-MS	about 9 hours	Tryptic digedt of mouse liver extract	-	[41]
IEF/RPLC	running buffer of 0.1% OG, 8 M urea, 2 M thiourea, 10 mM DTT, and 2.5% Biolyte ampholytes	-	30 × 53 mm nanoporous RP C_{18} (ODSI) column, gradients of water/acetonitrile (0.1% TFA, 0.3% formic acid) at 0.2 mL/min	MALDI and ESI-TOF MS	Over 13 h	Mapping of cultured normal ovarian surface epithelium cells and an epithelial ovarian cancer-derived cell line	-	[42]
OMJ-CIEF/RPLC	seven equal PEEK tubing segments (each 12 × 0.395 ID × 0.635 mm OD joined together by short insertions of tubular Nafion membrane carrier buffer consisting of 5% isopropanol and 0.5% Pharmalyte 3-10 at 100 V/cm. Several buffer solutions pH from 3-10	-	80 mm × 0.075 mm ID C_{18} column, gradients of acetonitrile and water both containing 0.1 % formic acid at 300 nL/min	MS/MS	Over 15 h	Digested yeast proteome	-	[43]
IEC/CGE	250 mm × 4 mm DNAPac PA200 gradients of 20/80 ACN/water (pH 11.5) and 20/80ACN/water containing 1.25 M NaCl (pH 11.5) at 0.3 mL/min	-	260 mm × 0.100 mm ID fused-silica capillary 50 mM Tris-Tricine (pH 8.1) and 5% (m/V) HPMC in the Tris-Tricine buffer −10 kV	UV	Over 15 h	oligonucleotides of therapeutic size.	1474	[44]
IPC/CGE	50 mm × 4.6 mm XBridgeC18 gradients of 100 mM TEA (pH 5.5) and ACN at 0.3 mL/min	-	24-array capillary (800 mm × 0.075 mm ID) 50 mM Tris-Tricine (pH 8.1) and 5% (m/V) HPMC in the Tris-Tricine buffer −15 kV	UV	About 2 h	oligonucleotides of therapeutic size	852	[44]

Hyphenation	^{1}D separation media and conditions	Interface	^{2}D separation media and conditions	Detector	Total analysis time *	Application	Peak capacity	Reference
SEC/CE and SEC/IEC/CE	700 ×16 mm Sefadex gel SEC column with 1% (v/v) acetic acid as mobile phase 250 mm × 4.6 mm Hamilton PRP X-100 column for IEC	-	1000 mm × 0.075 mm ID fused-silica capillary 10 mM Na_2HPO_4 with 0.88 mM cetyltriammonium bromide, pH 10.5 20 kV	ICP-MS	Over 2 h	mapping of seleno-compounds in aqueous extracts of selenised yeast	-	[45]
IEC/CEC	100 mm × 0.300 mm ID SCX stationary column, gradients of water–acetonitrile–TFA (95:5:0.1, v/v/v) and 0.5mol/L NH_4Cl–acetonitrile–TFA (95:5:0.1, v/v/v) at 0.003 mL/min (splitting ratio: 20:1)	-	550 mm × 0.150 mm ID C_{18} column, gradients of water–acetonitrile–TFA (95:5:0.1, v/v/v) and water–acetonitrile–TFA (5:95:0.1, v/v/v) at 400 nL/min, 3 kV or 5 kV (medicine)	UV	About 9 h	traditional Chinese medicine, bovine serum albumin (BSA) tryptic digest and real serum tryptic digest	880-1200	[46]
BAC/CIEF	Glyco-Tek affinity columns	-	300 mm × 0.050 mm ID Agilent DB-1 capillary Ampholyte solution was 2% (v/v) Pharmalyte pH 6.7 to 7.7 in methylcellulose solution (0.375% w/v in water). Catholoyte solution was 80 mM borate pH 10.25 with as catholyte and 100 mM phosphoric acid in methylcellulose solution as anolythe	UV	-	Glycated haemoglobin in blood	-	[47]
TLE/TLC	20 × 20 cm glass-backed cellulose plates 88% formic acid/glacial acetic acid/water (50:156:1794, v/v/v), pH 1.9 1.0 kV	-	1-butanol/pyridine/glacial acetic acid/water (75/50/15/60, v/v/v/v)	Autoradiography	Over 17 h	phosphoprotein digest	-	[48]
PEC/HPTLC	silica gel 60 glass-backed HPTLC plate 1-butanol/glacial acetic acid/pyridine//water (50/25/25/900, v/v/v/v), pH 4.7 300-400 V	-	1-butanol/glacial acetic acid/pyridine/water (30/6/20/24, v/v/v/v)	MALDI-TOF-MS	Over 3 h	phospholyrated peptides in various digests	6 250 000 (10 000 for MS)	[49]
HPTLC/PPEC	50 × 200 mm HPTLC RP18W plates with margins of silicone sealant 45% v/v methanol in citrate-phosphate buffer, pH 3.0. as mobile phase	-	75% acetonitrile in citrate-phosphate buffer pH 3.0 at 2.5 kV or 75% acetonitrile in glycine-NaCl-NaOH buffer pH 9.1 at 2.5 kV	DAD scanner	About an hour	Dye mixture	-	[50]

Hyphenation	^{1}D separation media and conditions	Interface	^{2}D separation media and conditions	Detector	Total analysis time *	Application	Peak capacity	Reference
UTLC/PEC	40 × 40 mm electrospun nanofibre stationary phase plate, 90:10 2-PrOH/ MeOH (v/v) over 25 mm of the plate	-	25:25:50 ACN/2-PrOH/25 mM citrate buffer, pH 5.6 (v/v/v), at 1 kV	UV	11 min	a mixture of 5 laser dyes	-	[51]
MEKC/TLC	620 mm × 0.050 mm ID fused silica capillary, 10 mM sodium tetraborate with 40 mM sodium dodecyl sulphate (pH ca. 9.5), 15 kV		Adsorbosil octadecyl modified RP-TLC plates, Acetonitrile/0.2 M β-CD in water (20:80 v/v) containing sodium chloride 0.6 M	LIF using CCD camera	Over 55 min	separation of dansylated-amino acid enantiomers	1100	[52]
RPLC/CAIEF	300 mm × 0.250 mm ID home-packed C8 column gradients of 5% acetonitrile/95% water and 5% water/95% acetonitrile (both containing 0.1 % TFA) at 0.002 mL/min		200 mm × 0.075 mm ID 60 HPC-coated capillaries, NaOH (40mM) and H_3PO_4 (100mM) as the catholyte and anolyte 3 kV	LIF-WCID	Less than 3 h	proteins in D20 liver cancer tissue	18 000	[53]
RPLC/CIEF	300 mm × 0.250 mm ID home-packed C8 column gradients of acetonitrile and water (both containing 0.1 % TFA) at 0.002 mL/min		200 mm × 0.100 mm ID HPC-coated capillary, 2% NH_4OH solution and 1% acetic acid as the catholyte and anolyte 10 kV	MALDI-MS	1.5 day	proteome of rat liver tissue extracts	9 000	[54]
IEF-FFE/RPLC	either aqueous 0.2% (w/v) HPMC or 25% v/v glycerol containing 0.4% (v/v) carrier ampholytes (Servalyte pH 3-10, 4-6, 5-7, 9-11, or Sinulyte pH 2-4, 3-5, 7-9, 2-11); electrode solutions 100 mM H_3PO_4 and 50 mM NaOH; 0.4% (w/v) HPMC and 0.8% (v/v) carrier ampholytes at a flow rate of 1.4-1.8 mL/min, 1250 V	-	100 mm × 2.1 mm ID octylsilica column, gradients of 0.1% TFA in water and 0.094% TFA/60% CH3CN, at 1 mL/min	UV and FLD	Over 8 h	proteins and peptides in total/ tryptic digested cellular lysate of the colon carcinoma cell line and a human urine specimen	6720	[55]

Hyphenation	^{1}D separation media and conditions	Interface	^{2}D separation media and conditions	Detector	Total analysis time *	Application	Peak capacity	Reference
Online approaches								
RPLC×CE	250 mm × 1 mm ID Brownlee Aquapore RP-300 column, gradients of 0.012 M potassium phosphate buffer (pH 6.9) and acetonitrile at 0.010 mL/min	Valve/ loop interface	380 mm × 0.041 mm ID (ovalbumin digest) and 380 mm × 0.050 mm ID (peptide standards) fused silica capillaries, 0.012 M potassium phosphate buffer (pH 6.9), -19 kV (ovalbumin digest) and, -22 kV (peptide standards)	FLD	Over 4 h	peptide standards and tryptic digest of ovalbumin	420	[56]
SEC×CE	1000 mm × 0.250 mm ID microcolumn. Packed with Zorbax GF450 particles, 10 mM tricine, 25 mM Na_2SO_4, 0.005% sodium azide (pH 8.32) at 360 nL/min	Valve/ loop interface connected to tee piece	380 mm × 0.050 mm ID fused silica capillary, 10 mM tricine, 25 mM Na_2SO_4, 0.005% sodium azide (pH 8.32), -8 kV	UV	about 2 h	human, horse and bovine sera	-	[57]
SEC×CE	1050 mm × 0.250 mm home-packed column, 10 mM tricine,25 mM Na_2SO_4, 0.005% w/v sodium azide (pH 8.23) at 180 or 360 nL/min	Valve/loop interface connected to a tee	Either 380 mm or 580 mm × 0.050 mm fused silica capillaries, 10 mM tricine, 25 mM Na_2SO_4, 0.005% w/v sodium azide (pH 8.23) -11 and -8 kV	UV-Vis	4 h (for 180 nL/min flow run)	mixture of protein standards as well as human serum (lyophilised powder)	-	[58]
RPLC×CE	150 mm × 2.1 mm Zorbax 300 SB-C_8 column, linear gradients from 20% to 70% acetonitrile in water with 0.1% v/v trifluoroacetic acid at 0.050 mL/min or 0.060 mL/min	8-port valve fitted with two 10 µL loops	140 mm × 0.015 mm fused silica capillary, 10 mM Na_2HPO_4, plus 20 mM TEA (pH 11.0), -12.5 to -13.5 kV	LIF	Over 50 min	horse heart cytochrome c	-	[58]
RPLC×CE	150 × 2.10 mm Vydac Protein & Peptide C 18 column, gradient from 100% 0.01 M Na_2HPO_4 (pH 6.85) to 100% (30% acetonitrile/7% CE buffer) at 0.0250 mL/min	Optical gating	120 mm × 0.010 mm ID capillary, 0.01 M Na_2HPO_4 (pH 6.85), 20 kV	LIF	20 min	horse heart cytochrome c	-	[58]
IC×CE	250 mm × 2 mm ID Dionex IonPac AS24 column, Gradient elution with potassium hydroxide at 0.3 mL/min	injection valve connected to a tee piece	150 mm × 0.025 mm ID fused silica capillary, 20 mM nicotinic acid and HEPES containing 0.1% PVP (pH 4.4), +30 kV	C^4D	56 or 35 min (depending on the gradient)	inorganic anions and haloacetic acids	498	[59]

Hyphenation	^{1}D separation media and conditions	Interface	^{2}D separation media and conditions	Detector	Total analysis time *	Application	Peak capacity	Reference
CIEF-RPLC	125 mm × 0.100 mm ID home-packed C_{18} column, Gradient of 5 to 80% acetonitrile (containing 0.02% heptafluorobutyric acid) at 0.001 mL/min	SPE trap columns for parking the IEF fractions	600 mm × 0.100 mm capillary coated with hydroxypropyl cellulose, 0.5% ammonium hydroxide (pH 10.5) and 0.1 M acetic acid (pH 2.5) as catholyte and anolyte, respectively. electric field strength of 300 V/cm	ESI-IT-MS	About 24 h	yeast tryptic peptides obtained from the soluble fraction of cell lysates	2 640	[60]
CIEF-RPLC	150 mm × 0.050 mm ID home-packed C_{18} column, linear gradient from 5 to 45% acetonitrile containing 0.02% HFBA and 0.02% formic acid at a flow rate of 200 nL/min	14 or 28 trap columns packed with C_{18} reversed-phase particles	840 mm × 0.100 mm ID CIEF capillary coated with hydroxypropyl cellulose, 0.5% ammonium hydroxide (pH 10.5) and 0.1 M acetic acid (pH 2.5) as catholyte and anolyte, respectively electric field strength of 300 V/cm	ESI-Q-TOF micro	18.5 h	micro-dissected tumor tissue	1 478-1539 distinct proteins were identified	[61]
CIEF-RPLC	150 mm × 0.075 mm ID C_{18} reversed-phase column, gradients of A (94.4% water, 5% acetonitrile, 0.5% formic acid, and 0.1% TFA) and B (94.4% acetonitrile, 5% water, 0.5% formic acid, and 0.1% TFA) at a flow rate of 200 nL/min	Two sampling loops attached to a microselection valve/ 20 cm PEEK tubings attached to a 10-port loop selection system/ C4 reversed-phase protein trap column attached to a six-port valve	With microdialysis membrane-based cathodic cell 700 mm × 0.075 mm ID polyacrylamide-coated capillary, 100 mM acetic acid (anolyte) and 0.5% ammonium hydroxide (catholyte), an electric field of 300 V/cm	API-ESI-QTOF	< 8 h	lysates of the green sulfur bacterium Chlorobium tepidum	160	[62]
CIEF-RPLC	50 mm × 0.300 mm ID C_4 reversed-phase column, gradients of A (94.4% water, 5% acetonitrile, 0.1% acetic acid) and B (94.4% acetonitrile, 5% water, 0.1% acetic acid) at a flow rate of 0.020 mL/min	A microslection valve with a loop connected to a six-port valve with a C_{18} trap column	With microdialysis membrane-based cathodic cell 550 mm × 0.050 mm ID eCAP neutral capillary; 91 mM H_3PO_4 (anolyte) and 20 mM NaOH (catholyte)), an electric field of 300 V/cm	API-ESI-QTOF-MS	About 2 hours	A mixture containing ribonuclease A, cytochrome c, myoglobin, insulin, and β - lactoglobulin, carbonic anhydrase II and bovine serum albumin, and CCK flanking peptide	70 (10^6 including MS)	[63]
CIEF-RPLC	50 mm × 0.300 mm ID C_4 reversed-phase column, gradients of A (94.4% water, 5% acetonitrile, 0.1% formic acid) and B (94.4% acetonitrile, 5% water, 0.1% acetic	A microslection valve with a loop connected/ a 10-port loop selection system/ six-port	With microdialysis membrane-based cathodic cell 550 mm × 0.100 mm ID eCAP neutral capillary, 400 mM acetic	API-ESI-QTOF-MS	About 11 hours	proteins from a complex yeast enzyme concentrate	-	[64]

Hyphenation	^{1}D separation media and conditions	Interface	^{2}D separation media and conditions	Detector	Total analysis time *	Application	Peak capacity	Reference
	acid) at a flow rate of 0.010 mL/min	valve with a a reversed-phase protein trap column	acid (anolyte) and 0.5% ammonium hydroxide (catholyte), an electric field of 500 V/cm					
CIEF-enzyme microreactor-RPLC	600 mm × 0.100 mm ID LPAA coated capillary anolyte, 1% v/v acetic acid; catholyte 1% v/v NH_4OH at 300 V/cm	hollow fiber membrane interface/ enzyme microreactor/ monolithic trap columns	340 mm × 0.075 mm ID monolithic RPLC column gradients of water and 70% acetonitrile both containing 0.1% formic acid at 300 nL/min	ESI-MS/MS	Over 4 hours	proteins extracted from *E. coli*	-	[65]
CIEF-CEC	440 mm × 0.050 mm ID HPC coated, either 20 mM phosphoric acid containing 0.1% HPMC, (pH 2.03) and 20 mM sodium hydroxide (pH 11.87) or 1% v/v acetic acid (pH 2.5) and 1% v/v ammonium hydroxide (pH 10.7) as anolyte and catholyte, respectively, 20 kV focusing voltage	A 6-port nanoinjector valve with ceramic internal pathway	410 mm × 0.100 mm ID neutral C_{17} monolith column, 40% (v/v) ACN in 20 mM sodium dihydrogen phosphate (pH 7.0) as mobile phase, running voltage 10 kV	UV-Vis	7 days (to realise the theoretical peak capacity)	standard proteins, human serum proteins	54 320 (theoretical peak capacity)	[66]
RPLC×CE	150 mm × 2.1 mm Vydac protein and peptide C_{18} column, gradient elution of CE buffer (A) 60% acetonitrile/40% A (v/v) at 0.250 mL/min	Optical gating	80 mm × 0.010 mm ID fused silica capillary, 0.01 M sodium phosphate buffer (pH 6.85), 20 kV applied voltage (1.1 kV separation voltage)	LIF-PMT	< 10 min	fluorescently tagged horse heart cytochrome c	650	[67]
SEC×CE	1500 mm × 0.250 mm and 1100 mm × 0.100 mm columns, buffer used for both separations was 10 mM tricine, 25 mM Na_2S0_4, 0.005% sodium azide (pH 8.23) at 360 nL/min (valve interface) and 235 nL/min (flow gated for 0.250 mm ID column) and 20 nL/min (0.100 um column with gated interface)	Valve/ sample loop and Flow gating interface	10 mM tricine, 25 mM Na_2S0_4, 0.005% sodium azide (w/v),pH 8.23 580 mm × 0.050 mm ID capillary with -11 kV (valve interface) 450 mm × 0.050 mm ID capillary with -10 kV separation voltage (0.250 mm column- gated) 530 mm × 0.050 mm ID capillary with -11 kV separation voltage (0.100 mm column- gated)	UV	about 2 hours	protein standards	-	[68]

Hyphenation	^{1}D separation media and conditions	Interface	^{2}D separation media and conditions	Detector	Total analysis time *	Application	Peak capacity	Reference
RPLC × CE	760 mm × 0.050 mm ID column packed with C_8 particles, gradients of water and acetonitrile both containing 0.1% TFA at 30-60 nL/min	Flow gating in a clear polycarbonate interface	250 mm × 0.017 mm ID coned inlet capillary, 10 mM phosphate with 0.22% TEA (v/v) and 15% acetonitrile (v/v), pH 10.5 -30 kV	LIF	4 h	human urine	over 400 peaks resolved	[69]
RPLC-CEIA	45 mm × 0.050 mm ID C_4 column, gradients of 10 mM phosphate buffer (pH 2.5) containing 5% 2-propanol/ 10 mM phosphate buffer (pH 2.5) containing 30% 2-propanol at 150 nL/min	Flow gating	72 mm × 0.010 mm fused silica capillary, 50 mM tricine at pH 8.3, 25 kV	LIF	< 10 min	glucagon secretion from single islets of Langerhans	-	[70]
RPLC-APCE	150mm × 3.0mm RP-C8 column, a binary mixture of solvent A (acetic acid/water, 0.1/99.9, v/v) and solvent (acetic acid/water/acetonitrile, 0.1/19.9/80, v/v/v) at 0.3 mL/min	Flow gating	75 mm × 0.010 mm ID separation capillary, 25mMTris, 192 mM glycine (pH 8.5) 15 kV	LIF	< 50 min	inhibitors of Src homology 2 domain–phosphopeptide binding in mixtures	-	[71]
RPLC×CE	33 mm × 1 mm ID POROS R/H II RPLC column, gradients of water acetonitrile both containing 0.05% trifluoroacetic acid at 0.015 mL/min (0.001 mL/min of the RPLC effluent flowing to the CE injection interface)	Flow gating	150 mm × 0.029 mm fused silica capillary, 0.4% triethylamine in water, +25 kV	Sheath flow ESI-MS	About 15 min	A glycosylated peptide mixture	500, 000 (including the peak capacity obtained by MS)	[72]
RPLC×CE	100-120 mm × 0.2 mm ID home-packed C_{18} column, gradient of 20 mM formic acid/ACN (90/10 mobile phase A, 10/90 mobile phase B, v/v) at 0.002 mL/min flow	PDMS flow-gating cross	200-250 mm × 0.050 mm ID 3-aminopropyl-trimethoxysilane coated fused silica capillaries, 50 mM phosphate buffers (pH 7) for positive injection mode and 10 mM acetic acid/acetonitrile (ACN) (50/50, v/v) In negative injection mode -15 kV	sheathless ESI-TOFMS	< 30 min	9-peptides standard mixture	3000 (48 chromatographic)	[73]
RPLC×CE	100–120 mm × 0.2 mm ID ODS-AQ C_{18} packed column, mobile phase gradients using solvent A: 9.2 mM acetic acid (HAc) : ACN (95 : 5, v : v), and solvent B: 1.6 M HAc : ACN (5.5 : 94.5, v : v), at 0.0015 mL/min	PDMS fabricated gating cross	PolyE-323 coated 0.050 mm ID capillaries at lengths of 190 and 260 mm, together with 4 cm of PDMS channel, 10 mM HAc : ACN 75 : 25, 30 kV	ESI-FTICR-MS	< 1 h	tryptic digested bovine serum albumin (BSA) and tryptic digests of human cerebrospinal fluid (CSF)	42–300	[74]
RPLC×CE	150 mm capillary packed with C8 RPLC, gradients of methanol water at 0.0015 mL/min	Pinched-injection glass microchip	40 mm long × 0.025 mm deep and 0.075 mm wide at half depth channel on a glass microchip CE, 30 mM TEA, 2.54 kV	LIF	90 min	peptides in (FITC)-labeled tryptic digests of bovine serum albumin	1000	[75]

Hyphenation	^{1}D separation media and conditions	Interface	^{2}D separation media and conditions	Detector	Total analysis time *	Application	Peak capacity	Reference
GFC×CE	600 mm × 7.5 mm ID 2 serially connected TSK gel G3000SW silica diol columns, isocratic elution 50 mM phosphate (pH 7.4) with 5 mM SDS at flow rate of 0.150 mL/min	Plexiglas Servo-actuated capillary array moving interface	250 mm × 0.025 mm capillaries, 50 mM pH 9.25 borate buffer containing 2 or 4 mM SDS, 20 kV	LIF with a PDMS multichannel sheath-flow cuvette	Over 165 min	FQ-labelled proteins in serum	90	[76]
Microchip IEF-RPLC	42 mm × 0.254 mm wide × 0.130 mm deep channels packed with C_{18} silica particles, gradients of 0–40% acetonitrile containing 0.1% TFA at 0.0025 mL/min	Multiplexed channels	70 mm × 0.254 mm wide × 0.180 mm deep channel coated with 0.4% HPMC, 0.5 MNaOH as catholyte and 0.5 M H_3PO_4 as anolyte, 1 KV	FLD and MALDI-MS	About 90 min	BSA digest	215	[77]
Microchip RPLC×CE	100 mm × 0.025 mm × 0.120 at full width LC channel packed with C18-bonded porous particles, gradients of 0.1% formic acid in water, and 0.1% formic acid in acetonitrile at 700 nL/min split to 570 nL/min for sample loading and 65 nL/min for separation	Flow gated interface at the end of the LC channel	Microchip CE channel, 50 mm × 0.008 mm deep and 0.050 mm at full width coated with PolyE-323, 0.1% formic acid with 25% acetonitrile (pH 2.5) and + 8 kV	Q-TOFMicro-MS	30 min LC run 18 s total CE separation time with overlapping injecitons occurring every 10 s	tryptic digests of bovine serum albumin, yeast enolase and *E. coli* cell lysate	640	[78]
RPLC×CE	LC channel inlet before split, 150 mm × 0.075 mm ID packed with C_{18} particles, on chip 13 mm; LC inlet after split 4 mm long, gradients of 0.5% acetonitrile with 0.1% formic acid, and 99.5% acetonitrile with 0.1% formic acid at 0.010 mL/min flow for trapping step and 500 nL/min for separation	On-chip flow splitting gated injections	Microchip CE channel, 91mm × depth of 0.010 mm, asymmetrically tapered down to a full width of 0.030 mm in serpentine turns coated with aminopropyltriethoxysilane, 50% acetonitrile, 0.1% formic acid, 800 V/cm	oa-TOF-MS	Over 60 min	tryptic digest of an immunoglobulin G2 (IgG2) monoclonal antibody	1400	[79]
Heart cutting RPLC-CE	100 mm × 0.100 mm capillary column packed with PS-DVB, AcN/phosphate (5 mM, pH 3), 30 : 70 at 0.0002 mL/min	PDMS fabricated droplet-based microchip connected to a PTFE tubing	200 mm x 0.100 mm fused silica capillary, 10 kV	UV	About 70 min	yeast cell proteins	2000	[80]
RPLC×CE	150 mm × 0.100 mm Ultimate XBC18 column, gradients of A: H2O+ 0.05% TFA and B: ACN + 0.05% TFA at 500 nL/min	PDMS droplet microchip and a olyethylene tube for sample storage	280 mm × 0.075 mm ID CE capillary, 10mM phosphate at pH 3.0, 10 kV	UV	6 days	human urinary protein digest	-	[81]
RPLC×CE	300 mm × 0.250 mm column packed with C8 particles, gradient of acetonitrile-water with 0.1% TFA, 0.0015 mL/min	hydrodynamic-sampling interface	300 mm × 0.075 mm untreated fused-silica capillary, 50 mM TEA running buffer, 30 kV	MALDI-TOF-TOF-MS	About 86 min	proteins in D_{20} liver cancer tissue	-	[82]

Hyphenation	^{1}D separation media and conditions	Interface	^{2}D separation media and conditions	Detector	Total analysis time *	Application	Peak capacity	Reference
GFC-CIEF	300 mm × 7.5 mm cross-linked polysaccharide column, 50 mM Tris-HCl and 100 mM KCl at pH 7.5 at 0.350 mL/min	Horseshoe shaped microdyalsis hollow fibre membrane module	50 mm × 0.100 mm ID fluorocarbon coated fused silica capillary, 10 mM H_3PO_4 as anolyte and 20 mM NaOH as catholyte, 3 kV separation voltage	Absorption image detector	About 30 min	myoglobin and bovine serum albumin (two proteins)	-	[83]
SCE	Cellulose coated 200 × 200 mm glass plate, Solvcnt/electrolytc: isopropanol(47.5 ml)-water(52.5 ml)-trichloroacetic acid (1 g) pH = 4.0	-	The same as the ^{1}D at 600 V separation voltage	Xray film	About 4 h	labellcd aquohalo complcxcs of tctrnvalcnt and trivalent iridium.	-	[84]
SCE	70 × 60 mm fluorescent and non-fluorescent Whatman PE SIL G plates For vitamins and amino acids: 1-propanol/1 mM aqueous ammonia (2:1) buffered to pH 9.3 For dyes: 1-propanol/1.0 mM aqueous glycine (2:1) buffered to pH 2.4	-	The same as the ^{1}D at 500 V	UV-Vis and Fluorescence	All in less than 30 min	mixtures of vitamins, amino acids and dyes	-	[85]
OPPEC	10 cm × 10 cm HPTLC RP18W chromatographic plate Mobile phase of acetonitrile and citrate-phosphate buffer at pH 3.0 at 0.060–0.100 mL/min	-	Separation voltage of 1.0-2.0 kV	Vis		Mixture of food dyes	-	[86]
RPLC×CE	250 mm × 4.6 mm Bio-Rad Hi-Pore RP-304 column, 12.5 mM potassium dihydroxyphosphate solution in a mixture containing 72.5% water, 25% acetonitrile, and 2.5% methanol, 1.0 mL/min	Stroboscopic sampling	600 mm × 0.050 mm ID fused-silica capillary, 20 mM sodium tetraborate, 20 kV	UV	About 1.5 h	tannic acid	-	[19]
IEC×CE	40 × 4 mm IonPac AG9-SC, 20 mM sodium tetraborate solution (pH 9) at 1.0 mL/min	Stroboscopic sampling	600 mm × 0.050 mm ID fused-silica capillary, 20 mM sodium tetraborate, 20 kV	UV	About 3 hours	phenols and aromatic carboxylic acids	-	[19]
RPLC×μFFE	150 mm × 0.075 mm ID packed C_{18} column, gradients of mobile phase A water with 0.05% TFA and mobile phase B 90:10 ACN/water with 0.05% TFA at 300 nL/min flow rate	A 0.020 mm ID fused silica capillary	0.010 mm deep × 10 mm wide × 25 mm long separation channel etched into borofloat glass wafers coated with coated with PEO, 300 μM Triton X-100, 8 M urea, and 50 mM MES hydrate (pH= 5.56), 0.5 mL/min, 150 V	LIF	About 25 min	BSA tryptic digest	776 (2352 theoretical value)	[20]

Hyphenation	^{1}D separation media and conditions	Interface	^{2}D separation media and conditions	Detector	Total analysis time *	Application	Peak capacity	Reference
IC×CE	250 × 0.25 mm Dionex Ion-Swift MAX−200 column, isocratic elution with 40 mM KOH at 0.005 mL/min	capillary batch injection modulator	205 mm × 0.025 mm ID separation capillary , 25 mM ammonium acetate buffer (pH = 9.15), 22.5 kV	ESI-micrOTOF-MS	about 15 min	model mixture of six nucleotides	-	[87]
Heart cutting RPLC-CEC and NPLC-CEC	100 mm × 4.6 mm ID S5W phenyl column, 70:30 acetonitrite:water at 0.5 mL/min 150 mm × 4.6 mm ID Spherisorb S5W silica column, hexane mobile phase at 0.5 mL/min	Flow gating with two perpendicular tee pieces	250 mm × 0.100 mm ID fused silica capillary packed with Waters Spherisorb S5W ODS1, 80:20 acetonitrile: 10 mM TRIS (pH 7.7) at 0.4 mL/min, 20 kV	UV	Over 30 min for separation of a single fraction	nitro compounds (Energetic Material), coal oil	-	[88]
Heart-cutting SEC-CE	30 × 4.6 mm ID hydrophilically modified silica column, water containing 1.6 mM glacial acetic acid and 16 mM ammonium acetate (pH 5.8), 0.200 mL/min	C_{18} bonded silica trap microcolumn connected to a home-made interface through a valve	900 mm × 0.050 mm ID fused silica capillary, 150 mM phosphoric acid (pH 3.1), -30 kV	UV	Over 25 min for a single fraction	enkephalins peptide drugs in cerebrospinal fluid	-	[89]
Heart-cutting SEC-CE	30mm × 4.6mm ID column, gradient of 16 mM ammonium acetate buffer (pH 5.8) at 0.050 mL/min	C_{18} trap column with tee-split interface	1200 mm × 0.075 mm ID fused silica capillary, 50 mM boric acid buffer (pH 8.0), -20 kV	UV	Over 40 min for analysis of the heart-cut	Enkephalins in cerebrospinal fluid (CSF)	-	[90]

* Approximate values regardless of sample preparation time. In some cases, the analysis time was estimated from the time axis on the graphs.

1.3 Offline approaches

The first combinations of LC and CE were conducted in an offline manner. The complementarity of LC and CE was realised when digested peptides of human growth hormone that co-eluted in LC could be resolved by CE [91] or when CE was used to assess the purity of peptide samples obtained after preparative LC [92]. Despite the fact that automated LC×CE appeared only a few months later than these works, offline LC/CE has continued to see vast use and further developments for the reasons listed below.

In an offline comprehensive 2D separation, fractions of ^{1}D separation are collected and are later subjected to ^{2}D separation subsequent to any kind of sample treatment, e.g., digestion, preconcentration or derivatisation. This approach offers substantial flexibility and simplicity as it can be implemented using commercially available instrumentation and detectors and potentially has no restrictions in terms of the separation chemistry in either ^{1}D or ^{2}D (e.g. any kind of stationary or mobile phase, electrophoretic media, background electrolyte composition or additives, column dimensions and separation flow rate or temperature can be used). This degree of flexibility, however, is obtained at a price of time as it may take several hours to complete an offline 2D run, especially when a very high resolution second dimension separation is performed, pre-^{2}D sample treatment is tedious, or automation is not easy to achieve.

So far various offline chromatographic and electrophoretic techniques have been introduced, including RPLC/CE [25-35], RPLC/CIEF [36], RPLC/MEKC [32, 37, 38], IEF/GPC [93], IEF/RPLC [39-43, 94], IPC/CGE [44], IEC/CGE [44], SEC/CE and SEC/IEC/CE [45], IEC/CEC [46], BAC/CIEF [47], TLE/TLC [48], PEC/TLC [49], TLC/PPEC [50], TLC/PEC [51], MEKC/TLC [52], etc. Highlights of these offline, coupled techniques will be briefly discussed in this section while an extended summary of these can be found in Table 1-1.

In a classic example of offline RPLC/CE, Issaq *et al.* demonstrated the separation of a proteolytic digest of cytochrome *c* and myoglobin [25]. In their work, LC fractions were collected in microliter wells every minute throughout a 40 min ^{1}D run. These 40 fractions were then dried under vacuum and reconstituted for injection into CE with LIF detection. With each CE run lasting 14 minutes, 2D analysis took approximately

9 hours to complete. This, as mentioned earlier, is a typical run time for an offline 2D separation.

To improve separation speed, the same group used a capillary array electrophoresis (CAE) instrument to allow parallel ^{2}D separation of fractions instead of using a single capillary [26]. This enabled more frequent sampling of LC effluent as well as a reduced total analysis time of less than an hour. Using the same approach with less sensitive UV detection instead of LIF for mapping of ovarian cancer cell extracts [27], He and coworkers noted that LC fractions needed to be more concentrated prior to injection into the 12-array capillary. As a result, large volume sample stacking with polarity switching was performed in conjunction with drying to enhance the sensitivity [27]. This work sheds light on another area of great concern in almost all two-dimensional liquid-phase separation approaches, which is the inevitable dilution of the eluate in ^{1}D and therefore reduced 2D sensitivity when compared to 1D approaches [95]. To address the ^{1}D dilution issue, several strategies such as sample preconcentration prior to ^{2}D, e.g., evaporation of solvent, solid phase extraction, large volume sample stacking, or derivatisation have been practiced. A few examples of these include RPLC/MEKC separation of *B. subtilis* cell extract metabolites where dynamic pH junction CE and sweeping MEKC were applied for early and late eluting fractions respectively, while the fractions in-between were subjected to both [32]; sweeping by SDS micelles for RPLC/MEKC analysis of natural antioxidants in red wine [38]; and, online solid phase extraction (SPE) at the inlet of CE capillary (SPE-CE) for preconcentration of RPLC fractions of digested bovine serum albumin [35].

While in the majority of approaches CE serves as ^{2}D, the use of other electrophoretic techniques have also been reported. Effective combination of RPLC/CIEF introduced by Zhang's group, for instance has enabled peak capacities as high as 10 000 [36]. In this work, fractions of capillary RPLC were collected every 1 min continuously throughout the LC run. Followed by fluorescent labelling, these fractions were injected into hydroxypropylcellulose-coated capillaries for IEF-LIF. One of the advantages of using IEF over CE is the ability to inject the whole capillary with sample making it more compatible with the larger volumes of the LC fraction. Like most of the other offline approaches, the use of a capillary array was also examined and different detection techniques were tested in later works of the same group [53, 54].

Although often expressed as one of the main advantages of offline 2D separation approaches over the online techniques, 2D LC/CE approaches can be prone to matrix effects from the first dimension elution solvent affecting the second dimension separation. An example of this is described in hyphenation of IEC with CGE [44], where specifically the varying NaCl content of IEC mobile phase does not allow sufficient transfer and discrimination-free electrokinetic injection of mixtures of poly adenosine, thymidine, cytosine and uracil homodeoxyoligonucleotides from ^{1}D effluent into CGE. As a result, hydrodynamic injection had to be employed which not only reduced the sensitivity of the approach but also didn't allow a multiplexed array of capillaries to be utilised in order to improve sample throughput. The authors, therefore, decided to choose IPC as an alternative ^{1}D, which is believed to be a more suitable candidate to couple with CGE due to substantially lower ionic strength of the eluent. IPC/CGE provided a lower peak capacity than IEC/CGE (852 against 1 474) while enabling higher sample throughput as well as more frequent fractionations.

In addition to various separation techniques, several detection approaches have been used in offline combinations. Amongst all of these detection technologies mass spectrometry, which is known to add additional resolution, has a special place. An early example of hyphenation with MS appeared in offline RPLC/CE/MALDI-TOFMS [31].

A less-explored area of hyphenated chromatographic and electrophoretic techniques is hyphenations in which the electromigration technique serves as ^{1}D. In work by Wall *et al.* IEF/RPLC was introduced as an alternative to traditionally-favoured 2D-PAGE for mapping of cellular proteins [39]. A commercially available IEF device was used to carry out the ^{1}D separations and IEF fractions were all collected at the same time and stored for subsequent ^{2}D separation by RPLC-MALDI-TOFMS. Comparison of the 2D electrophero-chromatogram obtained by this method against a 2D-PAGE map, showed that the gel approach provided better sensitivity for proteins above 50 kDa with p*I* values below 7 while IEF/RPLC improved the sensitivity for proteins below 50 kDa with p*I* values above 7. As a result, both approaches were concluded to be complementary rather than redundant and competitive. IEF/RPLC, nevertheless, was proven to be superior in regard to total analysis time as well as the possibility of automation.

In another interesting offline hyphenation of IEF with RPLC, FFE was used to fractionate proteins and peptides in total/ tryptic digested cellular lysate of the colon

carcinoma cell line and a human urine specimen based on the electrophoretic mobility of the components as well as their p*I* [55]. In this work, proteins were continuously introduced to a carrier ampholyte solution perpendicular to which an electric field was applied. A counterflow of glycerol or hydroxypropylmethylcellulose was used to avoid precipitation of proteins whose solubility around their p*I* was low. FFE-IEF fractions were then collected in a 96-well plate and stored at low temperature for ^{2}D analysis with RPLC-ESI-IT-MS. In contrast to gel-based IEF, this approach allowed the use of large sample volumes as well as the possibility of analysis of lower molar mass peptides which had also been noted in previous comparisons with gel-based technologies.

Besides improving the peak capacity, coupling IEF with RPLC eliminates the interferences from ampholytes, acids, and bases which complicate mass spectrometric detection of IEF-separated bands. Several technologies have been introduced to facilitate this purpose. In one approach, OFFGEL-IEF was used in the ^{1}D in 2D quantitative proteomics analysis of mouse liver tissue [41]. In OFFGEL-IEF, an immobilised pH gradient (IPG) gel strip is used for inducing the pH gradient at the bottom of a multicompartment chamber. As a result, there is no need for addition of ampholytes. Upon application of a perpendicular gradient voltage through the chamber, the charged species are removed while the neutral species whose p*I* is equal to the IPG pH remain in the solution and can be analysed further. OFFGEL-IEF /RPLC was shown to outperform single-dimensional LC or SCX/RPLC for improving the sensitivity of selected reaction monitoring in a mass spectrometer. In another work using OFFGEL technology, isoelectric focusing of cisplatin-binding proteins was achieved under reducing conditions followed by filter-aided sample preparation for buffer exchange, reduction, alkylation and tryptic digestion prior to SEC-ICP-MS and *n*LC-ESI-LTQ-MS/MS analysis [94]. In another recent CIEF/RPLC approach, an online multijunction (OMJ) capillary isoelectric focusing fractionator was developed by Pirmoradian *et al.* [43]. Constructed from PEEK capillaries with Nafion membrane windows immersed in electrolytic buffer solutions of 8 different pH values in different vials, this device offered high micropreparative loading capacity with a stabilised pH gradient for focusing, immobilisation and further refocusing of tryptic peptides of digested yeast proteome. The collected fractions were then introduced to LC-MS/MS as the ^{2}D.

Following Haugaard and Kroner's pioneering work on paper chromatography × electrophoresis, there have also been several reports on both offline and online coupling of thin layer chromatography (TLC) with thin layer electrophoresis (TLE) or planar electrochromatography (PEC). In fact, one of the most popular methods for analysis of phosphopeptides is the TLE/TLC method proposed by van der Geer and Hunter [48]. Using thin-layer cellulose plates, this method was based on electrophoresis of ^{32}P-labelled peptides in the ^{1}D followed by their partitioning in the ^{2}D and visualisation by autoradiography. Phosphoamino acid content of both intact phosphoproteins and individual phosphopeptides were also recovered after the 2D TLE/TLC for further separation by either TLE or TLE/TLE. A more recent variation of this work as PEC/HPTLC was employed by Panchagnula *et al.* for analysis of phosphopeptides by MALDI-TOF-MS which eliminated the complexities associated with radiolabelling [49]. The authors have shown that use of silica gel rather than cellulose plates helped improve the separation as a result of the stronger chromatographic interactions on silica gel. Therefore, PEC was used in the ^{1}D instead of TLE. Whether as PEC-TLC or TLC-PEC, couplings of TLC with PEC have proven to be of superior performance when compared with single-dimensional TLC, which is known to suffer from limited peak capacity due to the varying velocity of the capillary action- driven mobile phase with distance. Unlike TLC, the electroosmotic driven mobile phase in PEC has a constant velocity and is independent of the particle size. However, PEC is susceptible to Joule heating-related band-broadening. To eliminate the mobile phase evaporation and its flux to the stationary phase surface, forced-flow techniques such as pressurising of the separation layer has proven to be effective. The first example of hyphenation of TLC with pressurised planar electrochromatography (PPEC), was reported by Chomicki *et al.* to separate a number of dyes after HPTLC separation in ^{1}D followed by drying and pressurising of the thin layer by means of a hydraulic press and application of separation voltage within a device specifically designed for performing PPEC [50]. With a special focus on overcoming shortcomings such as long analysis time and poor separation efficiency, new materials have also been introduced. A recent example is new ultrathin electrospun polymer nanofiber layers used in the offline separation of a mixture of laser dyes by UTLC in ^{1}D and PEC in ^{2}D [51]. New simultaneous separation approaches of this kind are further discussed under the online planar approaches section of this chapter.

Undoubtedly, the majority of multidimensional chromatographic and electrophoretic hyphenations fall in the offline category using the approaches described above. An interesting example of an uncommon pairing is the coupling of a temporal separation (MEKC) with a spatial separation (TLC) for the separation of dansylated-amino acid enantiomers [52]. Similar to the CAE approaches described above, ^{2}D separation could be achieved simultaneously for all fractions as the TLC plate was used to store ^{1}D eluate. Sample transfer from the first to the second dimension was achieved using sheath flow electrospray (ES), which in contrast to the conventional ES usually used in mass spectrometry, was carried out at a lower voltage resulting in a more focused liquid filament rather than a broadened fine mist.

1.4 Online approaches

It wasn't long after proposing comprehensive two-dimensional liquid chromatography (LC×LC) [4], that Bushey and Jorgenson introduced online comprehensive two-dimensional liquid chromatography-capillary electrophoresis (LC×CE) [56]. In contrast to substantially longer offline approaches, an online 2D separation finishes in essentially the timeframe of the ^{1}D separation but generally provides inferior resolution to its offline counterpart.

The heart of an on-line 2D system is the interface, which needs to be positioned between the two dimensions to modulate the ^{1}D effluent for introduction to the ^{2}D. This interface captures, ideally re-focuses, and re-introduces the ^{1}D eluate into the ^{2}D. Various interfacing technologies have been implemented to enable online 2D analysis with maximised sampling frequency and transfer efficiency while minimising the instrumentation complexities and analysis time. Below is an overview of how the LC×CE interface has evolved throughout the past 25 years.

1.4.1 Valve-based interfaces

In the first attempt to comprehensively couple LC with CE, a six-port two-position injection valve with a 10 µL sample loop was used as an interface between the two dimensions [56]. As shown in Figure 1-2, the effluent from the RPLC column was collected in the loop every minute and flushed (at a higher flow rate than the LC flow rate through the use of a second pump) towards the CE capillary where it was electrokinetically injected. In order to provide a sufficient number of samples of the

[1]D peaks, the microbore LC column (250 mm × 1.0 mm) was operated at a low flow rate of 10 μL/min to produce slowly-eluting peaks (4 min wide at the base). Nevertheless, not only was the RP separation undersampled but the peak capacity was also sacrificed (peak capacity of 35 in the [1]D and 12 in the [2]D) and the data acquisition time was over 4 h for analysis of fluorescently-labelled peptides from an ovalbumin tryptic digest.

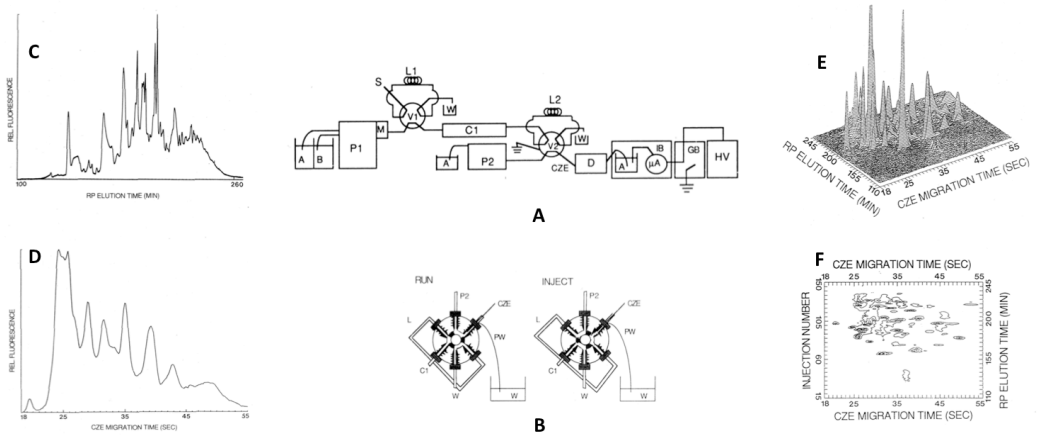

***Figure 1-2**: **A**: Schematic of 2D LC-CE instrumentation: P, pump; M, mixer; V, valve; S, injection syring; L, loop; C, column; W, waste; CZE, CZE capillary; D, detector; IB, interlock box; μA, microammeter; GB, grounding box and HV, high-voltage power supply. **B**: Two configurations of six-port computer-controlled valve interface. **C**: Single dimension RP chromatogram of fluorescamine labeled tryptic digest of ovalbumin. **D**: Single dimension electropherogram of the same sample as in C. **E**: Surfer generated chromatoelectropherogram of fluorescamine labeled tryptic digest of ovalbumin. **F**: Contour plot of same data set. For further experimental details the readers are referred to the source article. Reprinted with permission from [56].*

The valve-based interface has had variations since the original work. In the first work of coupling SEC with CE a microcolumn (0.250 mm ID) with a flow rate of 360 nL/min was used to separate proteins [57] to address the incompatibility of the large LC elution volume with the small CE injection volume. Instead of connecting the CE capillary directly to the valve, a tee-piece was used with a hollow stainless tube serving as both inlet electrode and wasteline and the CE capillary was positioned directly opposite the buffer flow in the tee. In later works, the sample loop was replaced with an internal loop of substantially lower volume for the SEC×CE separation of protein standards of thyroglobulin, bovine serum albumin, chicken egg albumin, horse heart myoglobin and human serum (lyophilised powder) [58]. Another

variation of the valve-based interface was shown in a RPLC×CE system [58], where two 10 µL loops were connected to an eight port valve similar to the initial LC×LC report. The loops were alternatively filled with the LC effluent; while the content of one loop was flushed (at a substantially higher flow rate than the LC flow) and a small portion was introduced onto the CE capillary, the other loop was filled with the ^{1}D effluent. CE runs in this work were substantially shorter compared to the previous works of the same group (total CE run time of 19 s). To allow more frequent injections of the ^{1}D, *overlapping* injections were used; with the first 7.5 s of each CE run showing no peaks, a new injection was made every 7.5 s. This maximised the utilisation of the ^{2}D separation space and guaranteed sufficient sampling of the ^{1}D effluent. This set-up was used for analysis of labelled tryptic digest of horse-heart cytochrome *c* with LIF as detection.

Our group has recently demonstrated a non-focusing valve-based interfacing approach to couple IC with CE [59]. Described in details in Chapter 2 of this thesis, the set-up comprised of a flow interface similar to the one described earlier by Lemmo *et al.* [57], a tee-piece (with the CE capillary in right angle to the ^{1}D effluent flow) was connected to a six-port two-position injection valve. This interface, however, differed from the other valve-based approaches in that it eliminated the use of a sample loop to collect the IC effluent and was therefore free from any loop-related extra-column broadening, which is often listed as one of the shortcomings of valve-based interfacing approaches. Instead of sampling the loop content, the fast CE separation enabled the comprehensive sampling of the IC effluent by switching the injection valve and directing the effluent to the tee-piece. This system was used for quantitative analysis of inorganic anions and haloacetic acids in water. In contrast to RPLC×CE, which is prone to matrix effects from the ^{1}D mobile phase composition, the coupling of suppressed IC with CE is not only free from any interferences but also allows the application of sample stacking techniques due to the low conductivity of the IC effluent.

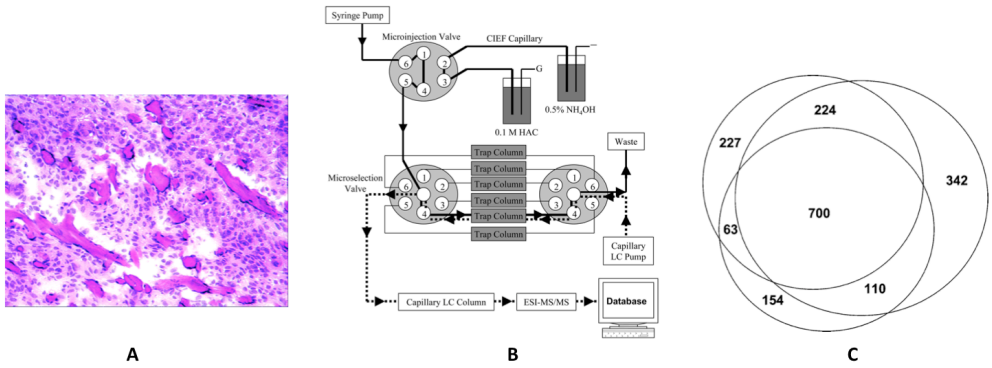

***Figure 1-3**: **A**: Optical microscope photograph of stained glioblastoma multiforme tissue section. **B**: Schematic of on-line integration of CIEF with RPLC as a concentrating and multidimensional separation platform. Solid and dashed lines represent the flow paths for the loading of CIEF fractions and the injection of fractions into a CRPLC column, respectively. **C**: Overlap in the proteins identified from three CIEF-nano-RPLC-ESI-MS/MS runs using a single tissue sample. A and C reprinted with permission from [61] and, B reprinted with permission from [60].*

In addition to LC×CE approaches, valves have also been used as an interface for CE×LC. CIEF was coupled with RPLC via the use of a number of trap columns in between the two dimensions using two valves; one before the trapping column and the other one after [60, 61, 96]. Focusing of the limited protein quantities from a microdissected tumor tissue was performed through the use of CIEF as the ^{1}D. As shown in Figure 1-3, the focused bands were consecutively transferred to a 400 nL loop on a microinjection valve and hydrodynamically loaded on to a series of C_{18} SPE trapping columns through the use of a microselection valve. Once the whole content of the CIEF capillary was loaded onto the SPE columns, the ampholytes used for CIEF were eluted from the column using a solution of acetic acid. Through the use of a second microselection valve the bands were eluted with LC mobile phase and separated by *n*RPLC-ESI-Q-TOFMS [61]. Various modifications of the same technology were subsequently introduced by the same group [62-64]. To constantly sample the CIEF separation, the traditional 2D LC two-loop approach was used followed by storage of samples in an array of loops connected to a microselection valve. To transfer these samples to the LC dimension, each fraction passed through a trap column connected to a six-port valve to remove the ampholytes and IEF markers prior to *n*LC-Q-TOF analysis. Several variations of this have emerged, with one example involving online digestion within a trypsin immobilised enzyme microreactor prior to RPLC-MS after desalting by use of parallel trap columns [65].

Although the valve interface is available off-the-shelf and easy to automate compared to other interfacing devices, there are a number of limitations. First, when employed in a system that utilises an electric field, the valve needs to be electrically isolated. This issue has been addressed by several groups through the grounding of the CE inlet [56-59] or use of metal-free valve material [66]. Second, and more importantly, is the contribution of the valve to extra-column band broadening when transferring the eluate between the two dimensions, as well as its mechanical and speed limitations when used with faster ^{2}D separations. This issue has been addressed by use of low-dead-volume valves and more frequently by the introduction of other interfacing approaches such as gated injection devices.

1.4.2 Gated interfaces

The gated injection technique, first introduced in 1991 [97], is by far the most popular approach for the online interfacing of LC with CE. In the initial technique, called optical-gating, the CE capillary was mounted vertically with one end in a tee-piece and the other in an outlet buffer reservoir (Figure 1-4). With the LC effluent coming from the opposite arm of the tee and the electric field on, LC bands electromigrated into the CE capillary continuously. Upon entering the capillary the band was exposed to two argon laser beams, the upper one with 95% of the total laser power which photolysed everything to nonfluorescent species. To perform an injection this laser was momentarily blocked using a shutter to provide a small zone of un-photolysed analytes. These migrated towards the second beam used for fluorescence detection. With a LC run time of 20 min and fast CE run time of 2 s, this system was used for separation of a tryptic digest of horse heart cytochrome *c* [58]. In an extension of this work, 2D separations of less than 10 min with a RPLC gradient of only over 2 min and CE separation time of 2.5 s were achieved [67]. This substantially faster analysis time, as mentioned earlier, limited the peak capacity in both dimensions (15 in RPLC and 43 in CE assuming unit resolution). The resulting total peak capacity of 650, however, was still high enough to enable the separation of FTC-tagged tryptic digests of horse heart cytochrome *c*.

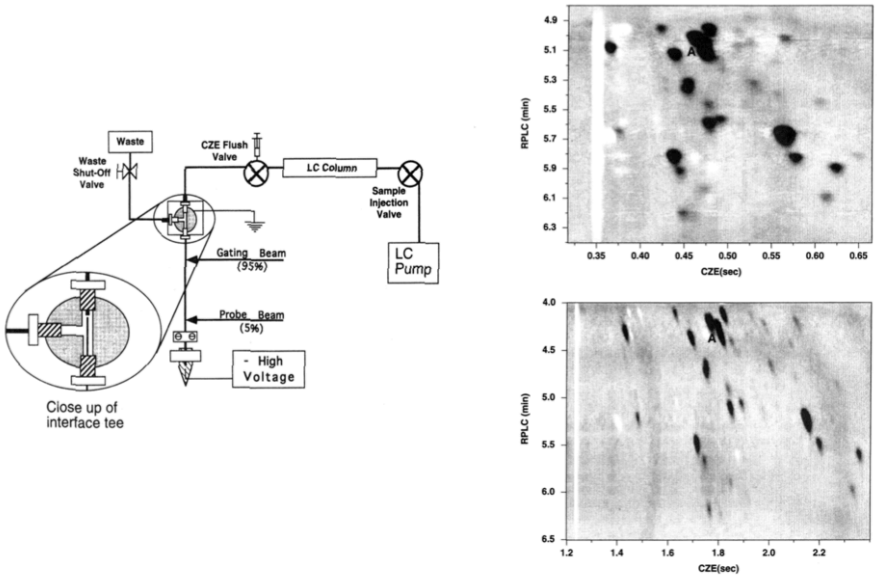

***Figure 1-4**: **A**: Two-dimensional optically gated RPLC-CE instrumental diagram. **B**: 2D RPLC-CE analysis with 2-min LC gradient and overlapped injections of FTC-tagged tryptic digest of horse heart cytochrome c. 0.7 s CE analyses (top) and 2.5-s CE analyses (bottom). Reprinted with permission from [67].*

The optically-gated interface was used in a 3D hyphenation of SEC×RPLC×CE [21]. A normal bore SEC column with a flow rate of 11 µL/min was used for ^{1}D, separating the components of fluorescently-tagged ovalbumin digest based on their molecular mass. This was followed by RPLC in a 2.1 mm ID LC column with a flow rate of 250 µL/min and subjected to fast CE separation in an 8 cm × 6 µm ID capillary with 1.7 cm effective length (electric field strength of +2.5 kV/cm). As the number of separation dimensions increased the chance of co-elution/co-migration dropped. This substantial improvement in the overall peak capacity of a 3D set-up, on the other hand, was accompanied by increased complexity. Apart from computational and data handling issues, there were other problems associated with 3D SEC×RPLC×CE separations. First, to accommodate large elution volumes of SEC into RPLC, a flow splitter with a split ratio of 1:10 was used which passed only 1 µL/min of the SEC sample to RPLC. The other issue was the incompatibility of the SEC solvent (methanol) with the RPLC mobile phase, for which the SEC effluent had to be diluted with CE BGE. Consequently, highly concentrated samples were required.

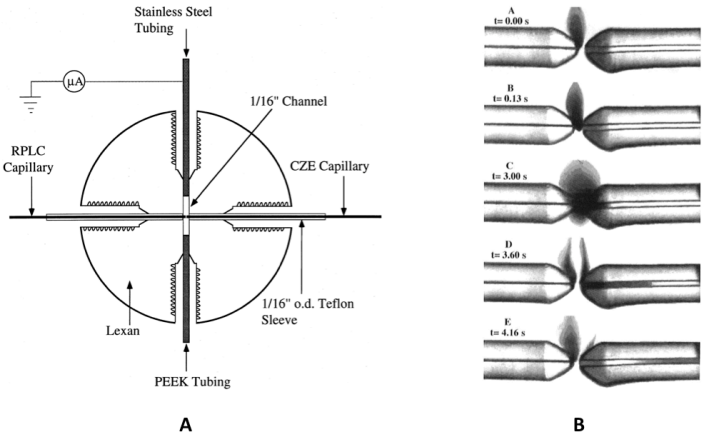

***Figure 1-5**: **A**: Schematic of the clear flow gating interface. **B**: Video images of the injection process of a solution of methylene blue dye flowing out from the left into the interface through which the transverse buffer flows. On the right is the CZE capillary. In (A), the voltage has been turned off while the transverse flow remains is running through. In (B), the transverse flow has been stopped to allow sample to flow across from the transfer capillary to the CZE capillary. The electrokinetic injection is occuring in (C). The transverse flow has been turned off and sample is swept out of the gap between the capillaries in (D). In (E), the gap between the capillaries is completely filled with buffer and the plug of dye is undergoing electrophoresis as the separation voltage is applied. Reprinted with permission from [69].*

One main limitation of optical-gating is that it is only applicable to fluorescent or fluorescently-tagged targets. On the other hand, transverse flow gating does not suffer from the same problem [68]. This interface was constructed of two stainless steel plates with a flow-through channel at the top of which the transverse flow of buffer entered and left through the port at the bottom. Right at the middle of this channel was the place where the SEC effluent line and the CE capillary met. These were both mounted at the opposite sides of the inner face of the flow. A transverse flow of CE buffer was used to prevent the SEC effluent from being injected into CE. When an injection was desired, the transverse flow was interrupted momentarily. Figure 1-5 shows a later modification of this interface which was fabricated on transparent material to facilitate easier capillary alignment and troubleshooting [69]. In the initial report [68] the transverse flow interface showed less dispersion/dilution than the loop interface with an 8-fold improvement in sensitivity due to higher transfer efficiency.

Apart from the separation of complex mixtures, the transverse flow gated LC×CE has been used for immunoassay screening purposes [70, 71]. In work by Liu and Kennedy, mixtures containing potential inhibitors of Src homology 2 domain–phosphopeptide binding were separated in the first dimension using LC. The LC eluate was then mixed with Src homology 2 domain and an affinity probe

phosphopeptide. Using this methodology, the reaction mix was monitored by CE where any variations in peak height of the affinity probe and the complex reflected the degree of binding between the inhibitor and the protein.

Before 1997, optical detection was the dominant detection technique in online LC×CE reports. In 1997, Lewis *et al.* reported the first LC×CE-ESI-MS separations with a total analysis time of about 15 min [72]. In this work, a transverse flow-gated interface was used with a high-pH CE buffer for separation of peptides while MS electrospray was carried using an acidic pH sheath flow. Unlike the previous work where CE inlet was grounded, the separation voltage had to be applied on the capillary inlet to allow coupling with the electrospray needle voltage of +3 kV. As a result, to isolate the high separation voltage of +25 kV from the rest of the system a polymethylmethacrylate box was used. Although separation of peptide standards and tryptic digests of ribonuclease B was demonstrated, adequate sampling of the CE effluent by MS was recognised to be as challenging as sampling of the LC effluent by CE [72]. To overcome this, CE peaks were broadened (by larger injection) which of course sacrificed the CE separation efficiency and peak capacity.

To address the issue of insufficient MS sampling, Bergström and co-workers chose to use TOF mass spectrometry [73] and FTICR-MS [74], which enabled faster sampling rates. They employed a sheathless ESI interface which resulted in no post-separation dilution or band broadening and was less complex when unified with the MS emitter [73]. A slightly different gated interface with a two-level PDMS structure was used and unlike the previous interfaces, the LC column was positioned at right angle to the CE capillary in the cross interface. This divergent design and orientation minimised the contact area between the channels and allowed use of lower transverse flow rates when compared to previously introduced gated interfaces. Use of a PEEK injection valve [73] and a power isolation transformer [74] facilitated the electrical isolation of the CE voltage.

1.4.3 Microfluidic chip-based interfaces

Since the first introduction of electrodriven separations on microchips by Manz *et al.* [98, 99] followed by 2D electrophoresis on chips [100], several reports of single- and multidimensional on-chip technologies have emerged. Miniaturised chip-based interfaces allow integration of almost any type of design with almost-zero dead volume. The possibility of handling extremely small sample sizes as well as high

sample throughput due to smaller channel size and higher speed separations are two of the other advantages of such techniques when compared to column-based approaches. LC×CE has also been influenced by the microfluidic revolution; use of polymeric or glass substrate to fabricate LC×CE interfaces has become increasingly popular in recent years. Examples include glass microchip CE interfaces [75, 78, 79], a PDMS fabricated interface [74], a Plexiglas fabricated device [76] and a cyclicolefin chip device [77].

Coupling capillary RPLC with microchip CE was first presented by Yang *et al.*[75]. In this work, *c*LC eluate was sampled through a microhole fabricated on the cover plate of a conventional cross-channel microchip CE. Using pinched injections every 20 s, separation of FITC-labeled tryptic digest of bovine serum albumin was shown. Although it allowed the coupling of the high-pressure LC flow with microchip CE, this method only enabled transfer of 1/300 of the ^{1}D effluent to the ^{2}D. The authors also concluded that the overall repeatability of the 2D separation was insufficient and attributed this to the changing surface of the triethylamine-coated microchip.

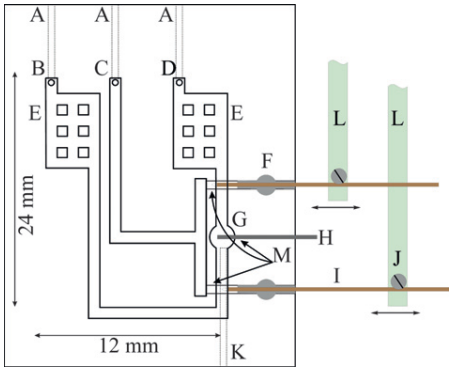

***Figure 1-6**: Top down view of the Plexiglas fabricated GFC–CE interface chip. (A) Connection points for sample and BGE supplies, (B) beginning of ''bottom BGE channel'' machined into face of the chip, (C) beginning of sample channel, (D) beginning of ''top BGE channel,'' (E) bubble trap/structure, (F) PDMS seal, (G) drain hole to waste connection, (H) ground electrode, (I) ''bottom'' separation capillary, (J) screw and washer attaching capillary onto the servo actuated arm (L) and (K) waste connection point. (M) The channels drilled through to house the separation capillaries. - Reproduced by permission from [76]*

A device machined into a piece of Plexiglas for coupling gel filtration chromatography (GFC) with CE to analyse fluorescently-labelled proteins in serum was introduced by Skinner [76]. As shown in Figure 1-6, this interface consisted of one sample channel and two BGE channels accommodating two separation capillaries which were connected to servo actuated arms. The two capillaries moved back and forth in turns using the servo arms. Depending on the position of the capillaries in the

sample channel, sample was injected into one capillary while the other one was moved back into the stagnant BGE channel to separate the LC eluate (Figure 1-6). Despite improvements in sampling frequency and therefore transfer efficiency, this device was not compatible with LC mobile phases containing organic solvents.

The first microfluidic platform combining both electro- and pressure-driven separations on the same device was introduced by Liu *et al.* to perform IEF-LC followed by fluorescence or MALDI-MS analysis of a protein digest [77]. Shown in Figure 1-7, this device consisted of an individual IEF channel intersected with an array of RPLC microcolumns which were fabricated on a cyclicolefin polymer chip. After conditioning of the RPLC channels, the external microvalve was closed and the selection valve was blocked to seal the inlet of the device in order to vacuum fill the IEF channel with HPMC. The catholyte and anolyte reservoirs were then filled and a separation voltage was applied. Upon completion of the separation, the microvalves were opened and the selection valve was switched to deliver the LC solvent(s) and inject the IEF focused bands in the LC channels for separation. Through the use of a flow splitter, LC elution was performed at an average flow rate of 2.5 µL/min. Fluorescent detection was performed in the region close to the waste reservoirs while these were replaced by needle interfaces to collect fractions for MALDI analysis. Despite being integrated on a single platform as well as a simple interfacing approach, which allowed effective transfer of the ^{1}D focused bands into the ^{2}D, the valving elements in this device were

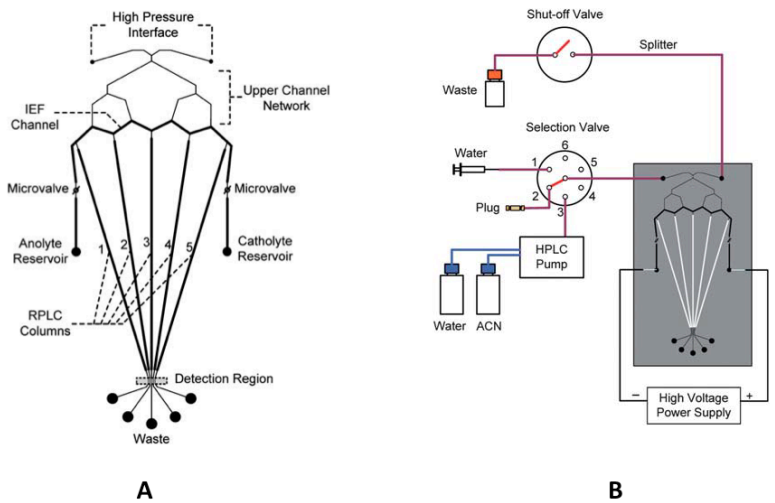

***Figure 1-7**: A: Schematic diagram of the IEF-RPLC chip. B: IEF-RPLC experimental setup. - Reproduced by permission from [89].*

controlled manually and the entire separation was not fully automated.

Full-on-chip-integrated LC×CE was introduced by Chambers *et al.* in 2011 [78]: a glass RPLC×CE-ESI platform which consisted of a previously fabricated CE-ESI microchip [101] incorporated with a LC channel. Tryptic digests of bovine serum albumin, yeast enolase, and *E. coli* cell lysate were analysed using this system (Figure 1-8). Sample injection in ^{1}D was performed using a conventional LC pump and injection valve. The pump flow was, however, split before entering the microchip-LC channel as the device fittings could resist a certain degree of pressure. A sample-trapping region packed with commercial C_{18} particles was integrated on the device which enabled sample preconcentration and clean-up prior to LC separation. A 30 min single ramp gradient elution at a flow rate of 65 nL/min was performed in the ^{1}D. The pressure-driven flow from the LC channel carried the eluate into the intersection at the end of the LC channel where CE injections were performed at a cross intersection in an overlapped gated manner. To enable electrospray at the end of the CE channel, an electroosmotic (EO) pump was integrated on the microchip to create a positive pressure at the intersection in order to pump the eluate towards the electrospray orifice. With the inlet of the mass spectrometer grounded, the voltage at the intersection of CE and EO channels provided the electrospray potential. Similar to Lewis' work, due to the slow sampling rate of the mass spectrometer, CE separation

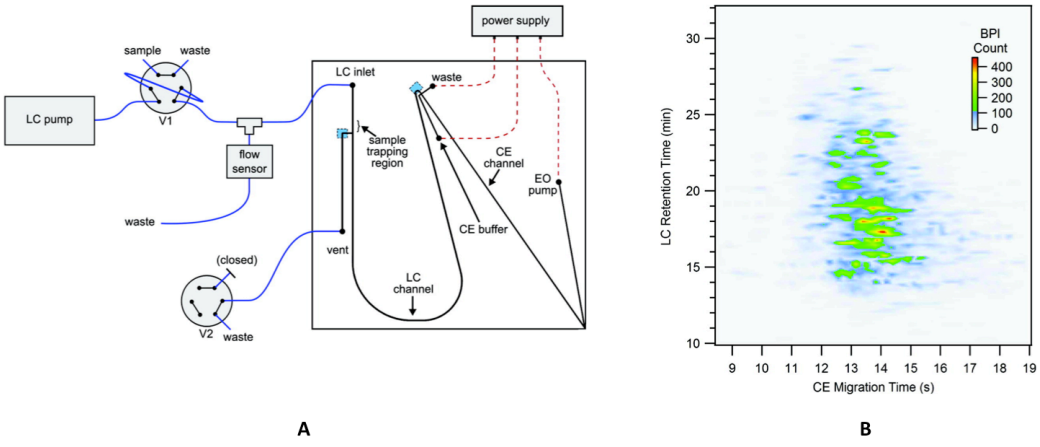

***Figure 1-8**: **A**: Schematic for the microchip-based LC-CE-MS system. The blue squares on the microchip denote the location of the weirs (channel segments etched 6 µm deep) that were used to retain the packed particles. Valve 1 (V1) was used to perform LC injections, and valve 2 (V2) was used to open and close the vent line. Valves are shown in the "sample loading" configuration. Electrospray was performed from the lower right corner of the microchip. **B**: Two-dimensional plot of LC-CE-MS analysis of 800 ng of an E. coli cell lysate tryptic digest. Reprinted with permission from [86].*

efficiency had to be sacrificed by performing longer injections to allow mass spectrometric detection. Even with the longer CE injection times, each ^{1}D peak was only sampled 1.6 times. In a similar work with slight variations (an on-chip flow splitter), the same group demonstrated the characterisation of *N*-linked glycosylation of a monoclonal antibody by glycopeptide mapping using RPLC×CE-ESI consisting of a commercial nanoUPLC system and the CE-ESI microchip [79].

Apart from relying mainly on gated injection technology, which like many other electrodriven injection techniques suffers from electrokinetic bias, the presence of open channels in microfluidic devices makes maintaining the flow rate difficult and necessitates proper sealing of the connections. In addition to the fabrication challenges, a sufficient coating of all the channels within the device is necessary in order to avoid analyte adsorption to the walls.

1.4.4 Droplet-based interfaces

Niu *et al.* developed a droplet based interface for coupling RPLC with CE [80]. In this device, droplet technology was used to segment ^{1}D eluate into nanolitre droplets encapsulated between oil droplets. As in Figure 1-9, which shows a later application of this interface [81], the sample stream from the LC separation met with an oil flow in a tee junction on the PDMS device where aqueous LC droplets were trapped in an oil stream. Using one syringe pump in constant volume mode, the droplets were transferred along a hydrophobic tube downstream towards the PDMS merging chamber where integration of pillar elements and use of another syringe pump in aspiration mode helped to evacuate the oil and load the merged droplets into CE. Depending on the length of tubing used between the two dimensions, the droplet interface offered the possibility of offline or online hyphenation with no sacrifice in ^{1}D resolution as in other interfacing approaches. And there was no need for high speed ^{2}D separation since the droplets were stored. In addition, the closed sample storage approach eliminated the sample loss normally encountered in offline approaches. This work presented a proof-of-principle comprehensive separation of a peptide mixture as well as a heart-cutting separation of yeast cell proteins. In the comprehensive separation with a 100-s capillary LC separation, each ^{1}D peak was sampled three times, 25 droplets with an approximate volume of 10 nL were formed and pushed towards the CE channel before which the pillar elements helped to evacuate the oil and load the merged droplets into the channel. Right after injection, a

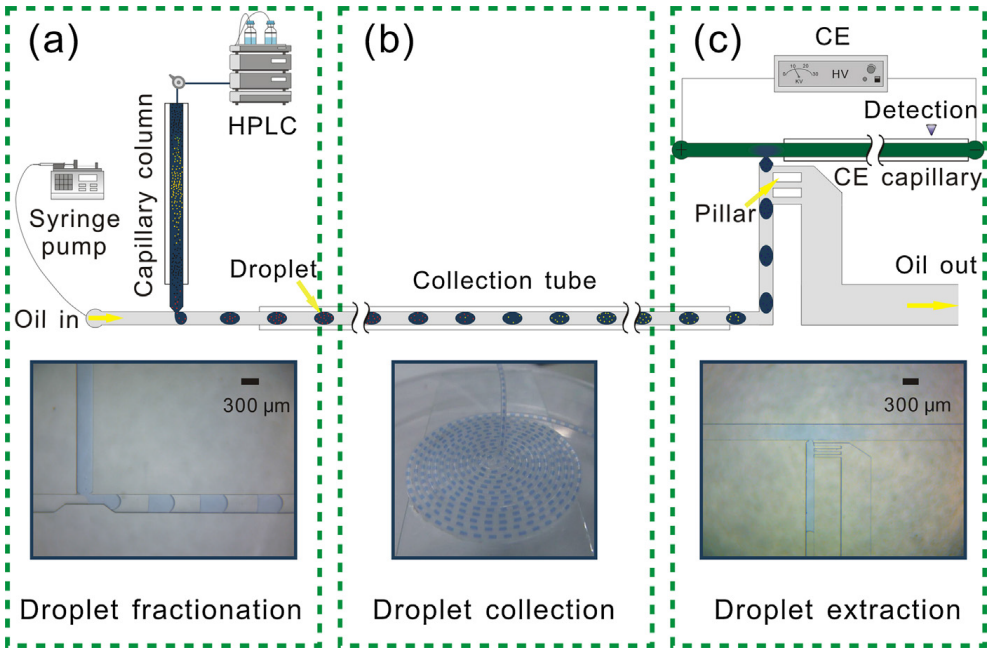

***Figure 1-9**: A droplet-interfaced 2D nanoLC–CE system. HPLC effluent was fractionated into a series of nanoliter droplet units right after chromatography (panel a), and collected and stored in a tube (panel b), before drop-wise analysis in CE (panel c). Photographs for each stage of the workflow are shown at the bottom. Blue ink was used to represent aqueous droplets, which were spaced by an oil phase. Reprinted from [92].*

10 kV separation voltage was applied to a 20 cm × 100 µm fused silica capillary. The same interface was used later for the separation of a human urinary protein digest [81]. A total of 353 droplets were formed in a 28.3-min chromatographic window and then collected and analysed in 25 min CE runs resulting in a total analysis time of 6 days for each sample. However, due to the sealed, low-temperature storage of droplet segments as well as the long-term reproducibility of CE operation and stability of droplet storage, the lengthy analysis time did not result in deterioration of system performance. Complete sample transfer and high spatiotemporal resolution were obtained in this work albeit at the expense of time.

In another work by Zhang and coworkers, droplets were formed and utilised in a totally different approach [82]. A hanging droplet siphoning interface was used to separate proteins/peptides from D_{20} liver cancer tissue by *c*LC×CE-MALDI-TOF-TOF-MS. In this interface, the microdroplet formed at the tip of the *c*LC column was hydrostatically introduced to the ^{2}D with a moving slide bar to which the inlet of the CE capillary was fixed. With the slide bar moving up to the injection position, LC effluent was introduced to CE. The slide bar was then moved down and upon insertion of the capillary into the inlet buffer vial, a separation voltage was applied.

The solution emerging from the CE capillary was then directed onto the MALDI targets for mass spectrometric detection. To improve the ^{1}D sample utilisation and preconcentration of peptides, the LC mobile phase was evaporated by a post column sweep of heated nitrogen.

1.4.5 Membrane-based interface

To couple GFC with CIEF, Tragas and Pawliszyn used a microdialysis hollow fibre [83]. As the salt concentration of the GFC effluent was too high to permit direct introduction of the proteins into IEF, a desalting step was necessary for the coupling of these techniques. The dialysis hollow fibre was inserted in a glass tube and connected to an 8-port injection valve. With the valve in the inject position the ^{1}D effluent entered the dialysis fibre lumen while, through a concurrent flush of carrier ampholyte (CA) in the glass tube using a syringe pump, the fibre content was stripped of the salts and mixed with the CA for IEF separation. This interface was used for heart-cutting separation of two model proteins with a total analysis time of 24 minutes.

In a different approach, a membrane-based interface to couple IC with CE was introduced by Kar and Dasgupta for IC×CE separation of propionate, acetate, nitrate, chlorate and fluoride [102]. In their work, approximately 10% of the suppressed IC eluate was passed through a membrane saturated with CE background electrolyte and injected into the second dimension *via* electromigration and electroosmotic flow.

1.4.6 Couplings involving planar techniques

As mentioned earlier, the first 2D chromatography × electrophoresis separations were performed in a discontinuous manner and required a long time to complete. To enable faster analysis as well as improved separation efficiency, simultaneous chromatography and electrophoresis (SCE), also known as *chromatophoresis*, was introduced [84, 103, 104]. Not to be confused with planar electrochromatography, in SCE the electric field is orthogonal, rather than parallel, to the direction of analyte migration. As a result, this technique can be classified as two-dimensional. One of the early apparatus specifically designed for performing chromatophoresis was presented by van Ooji in 1973 [84]. Using a polymethylmethacrylate device incorporating eight electrolyte reservoirs and two graphite electrode blocks, mixtures of the aquochloro complexes of trivalent iridium were separated on a glass or plastic sheet coated with

cellulose layer placed underneath the PMMA block as the solvent penetrated the thin layer material while voltage was applied in the right angle through the electrodes. In a more recent work, a dual reservoir device was introduced by Stevenson *et al.* to perform SCE of vitamins, amino acids, and dyes [85]. In this set-up a small glass vessel containing the cathode was placed inside a larger glass vessel accommodating the anode, both vessels contained the same separation solvent in order to maximise the current flow through the chromatographic plate rather than in the vicinity of the electrodes. The chromatographic plate was placed inside the large vessel to enable vertical capillary action while the current flew horizontally.

A great advantage of SCE is that separation happens concurrently rather than sequentially in both dimensions, hence common limitations such as the need for substantially fast ^{2}D separation or undersampling of the ^{1}D eluent are eliminated. In addition, it is possible to load multiple samples along the thin layer. However, it is challenging to find a solvent that is suitable to function as both background electrolyte and mobile phase. Furthermore, the shortcomings of PEC mentioned earlier in the offline section apply to this technique as well. As a result, Dzido's group introduced orthogonal pressurised planar electrochromatography (OPPEC), which combines overpressured layer chromatography (OPLC) and pressurised planar electrochromatography (PPEC) simultaneously [86, 105, 106]. In this technique, which is capable of performing both analytical and micropreparative separations, PPEC is performed along with a flow of separation buffer pumped through the thin layer at a right angle to the applied electric field.

Geiger *et al.* reported online *n*LC × *μ*FFE [20]. *μ*FFE was used to solve the commonly-faced problem of ^{1}D undersampling which usually arises from an insufficiently fast ^{2}D separation. The pressure-driven LC band was introduced to the planar *μ*FFE device, where an electric field was applied at 90 degrees to the liquid flow to separate the components by their electrophoretic mobilities. A photolithographically-fabricated *μ*FFE device with a capillary inserted through the side into the sample channel etched in the device served as the interface with minimised dead volume (*side-on* interface as the authors termed it) and was connected online with a commercial *n*LC instrument (Figure 1-10). Images of the *μ*FFE separation were recorded every 500 ms using a CCD for fluorescence detection. Due to the continuous nature of the FFE, the ^{1}D effluent was fully utilised and practical peak capacity was calculated to be 776 for a 10 min separation window within a 25

min LC separation of labelled BSA tryptic digest. The same group later employed this set-up to study the effect of surface adsorption on band broadening in μFFE [107] as well as to discuss sample dimensionality and to demonstrate dependence of *n*LC × μFFE peak capacity on the choice of fluorescent label used for tagging the analytes [108]. Despite its simplicity, no need for special interfacing or modulation technologies, and high utilisation of the ^{1}D separation, this method mainly relies on highly sensitive LIF detection and has limitations when it comes to application of alternative detection techniques such as mass spectrometry.

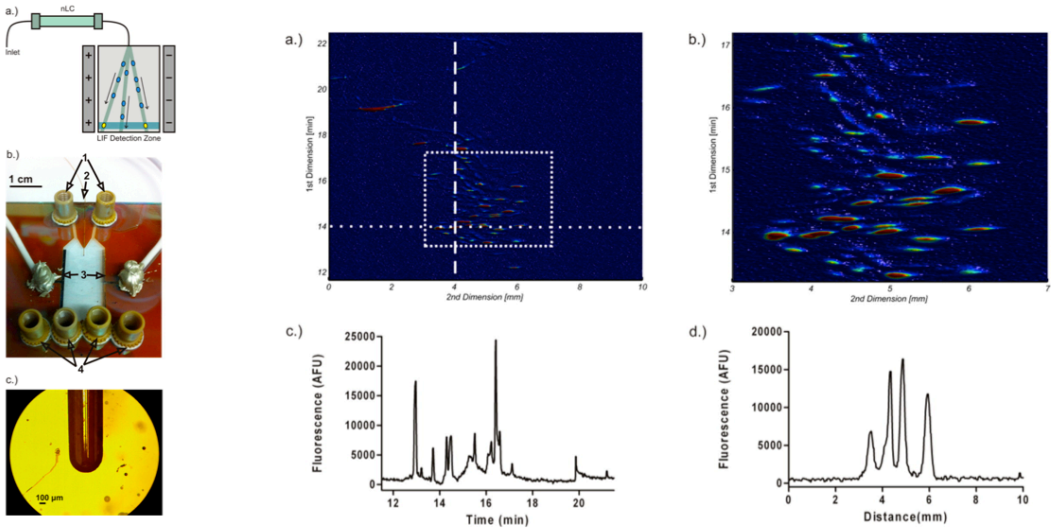

***Figure 1-10**: **A**: (a) Schematic of the nLC × µFFE system. (b) Image of the µFFE device. (1) buffer inlets, (2) sample inlet capillary, (3) electrodes, and (4) buffer outlets. (c) Image of the interface. The sample inlet capillary enters from the top of the image and is fixed in a 250 µm channel that extends from the edge of the µFFE device into the separation channel. **B**: 2D nLC × µFFE separation of the Chromeo P503 labeled BSA tryptic digest. (a) Top view and (b) expanded view of region enclosed in the dotted box in a). (c) Extracted chromatogram from the 1D measured at 4 mm on the µFFE device (shown as the vertical dashed line in a). (d) Line scan across the 2D dimension taken at 14.0 min in the 1D (shown as the horizontal dotted line in a). Reprinted with permission from [20].*

1.4.7 Other interfacing approaches

Ehala *et al.* transferred ^{1}D eluate from IC or RPLC to CE via a pneumatic sampler described as *stroboscopic* [19], referring to the repetitive injection of the sample into the ^{1}D followed by ^{2}D sampling at increasing time intervals for each ^{1}D injection. The LC effluent exiting the detector was forced through a sample line which consisted of two membranes. In the absence of pressure the effluent was directed to waste. By application of a pressure pulse to these membranes, a small volume of the effluent was introduced to CE capillary both hydrodynamically and electrokinetically. As a result of the repeated analysis of ^{1}D effluent at different intervals, the need for a rapid separation in the ^{2}D to ensure sufficient sampling was eliminated. However, the fact that replicated analysis needed to be performed imposes a limitation on the speed of the ^{1}D separation. In addition, due to repeated analysis which requires large sample size this method is not applicable to small-quantity samples. This interface was used to showcase the separation of organic acids and phenolic compounds.

In another report based on previously introduced capillary batch injection [109], IC was coupled with CE-MS/MS to separate a model mixture of six nucleotides [87]. In this work, instead of interrupting the ^{1}D effluent through a valve-based or gating interface, eluate from a *c*IC was introduced to CE separation capillary using a movable injection capillary, which also served as the transfer line connecting the two dimensions.

1.5 Conclusions

Although initially targeted to replace the 2D-gel approaches, column-based multidimensional electrophoretic and chromatographic separations have been shown to be powerful complementary techniques to 2D-GE for the analysis of lower molecular mass molecules in addition to proteins and peptides. Throughout all these years, there have been a considerable number of publications on chromatographic-electromigration and electromigration-chromatographic multidimensional liquid-phase separations. Along with instrumentation advances in liquid-chromatographic, electrophoretic and detection techniques, such as the emergence of narrower ID separation columns, nanolitre-flow rate instrumentation, higher field electromigration separations, on-chip technologies, etc., the interfacing technology has also improved. However, the accommodation of small injection volumes and the need for efficient

sampling by the second dimension which necessitates large splitting ratio, similar to the rest of 2D liquid-phase separations, has placed a great burden on detection [95]. While this limitation has been noticed, and to an extent addressed especially in offline approaches, no ultimate solution has been introduced and there is still a need for the development of modulation approaches which incorporate preconcentration/focusing methods to improve transfer of analyte from the first to the second dimension; as increasing the sample size alone without applying a focusing step would result in broader ^{2}D peaks and therefore reduced peak capacity.

Another often neglected areas hidden under the shadow of the progress in separation technologies are method development and optimisation of 2D separations as well as data processing and the construction of 2D plots, which despite the advances in computer science and data processing compared to the early days, are yet to be fully addressed.

1.6 References

[1] J.C. Giddings, Two-dimensional separations: concept and promise, Anal. Chem., 56 (1984) 1258A-1270A.

[2] G. Haugaard, T.D. Kroner, Partition Chromatography of Amino Acids with Applied Voltage, JACS, 70 (1948) 2135-2137.

[3] R. Consden, A.H. Gordon, A.J. Martin, Qualitative analysis of proteins: a partition chromatographic method using paper, Biochem. J., 38 (1944) 224-220.

[4] M.M. Bushey, J.W. Jorgenson, Automated instrumentation for comprehensive two-dimensional high-performance liquid chromatography of proteins, Anal. Chem., 62 (1990) 161-167.

[5] P.J. Marriott, Z. Wu, P. Schoenmakers, Nomenclature and Conventions in Comprehensive Multidimensional Chromatography – An Update, LCGC Europe, 25 (2012).

[6] R.E. Murphy, M.R. Schure, J.P. Foley, Effect of Sampling Rate on Resolution in Comprehensive Two-Dimensional Liquid Chromatography, Anal. Chem., 70 (1998) 1585-1594.

[7] J.V. Seeley, Theoretical study of incomplete sampling of the first dimension in comprehensive two-dimensional chromatography, J. Chromatogr. A, 962 (2002) 21-27.

[8] W. Khummueng, J. Harynuk, P.J. Marriott, Modulation Ratio in Comprehensive Two-dimensional Gas Chromatography, Anal. Chem., 78 (2006) 4578-4587.

[9] K. Horie, H. Kimura, T. Ikegami, A. Iwatsuka, N. Saad, O. Fiehn, N. Tanaka, Calculating Optimal Modulation Periods to Maximize the Peak Capacity in Two-Dimensional HPLC, Anal. Chem., 79 (2007) 3764-3770.

[10] P.H. O'Farrell, High resolution two-dimensional electrophoresis of proteins, J. Biol. Chem., 250 (1975) 4007-4021.

[11] J.L. López, Two-dimensional electrophoresis in proteome expression analysis, J. Chromatogr. B, 849 (2007) 190-202.

[12] G. Guiochon, M.F. Gonnord, M. Zakaria, L.A. Beaver, A.M. Siouffi, Chromatography with a two-dimensional column, Chromatographia, 17 (1983) 121-124.

[13] C. Evans, J. Jorgenson, Multidimensional LC-LC and LC-CE for high-resolution separations of biological molecules, Anal. Bioanal. Chem., 378 (2004) 1952-1961.

[14] T. Stroink, M.C. Ortiz, A. Bult, H. Lingeman, G.J. de Jong, W.J.M. Underberg, On-line multidimensional liquid chromatography and capillary electrophoresis systems for peptides and proteins, J. Chromatogr. B, 817 (2005) 49-66.

[15] R. Tomáš, K. Klepárník, F. Foret, Multidimensional liquid phase separations for mass spectrometry, J. Sep. Sci., 31 (2008) 1964-1979.

[16] F.J. Kohl, L. Sánchez-Hernández, C. Neusüß, Capillary electrophoresis in two-dimensional separation systems: Techniques and applications, Electrophoresis, 36 (2015) 144-158.

[17] W. Grochocki, M.J. Markuszewski, J.P. Quirino, Multidimensional capillary electrophoresis, Electrophoresis, 36 (2015) 135-143.

[18] P.A. Kler, D. Sydes, C. Huhn, Column–coupling strategies for multidimensional electrophoretic separation techniques, Anal. Bioanal. Chem., 407 (2015) 119-138.

[19] S. Ehala, M. Kaljurand, M. Kudrjashova, M. Vaher, Stroboscopic sampling in comprehensive high-performance liquid chromatography-capillary electrophoresis via a pneumatic sampler, Electrophoresis, 25 (2004) 980-989.

[20] M. Geiger, N.W. Frost, M.T. Bowser, Comprehensive Multidimensional Separations of Peptides Using Nano-Liquid Chromatography Coupled with Micro Free Flow Electrophoresis, Anal. Chem., 86 (2014) 5136-5142.

[21] A.W. Moore Jr, J.W. Jorgenson, Comprehensive three-dimensional separation of peptides using size exclusion chromatography/ reversed phase liquid chromatography/optically gated capillary zone electrophoresis, Anal. Chem., 67 (1995) 3456-3463.

[22] M.R. Schure, S.A. Cohen, Introduction, in: Multidimensional Liquid Chromatography, John Wiley & Sons, Inc., 2008.

[23] W.C. Peter, M.D. Joe, C.R. Sarah, R.S. Dwight, Principles of Online Comprehensive Multidimensional Liquid Chromatography, in: Advances in Chromatography, Volume 50, CRC Press, 2012, pp. 139-235.

[24] D.R. Stoll, X. Li, X. Wang, P.W. Carr, S.E.G. Porter, S.C. Rutan, Fast, comprehensive two-dimensional liquid chromatography, J. Chromatogr. A, 1168 (2007) 3-43.

[25] H.J. Issaq, K.C. Chan, G.M. Janini, G.M. Muschik, A simple two-dimensional high performance liquid chromatography/high performance capillary electrophoresis set-up for the separation of complex mixtures, Electrophoresis, 20 (1999) 1533-1537.

[26] H.J. Issaq, K.C. Chan, C. Liu, Q. Li, Multidimensional high performance liquid chromatography – capillary electrophoresis separation of a protein digest: An update, Electrophoresis, 22 (2001) 1133-1135.

[27] Y. He, E.S. Yeung, K.C. Chan, H.J. Issaq, Two dimensional mapping of cancer cell extracts by liquid chromatography–capillary electrophoresis with ultraviolet absorbance detection, J. Chromatogr. A, 979 (2002) 81-89.

[28] J. Liu, H. Zhao, K.J. Volk, S.E. Klohr, E.H. Kerns, M.S. Lee, Analysis of monoclonal antibody and immunoconjugate digests by capillary electrophoresis and capillary liquid chromatography, J. Chromatogr. A, 735 (1996) 357-366.

[29] H.J. Issaq, K.C. Chan, G.M. Janini, G.M. Muschik, MULTIDIMENSIONAL MULTIMODAL INSTRUMENTAL SEPARATION OF COMPLEX MIXTURES, J. Liq. Chromatogr. Rel. Technol., 23 (2000) 145-154.

[30] G.M. Janini, K.C. Chan, T.P. Conrads, H.J. Issaq, T.D. Veenstra, Two-dimensional liquid chromatography-capillary zone electrophoresis-sheathless electrospray ionization-mass spectrometry: Evaluation for peptide analysis and protein identification, Electrophoresis, 25 (2004) 1973-1980.

[31] S. Udiavar, A. Apffel, J. Chakel, S. Swedberg, W.S. Hancock, E. Pungor, The Use of Multidimensional Liquid-Phase Separations and Mass Spectrometry for the Detailed Characterization of Posttranslational Modifications in Glycoproteins, Anal. Chem., 70 (1998) 3572-3578.

[32] L. Jia, B.-F. Liu, S. Terabe, T. Nishioka, Two-Dimensional Separation Method for Analysis of Bacillus subtilis Metabolites via Hyphenation of Micro-Liquid Chromatography and Capillary Electrophoresis, Anal. Chem., 76 (2004) 1419-1428.

[33] L. Jia, N. Tanaka, S. Terabe, Two-dimensional separation system of coupling capillary liquid chromatography to capillary electrophoresis for analysis of Escherichia coli metabolites, Electrophoresis, 26 (2005) 3468-3478.

[34] K. Faserl, L. Kremser, M. Müller, D. Teis, H.H. Lindner, Quantitative Proteomics Using Ultralow Flow Capillary Electrophoresis–Mass Spectrometry, Anal. Chem., 87 (2015) 4633-4640.

[35] M.A. Strausbauch, B.J. Madden, P.J. Wettstein, J.P. Landers, Sensitivity enhancement and second-dimensional information from solid phase extraction-capillary electrophoresis of entire high-performance liquid chromatography fractions, Electrophoresis, 16 (1995) 541-548.

[36] Y. Mao, X. Zhang, Comprehensive two-dimensional separation system by coupling capillary reverse-phase liquid chromatography to capillary isoelectric focusing for peptide and protein mapping with laser-induced fluorescence detection, Electrophoresis, 24 (2003) 3289-3295.

[37] P. Česla, J. Fischer, P. Jandera, Separation of phenolic acids and flavone natural antioxidants by two-dimensional method combining liquid chromatography and micellar electrokinetic capillary chromatography, Electrophoresis, 31 (2010) 2200-2210.

[38] P. Česla, J. Fischer, P. Jandera, Improvement of the sensitivity of 2D LC-MEKC separation of phenolic acids and flavonoids natural antioxidants using the on-line preconcentration step, Electrophoresis, 33 (2012) 2464-2473.

[39] D.B. Wall, M.T. Kachman, S. Gong, R. Hinderer, S. Parus, D.E. Misek, S.M. Hanash, D.M. Lubman, Isoelectric Focusing Nonporous RP HPLC: A Two-Dimensional Liquid-Phase Separation Method for Mapping of Cellular Proteins with Identification Using MALDI-TOF Mass Spectrometry, Anal. Chem., 72 (2000) 1099-1111.

[40] M. Guijarro-Díez, M.C. García, A.L. Crego, M.L. Marina, Off-line two dimensional isoelectrofocusing-liquid chromatography/mass spectrometry (time of flight) for the determination of the bioactive peptide lunasin, J. Chromatogr. A, 1371 (2014) 117-124.

[41] A. Schäfer, C. von Toerne, S. Becker, H. Sarioglu, S. Neschen, M. Kahle, S.M. Hauck, M. Ueffing, Two-Dimensional Peptide Separation Improving Sensitivity of Selected Reaction Monitoring-Based Quantitative Proteomics in Mouse Liver Tissue: Comparing Off-Gel Electrophoresis and Strong Cation Exchange Chromatography, Anal. Chem., 84 (2012) 8853-8862.

[42] M.T. Kachman, H. Wang, D.R. Schwartz, K.R. Cho, D.M. Lubman, A 2-D Liquid Separations/Mass Mapping Method for Interlysate Comparison of Ovarian Cancers, Anal. Chem., 74 (2002) 1779-1791.

[43] M. Pirmoradian, B. Zhang, K. Chingin, J. Astorga-Wells, R.A. Zubarev, Membrane-Assisted Isoelectric Focusing Device As a Micropreparative Fractionator for Two-Dimensional Shotgun Proteomics, Anal. Chem., 86 (2014) 5728-5732.

[44] P. Álvarez Porebski, F. Lynen, Combining liquid chromatography with multiplexed capillary gel electrophoresis for offline comprehensive analysis of complex oligonucleotide samples, J. Chromatogr. A, 1336 (2014) 87-93.

[45] S. Mounicou, S. McSheehy, J. Szpunar, M. Potin-Gautier, R. Lobinski, Analysis of selenized yeast for selenium speciation by size-exclusion chromatography and capillary zone electrophoresis with inductively coupled plasma mass spectrometric detection (SEC-CZE-ICP-MS), J. Anal. At. Spectrom., 17 (2002) 15-20.

[46] Y. Wu, Y. Wang, X. Gu, L. Zhang, C. Yan, Two-dimensional strong cation-exchange liquid chromatography/reversed-phase pressurized capillary electrochromatography for separation of complex samples, J. Sep. Sci., 34 (2011) 1027-1034.

[47] J.M. Hempe, A.M. McGehee, S.A. Chalew, Two-dimensional analysis of glycated hemoglobin heterogeneity in pediatric type 1 diabetes patients, Anal. Biochem., 442 (2013) 205-212.

[48] P. van der Geer, T. Hunter, Phosphopeptide mapping and phosphoamino acid analysis by electrophoresis and chromatography on thin-layer cellulose plates, Electrophoresis, 15 (1994) 544-554.

[49] V. Panchagnula, A. Mikulskis, L. Song, Y. Wang, M. Wang, T. Knubovets, E. Scrivener, E. Golenko, I.S. Krull, M. Schulz, H. Heinz Emil, W.F. Patton, Phosphopeptide analysis by directly coupling two-dimensional planar electrochromatography/thin-layer chromatography with matrix-assisted laser desorption/ionization time-of-flight mass spectrometry, J. Chromatogr. A, 1155 (2007) 112-123.

[50] A. Chomicki, P. Ślązak, T.H. Dzido, Preliminary results for 2-D separation with high-performance thin-layer chromatography and pressurized planar electrochromatography, Electrophoresis, 30 (2009) 3718-3725.

[51] T.E. Newsome, S.V. Olesik, Planar Electrochromatography Using an Electrospun Polymer Nanofiber Layer, Anal. Chem., 86 (2014) 10961-10969.

[52] G.L. DeVault, M.J. Sepaniak, Two-dimensional capillary electrophoresis-thin layer chromatography separations of amino acid enantiomers using electro-filament transfer, J. Micro. Sep., 12 (2000) 419-428.

[53] Y. Mao, Y. Li, X. Zhang, Array based capillary IEF with a whole column image of laser-induced fluorescence in coupling to capillary RPLC as a comprehensive 2-D separation system for proteome analysis, Proteomics, 6 (2006) 420-426.

[54] W. Yu, Y. Li, C. Deng, X. Zhang, Comprehensive two-dimensional separation in coupling of reversed-phase chromatography with capillary isoelectric focusing followed by MALDI-MS identification using on-target digestion for intact protein analysis, Electrophoresis, 27 (2006) 2100-2110.

[55] R.L. Moritz, H. Ji, F. Schütz, L.M. Connolly, E.A. Kapp, T.P. Speed, R.J. Simpson, A Proteome Strategy for Fractionating Proteins and Peptides Using Continuous Free-Flow Electrophoresis Coupled Off-Line to Reversed-Phase High-Performance Liquid Chromatography, Anal. Chem., 76 (2004) 4811-4824.

[56] M.M. Bushey, J.W. Jorgenson, Automated instrumentation for comprehensive two-dimensional high-performance liquid chromatography/capillary zone electrophoresis, Anal. Chem., 62 (1990) 978-984.

[57] A.V. Lemmo, J.W. Jorgenson, Two-dimensional protein separation by microcolumn size-exclusion chromatography-capillary zone electrophoresis, J. Chromatogr. A, 633 (1993) 213-220.

[58] J.P. Larmann, A.V. Lemmo, A.W. Moore, J.W. Jorgenson, Two-dimensional separations of peptides and proteins by comprehensive liquid chromatography-capillary electrophoresis, Electrophoresis, 14 (1993) 439-447.

[59] L. Ranjbar, A.J. Gaudry, M.C. Breadmore, R.A. Shellie, Online comprehensive two-dimensional ion chromatography × capillary electrophoresis, Anal. Chem., 87 (2015) 8673–8678.

[60] J. Chen, B.M. Balgley, D.L. DeVoe, C.S. Lee, Capillary Isoelectric Focusing-Based Multidimensional Concentration/Separation Platform for Proteome Analysis, Anal. Chem., 75 (2003) 3145-3152.

[61] Y. Wang, P.A. Rudnick, E.L. Evans, J. Li, Z. Zhuang, D.L. DeVoe, C.S. Lee, B.M. Balgley, Proteome Analysis of Microdissected Tumor Tissue Using a Capillary Isoelectric Focusing-Based Multidimensional Separation Platform Coupled with ESI-Tandem MS, Anal. Chem., 77 (2005) 6549-6556.

[62] F. Zhou, T.E. Hanson, M.V. Johnston, Intact Protein Profiling of Chlorobium tepidum by Capillary Isoelectric Focusing, Reversed-Phase Liquid Chromatography, and Mass Spectrometry, Anal. Chem., 79 (2007) 7145-7153.

[63] F. Zhou, M.V. Johnston, Protein Characterization by On-Line Capillary Isoelectric Focusing, Reversed-Phase Liquid Chromatography, and Mass Spectrometry, Anal. Chem., 76 (2004) 2734-2740.

[64] F. Zhou, M.V. Johnston, Protein profiling by capillary isoelectric focusing, reversed-phase liquid chromatography, and mass spectrometry, Electrophoresis, 26 (2005) 1383-1388.

[65] T. Wang, J. Ma, S. Wu, H. Yuan, L. Zhang, Z. Liang, Y. Zhang, Integrated platform of capillary isoelectric focusing, trypsin immobilized enzyme microreactor and nanoreversed-phase liquid chromatography with mass spectrometry for online protein profiling, Electrophoresis, 32 (2011) 2848-2856.

[66] M. Zhang, Z. El Rassi, Two-Dimensional Microcolumn Separation Platform for Proteomics Consisting of On-Line Coupled Capillary Isoelectric Focusing and Capillary Electrochromatography. 1. Evaluation of the Capillary-Based Two-Dimensional Platform with Proteins, Peptides, and Human Serum, Journal of Proteome Research, 5 (2006) 2001-2008.

[67] A.W. Moore, J.W. Jorgenson, Rapid comprehensive two-dimensional separations of peptides via RPLC-optically gated capillary zone electrophoresis, Anal. Chem., 67 (1995) 3448-3455.

[68] A.V. Lemmo, J.W. Jorgenson, Transverse flow gating interface for the coupling of microcolumn LC with CZE in a comprehensive two-dimensional system, Anal. Chem., 65 (1993) 1576-1581.

[69] T.F. Hooker, J.W. Jorgenson, A Transparent Flow Gating Interface for the Coupling of Microcolumn LC with CZE in a Comprehensive Two-Dimensional System, Anal. Chem., 69 (1997) 4134-4142.

[70] I. German, R.T. Kennedy, Reversed-Phase Capillary Liquid Chromatography Coupled On-Line to Capillary Electrophoresis Immunoassays, Anal. Chem., 72 (2000) 5365-5372.

[71] P. Yang, R.T. Kennedy, High performance liquid chromatography coupled on-line to capillary electrophoresis with laser-induced fluorescence detection for detecting inhibitors of Src homology 2 domain–phosphopeptide binding in mixtures, J. Chromatogr. A, 1194 (2008) 225-230.

[72] K.C. Lewis, G.J. Opiteck, J.W. Jorgenson, D.M. Sheeley, Comprehensive on-line RPLC-CZE-MS of peptides, J. Am. Soc. Mass. Spectrom., 8 (1997) 495-500.

[73] S.K. Bergström, J. Samskog, K.E. Markides, Development of a Poly(dimethylsiloxane) Interface for On-Line Capillary Column Liquid Chromatography−Capillary Electrophoresis Coupled to Sheathless Electrospray Ionization Time-of-Flight Mass Spectrometry, Anal. Chem., 75 (2003) 5461-5467.

[74] S.K. Bergstrom, A.P. Dahlin, M. Ramstrom, M. Andersson, K.E. Markides, J. Bergquist, A simplified multidimensional approach for analysis of complex biological samples: on-line LC-CE-MS, Analyst, 131 (2006) 791-798.

[75] X. Yang, X. Zhang, A. Li, S. Zhu, Y. Huang, Comprehensive two-dimensional separations based on capillary high-performance liquid chromatography and microchip electrophoresis, Electrophoresis, 24 (2003) 1451-1457.

[76] C.D. Skinner, A liquid chromatography to capillary array electrophoresis interface for two-dimensional separations, Analyst, 135 (2010) 358-367.

[77] J. Liu, C.-F. Chen, S. Yang, C.-C. Chang, D.L. DeVoe, Mixed-mode electrokinetic and chromatographic peptide separations in a microvalve-integrated polymer chip, Lab on a Chip, 10 (2010) 2122-2129.

[78] A.G. Chambers, J.S. Mellors, W.H. Henley, J.M. Ramsey, Monolithic Integration of Two-Dimensional Liquid Chromatography−Capillary Electrophoresis and Electrospray Ionization on a Microfluidic Device, Anal. Chem., 83 (2011) 842-849.

[79] J.S. Mellors, W.A. Black, A.G. Chambers, J.A. Starkey, N.A. Lacher, J.M. Ramsey, Hybrid Capillary/Microfluidic System for Comprehensive Online Liquid Chromatography-Capillary Electrophoresis-Electrospray Ionization-Mass Spectrometry, Anal. Chem., 85 (2013) 4100-4106.

[80] X.Z. Niu, B. Zhang, R.T. Marszalek, O. Ces, J.B. Edel, D.R. Klug, A.J. deMello, Droplet-based compartmentalization of chemically separated components in two-dimensional separations, Chem. Commun., (2009) 6159-6161.

[81] L. Ye, X. Wang, J. Han, F. Gao, L. Xu, Z. Xiao, P. Bai, Q. Wang, B. Zhang, Two dimensional separations of human urinary protein digest using a droplet-interfaced platform, Anal. Chim. Acta, 863 (2015) 86-94.

[82] J. Zhang, H. Hu, M. Gao, P. Yang, X. Zhang, Comprehensive two-dimensional chromatography and capillary electrophoresis coupled with tandem time-of-flight mass spectrometry for high-speed proteome analysis, Electrophoresis, 25 (2004) 2374-2383.

[83] C. Tragas, J. Pawliszyn, On-line coupling of high performance gel filtration chromatography with imaged capillary isoelectric focusing using a membrane interface, Electrophoresis, 21 (2000) 227-237.

[84] W.J. van Ooij, A simple apparatus for simultaneous chromatography and electrophoresis on thin layers, J. Chromatogr. A, 81 (1973) 190-193.

[85] P. Stevenson, B. Dunlap, P. Powell, B. Petersen, C. Hatch, H. Chan, G. Still, M. Fulton, J. McKell, D. Collins, Simultaneous chromatography and electrophoresis: two-dimensional planar separations, Anal. Bioanal. Chem., 405 (2013) 3085-3089.

[86] T.H. Dzido, E. Łopaciuk, P.W. Płocharz, A. Chomicki, M. Zembrzycka, H. Frank, Equipment and preliminary results for orthogonal pressurized planar electrochromatography, J. Chromatogr. A, 1334 (2014) 149-155.

[87] A. Beutner, S. Kochmann, J.J.P. Mark, F.-M. Matysik, Two-dimensional separation of ionic species by hyphenation of capillary ion chromatography x capillary electrophoresis - mass spectrometry, Anal. Chem., 87 (2015) 3134-3138.

[88] M.M. Robson, K.D. Bartle, P. Myers, Simple interface for gradient elution CEC and coupled HPLC-CEC, Chromatographia, 50 (1999) 711-715.

[89] T. Stroink, G. Wiese, J. Teeuwsen, H. Lingeman, J.C.M. Waterval, A. Bult, G.J. de Jong, W.J.M. Underberg, On-line coupling of size exclusion and capillary zone electrophoresis via a reversed-phase C18 trapping column for the analysis of structurally related enkephalins in cerebrospinal fluid, Electrophoresis, 24 (2003) 897-903.

[90] F.W.A. Tempels, G. Wiese, W.J.M. Underberg, G.W. Somsen, G.J. de Jong, On-line coupling of size exclusion chromatography and capillary electrophoresis via solid-phase extraction and a Tee-split interface, J. Chromatogr. B, 839 (2006) 30-35.

[91] R.G. Nielsen, R.M. Riggin, E.C. Rickard, Capillary zone electrophoresis of peptide fragments from trypsin digestion of biosynthetic human growth hormone, J. Chromatogr. A, 480 (1989) 393-401.

[92] P.S.L. Janssen, J.W. Van Nispen, M.J.M. Van Zeeland, P.A.T.A. Melgers, Complementary information from isotachophoresis and high-performance liquid chromatography in peptide analysis, J. Chromatogr. A, 470 (1989) 171-183.

[93] K. Hayakawa, M. Hirano, J. Oizumi, M. Hosoya, Isoelectric focusing of biotinidase and lipoamidase with the addition of non-ionic detergent, Anal. Chim. Acta, 372 (1998) 281-289.

[94] I. Moraleja, E. Moreno-Gordaliza, M.L. Mena, M.M. Gómez-Gómez, Combining TBP-based rOFFGEL-IEF with FASP and nLC–ESI-LTQ-MS/MS for the analysis of cisplatin-binding proteins in rat kidney, Talanta, 120 (2014) 433-442.

[95] M.R. Schure, Limit of Detection, Dilution Factors, and Technique Compatibility in Multidimensional Separations Utilizing Chromatography, Capillary Electrophoresis, and Field-Flow Fractionation, Anal. Chem., 71 (1999) 1645-1657.

[96] W. Wang, T. Guo, P.A. Rudnick, T. Song, J. Li, Z. Zhuang, W. Zheng, D.L. DeVoe, C.S. Lee, B.M. Balgley, Membrane Proteome Analysis of Microdissected Ovarian Tumor Tissues Using Capillary Isoelectric Focusing/Reversed-Phase Liquid Chromatography−Tandem MS, Anal. Chem., 79 (2007) 1002-1009.

[97] C.A. Monnig, J.W. Jorgenson, On-column sample gating for high-speed capillary zone electrophoresis, Anal. Chem., 63 (1991) 802-807.

[98] D.J. Harrison, A. Manz, Z. Fan, H. Luedi, H.M. Widmer, Capillary electrophoresis and sample injection systems integrated on a planar glass chip, Anal. Chem., 64 (1992) 1926-1932.

[99] D.J. Harrison, K. Fluri, K. Seiler, Z. Fan, C.S. Effenhauser, A. Manz, Micromachining a Miniaturized Capillary Electrophoresis-Based Chemical Analysis System on a Chip, Science, 261 (1993) 895-897.

[100] H. Becker, K. Lowack, A. Manz, Planar quartz chips with submicron channels for two-dimensional capillary electrophoresis applications, Journal of Micromechanics and Microengineering, 8 (1998) 24.

[101] J.S. Mellors, K. Jorabchi, L.M. Smith, J.M. Ramsey, Integrated Microfluidic Device for Automated Single Cell Analysis Using Electrophoretic Separation and Electrospray Ionization Mass Spectrometry, Anal. Chem., 82 (2010) 967-973.

[102] S. Kar, P.K. Dasgupta, Direct coupling of ion chromatography with suppressed conductometric capillary electrophoresis, J. Micro. Sep., 8 (1996) 561-568.

[103] H.H. Strain, J.C. Sullivan, Analysis by Electromigration plus Chromatography, Anal. Chem., 23 (1951) 816-823.

[104] D.P. Burma, Electro chromatography on paper, Anal. Chim. Acta, 9 (1953) 518-524.

[105] R. Gajos, E. Łopaciuk, T.H. Dzido, Influence of some operation variables on continuous separation process of orthogonal pressurized planar electrochromatography, J. Chromatogr. A, 1396 (2015) 131-139.

[106] R. Gajos, E. Łopaciuk, T.H. Dzido, Application of orthogonal pressurized planar electrochromatography to micropreparative separation of test dye mixture — Preliminary results, JPC - Journal of Planar Chromatography - Modern TLC, 29 (2016) 77-81.

[107] M. Geiger, R. Harstad, M.T. Bowser, Effect of Surface Adsorption on Temporal and Spatial Broadening in Micro Free Flow Electrophoresis, Anal. Chem., 87 (2015) 11682-11690.

[108] M. Geiger, M.T. Bowser, Effect of Fluorescent Labels on Peptide and Amino Acid Sample Dimensionality in Two Dimensional nLC × μFFE Separations, Anal. Chem., 88 (2016) 2177-2187.

[109] F.-M. Matysik, Capillary batch injection – A new approach for sample introduction into short-length capillary electrophoresis with electrochemical detection, Electrochem. Commun., 8 (2006) 1011-1015.

Part 1

Instrumentation

2 Online comprehensive two-dimensional ion chromatography × capillary electrophoresis

"Technology has to be invented or adopted."
—Jared Diamond

This chapter has been published as a research article in Anal. Chem., 87 (2015) 8673–8678. It is reproduced here with minor modification of the introduction to remove replication of content with the preceding chapters.

2.1 Overview

A comprehensively coupled online two-dimensional ion chromatography-capillary electrophoresis (IC×CE) system for quantitative analysis of inorganic anions and organic acids in water is introduced. The system employs an in-house built sequential injection-capillary electrophoresis instrument and a non-focusing modulation interface comprising a tee-piece and a six-port two-position injection valve that allows comprehensive sampling of the IC effluent. High field strength (+ 2 kV/cm) enables rapid second dimension separations in which each peak eluted from the first-dimension separation column is analysed at least three times in the second-dimension. The IC×CE approach has been successfully used to resolve a suite of haloacetic acids, dalapon and common inorganic anions. Two-dimensional peak capacity for IC×CE was 498 with a peak production rate of production of 9 peaks/min. Linear calibration curves were obtained for all analytes from 5-225 ng/mL (except dibromoacetic acid (10-225 ng/mL) and tribromoacetic acid (25-225 ng/mL)). The developed approach was used to analyse a spiked tap water sample, with good measured recoveries (69-119%).

2.2 Introduction

Ion chromatography (IC) and CE are the two major techniques utilised in analysis of ionic and ionogenic analytes. Two-dimensional separations using these building blocks are unquestionably superior to the individual techniques due to the genuine orthogonality of separation mechanisms as described in Chapter 1. Suppressed IC uses a highly conducting eluent such as hydroxide, carbonate or sulfonate to elute the analytes from an ion-exchange resin stationary phase. When used with conductivity detection, the eluent is suppressed to a low conductivity medium allowing sensitive detection of analytes. In the case of hydroxide eluent, analytes are left in water, which is a perfect matrix for injection into CE enabling sample concentration techniques such as stacking with minimum matrix effects.

The first report of online coupling of IC with CE was by Kar and Dasgupta for the separation of propionate, acetate, nitrate, chlorate and fluoride [1]. In their work, approximately 10% of the suppressed IC eluate was passed through a membrane saturated with CE background electrolyte and injected into the second dimension *via* electromigration and electroosmotic flow. Although IC-CE analysis was described almost 20 years ago, an equivalent comprehensive coupling (IC×CE) was not described in the literature until recently. While preparing the manuscript for the results presented in this chapter, Beutner and co-workers briefly described an IC×CE-MS approach [2] using a capillary batch injection modulator [3]. In their proposed interface, eluate from a capillary IC separation was introduced to the CE separation capillary using a movable injection capillary, which also served as the transfer line connecting the two dimensions. This set-up was used to separate a model mixture of six nucleotides.

The present chapter describes an IC×CE system based on non-focusing modulation of IC effluent and investigates the suitability of this system for quantitative analysis. A sequential injection-capillary electrophoresis instrument (SI-CE) [4] with capacitively coupled contactless conductivity detection (C^4D) was adapted to sample the first dimension eluate. Previous description of this SI-CE system showed suitability for high sample throughput of 60 samples/h and repeatability of 3.4-12.5% (peak area) using an internal standard for electrokinetic injection of inorganic anions across 240 injections. Later a modified version of the same SI-CE system for simultaneous analysis of anions and cations in environmental and industrial samples

was described [5]. Analysis of 23 inorganic and small organic ions and extended automated analysis of tap water for a period of 48 h was shown. High throughput with repeatability of 1.48-6.81% for corrected peak areas were observed. These performance attributes indicate the SI-CE system is amenable to online comprehensive coupling with a separation step with further optimisation.

Compared to previously described IC-CE approaches which require exclusively-designed instrumentation, interfacing between the two dimensions in the present investigation was accomplished by simply plumbing the IC detector outflow to the six-port two-position injection valve in SI-CE with no further hardware modification needed. Injection into the second dimension occurred by altering the position of the valve and directing the IC eluate to the SI-CE sampling tee interface followed by application of voltage.

2.3 Materials and methods

2.3.1 Chemicals and reagents

Analytical grade chemicals were used for all the experiments. Haloacetic acid standards: monobromoacetic acid (MBAA), dibromoacetic acid (DBAA), tribromoacetic acid (TBAA), monochloroacetic acid (MCAA), dichloroacetic acid (DCAA), trichloroacetic acid (TCAA), bromochloroacetic acid (BCAA) and chlorodibromoacetic acid (CDBAA) were all purchased from Sigma-Aldrich (St. Louis, MO, USA) except bromodichloroacetic acid (BDCAA) which was from Supelco (Bellefonte, PA, USA). Other analytes purchased from Sigma-Aldrich include: sodium phosphate, sodium chlorate, potassium nitrate, sodium bromide and potassium bromate. Dalapon and sodium chloride were obtained from Fluka (Sigma-Aldrich, St. Louis, MO, USA) and sodium nitrite was from Ajax (Sydney, NSW, Australia).

Background electrolyte (BGE) components: nicotinic acid (NA), 4-(2-Hydroxyethyl)piperazine-1-ethanesulfonic acid (HEPES) and poly(vinylpolypyrrolidone) (PVP) were also from Sigma-Aldrich. Reagents used for flushing the capillary included: sodium hydroxide (Sigma-Aldrich), hydrochloric acid and methanol (Merck, Darmstadt, Germany).

Milli-Q water obtained from Millipore water purifier equipped with a 0.2 µm filter (Millipore, Bedford, MA, USA) was used as IC eluent and external water feeding the suppressor and to prepare all solutions.

2.3.2 Instrumentation - ion chromatography

First dimension separations were performed using a Dionex ICS-3000 ion chromatograph equipped with suppressed conductivity detector (Thermo Fisher Scientific, Sunnyvale, CA, USA). Dionex IonPac AS24 (250 mm × 2 mm ID) and AG24 (50 mm × 2 mm ID) were used as analytical and guard column, respectively. All analyses were performed in gradient elution mode, details of which are provided in the figure legends. The column temperature of 15 °C was maintained while the detector compartment temperature was set to 18 °C. Use of sub-ambient separation temperature is due to temperature dependent degradation of MBAA, CDBAA, and TBAA at high eluent pH [6]. Column flow rate was 0.300 mL/min. Injection volume of 1000 µL was used for all the experiments. The injection valve position was altered to load position after complete transfer of the sample (void time was taken as reference) within the initial isocratic conditions to eliminate the large sample loop volume contributing to dwell volume.

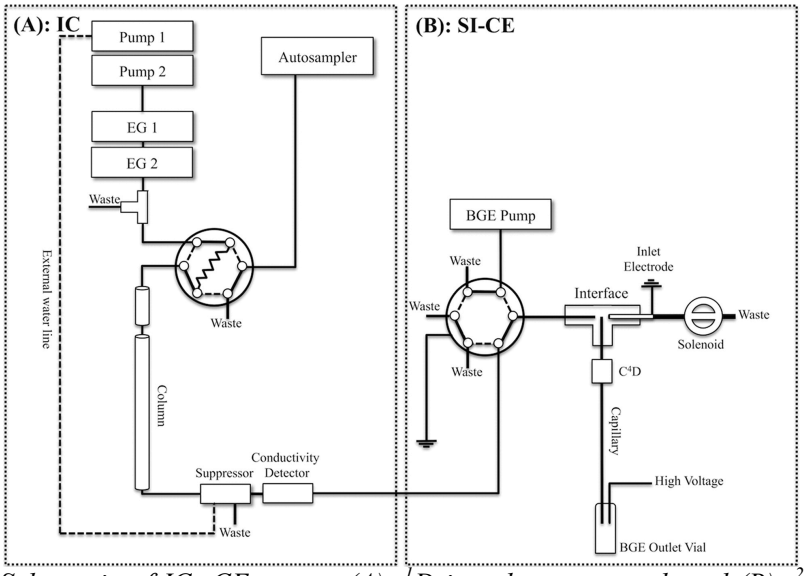

***Figure 2-1**: Schematic of IC×CE set-up. (A): ^{1}D ion chromatograph and (B): ^{2}D sequential injection-capillary electrophoresis system.*

2.3.3 Instrumentation - capillary electrophoresis

Second dimension electrophoretic separations were performed using a SI-CE system described elsewhere [4, 5, 7]. A schematic of the SI-CE instrument where the sample pump was replaced by IC outflow for 2D separations is shown in **Figure 2-1**B. The system hardware consisted of Spellman +/−30 kV CZE1000R high voltage power supply (Hauppage, NY, USA); two milliGAT pumps (GlobalFIA, Fox Island, WA, USA) one delivering background electrolyte and the other offline sample to the SI separation interface; a two-position six-port injection valve (Rheodyne, Oak Harbour, WA, USA) to switch between IC effluent and background electrolyte; a PEEK tee piece connector (P-727, Upchurch Scientific, Oak Harbour, WA, USA) connected to the valve by 60 mm × 250 μm ID PEEK tubing (Thermo Fisher Scientific) to enable sequential injection; a 30 mm cut stainless steel syringe needle (0.72 mm OD) serving both as outlet line and ground electrode; and, an isolation valve (NResearch, West Caldwell, NJ, USA) on the waste line to enable hydrodynamic injection and flushing of the separation capillary. Detection was carried out using Tracedec C^4D (Innovative Sensor Technologies, Strassahof, Austria).

The system was controlled from a personal computer via a program written in LabVIEW (LabVIEW 2011, National Instruments, Austin, TX, USA). A NI USB-6212 data acquisition device was used to interface all the components except detector and pumps, which were respectively connected via a RS232 serial connection and a RS422 serial cable.

All CE experiments were conducted in a 150 mm × 0.025 mm ID bare fused-silica capillary (Polymicro, Phoenix, AR, USA) at room temperature. The capillary was positioned inside the tee interface with the detector placed 30 mm from the inlet. The outlet was placed in a 15 mL background electrolyte vial where the positive electrode was immersed. To align the capillary in the tee piece another piece of capillary was inserted in the flow-through arm to ensure a 0.36 mm gap. Prior to first use, the separation capillary was initially conditioned by flushing methanol followed consecutively by 0.1 M sodium hydroxide, Milli-Q water, methanol, 0.1 M hydrochloric acid, Milli-Q water and finally BGE; each step for 5 min at 0.17 mL/min. Voltage of + 30 kV was then applied for 30 min to stabilise the inner surface of the channel. BGE consisted of 20 mM nicotinic acid and 0.1% (w/V) PVP at pH 4.4 adjusted by 1 M HEPES.

2.3.4 Instrumentation - interfacing and IC×CE operation

The two dimensions were interfaced through the six-port injection valve in the SI-CE system according to Figure 1-1. To carry out online 2D separations, the IC detector outflow was directed to the sample inlet on the valve using a 700 mm × 0.25 mm ID PEEK tubing (Thermo Fisher Scientific). Suppression of the eluent was achieved in external water mode where Milli-Q water was fed into the REGEN IN port of the suppressor.

IC effluent was sequentially sampled by CE with a sampling period of 18.4 s throughout the whole first dimension run time. SI-CE sampling cycle was initiated at the same time as the sample was injected in IC in the following sequence; the interface was initially filled with the IC fraction within 1.0 s followed by application of +5 kV voltage lasting for 1.0 s to electrokinetically inject the anions from the flowing stream into the capillary. The interface was then flushed for 2.0 s at 2.400 mL/min with BGE to remove the sample remaining in the valve-to-interface transfer line, BGE flow rate was then reduced to 0.024 mL/min and the separation voltage of +30 kV was applied for 12.0 s. These in addition to post-separation dead time of approximately 2.4 s, adds up to an injection-to-injection time of 18.4 s.

2.3.5 Data processing

Data collection and storage were achieved using LabVIEW. With each CE run stored as a single .csv file, the data for consecutive CE runs were merged and stacked into a two-column string using Origin 9.0 (OriginLab Northampton, MA, USA). The data were then processed into 2D chromato-electropherograms using GC Image (GC Image LLC, Lincoln, NE, USA). Integration and peak identification were also performed using GC Image; peak identification was achieved using retention times in the first dimension and migration times in the second dimension.

Due to 6.4 s of dead time during which no data were recorded (4.0 s prior to each separation for sum of sample flow, sample injection and interface cleaning time; in addition to approximately 2.4 s post-separation for data storage), the designated retention times in the first dimension did not match the actual values in the GC Image constructed images. As result, the 2D chromato-electropherograms presented in this chapter were plotted by loading the matrix of merged second dimension runs into Transform 3.3 (Fortner Research, Sterling, VA, USA).

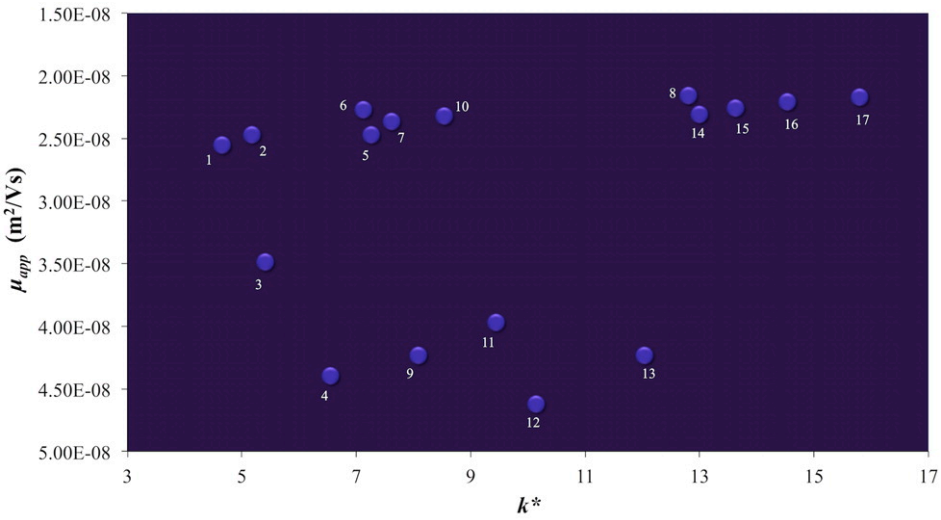

***Figure 2-2**: Predicted chromato-electropherogram derived from experimentally measured retention factor and electrophoretic mobility data; Peak identifications as in **Table 2-1**.*

2.4 Results and discussion

The predictable orthogonality of IC and CE is illustrated in **Figure 2-2** by plotting electrophoretic mobilities (μ_{app}) against IC effective retention factors (k^*) for a suite of organic- and inorganic-anions. These anions represent some typical drinking water matrix anions and drinking water disinfection byproducts regulated by the US-EPA. IC is the gold-standard technology for water disinfectant byproduct analysis however, despite considerable column chemistry development, the challenge to resolve all 17 anions using IC remains unmet. As a result, US-EPA method 557 for determination of these analytes requires use of tandem mass spectrometry with matrix diversion to enhance selectivity [6]. While the primary purpose of this investigation is not to develop competitive methodology for water disinfection byproducts analysis, this application provides ideal sample dimensionality to utilise the ordered two-dimensional separation space for qualitative interpretation and to maximise analyte resolution [8]. **Figure 2-2** highlights the appropriate selectivity of the orthogonal separation dimensions to separate the two sets of solutes (namely homologous organic anions and inorganic anions) present in the sample.

One of the main challenges in developing an online IC×CE approach is to ensure a sufficiently high sampling rate, which may be described as the modulation ratio (M_R) [9]. For separations where the utmost precision in measuring trace analytes is important, a $M_R \geq 3$ should be chosen [9] and this places a constraint on time required to complete the second-dimension (^{2}D) CE separation. Using the gradient IC

***Table 2-1**: Figures of merit for 2D IC×CE analysis of haloacetic acids, dalapon, bromate and common inorganic anions.*

Spot number	Analyte	Retention time RSD% (n=3)[a]	Migration time RSD% (n=3)	Peak area RSD (%)[b]	Dynamic linear range (ng/mL)	Correlation coefficient	Recovery % (40 ng/mL)	Recovery % (150 ng/mL)
1	MCAA	0.0	0.3	12.8	5-225	0.9229	69	89
2	MBAA	0.0	0.3	8.3	5-225	0.9533	80	84
3	Bromate	0.0	0.5	16.1	5-225	0.9792	93	108
4	Chloride	0.0	0.6	1.0	5-225	0.9737	-	-
5	DCAA	0.0	0.3	8.8	5-225	0.9894	105	96
6	Dalapon	0.0	0.5	12.0	5-225	0.9639	84	80
7	BCAA	0.0	0.3	5.1	5-225	0.9911	96	96
8	Phosphate	0.0	0.7	11.7	5-225	0.9944	80	85
9	Nitrite	0.0	0.0	17.8	5-225	0.9692	74	74
10	DBAA	0.0	0.0	14.0	10-225	0.9702	92	106
11	Chlorate	0.0	1.2	12.7	5-225	0.9656	73	78
12	Bromide	0.0	1.4	10.0	5-225	0.9746	119	115
13	Nitrate	0.0	1.1	9.3	5-225	0.9638	85	119
14	TCAA	0.9	0.6	17.4	5-225	0.9769	94	117
15	BDCAA	0.0	0.3	2.8	5-225	0.9868	94	117
16	CDBAA	0.0	0.5	0.8	5-225	0.9893	87	110
17	TBAA	0.0	0.5	10.5	25-225	0.9515	70	104

[a] the peak maxima were each collected within consistent modulation events between runs

[b] for tap water sample spiked with 150 ng/mL of the analyte set

conditions described above, average ^{1}D peak widths (4σ) are on the order of 0.9 min, so the CE cycle must be completed on the order of 18 s to maintain appropriate modulation ratio. The highest separation speeds reported using the SI-CE system employed in previous investigation are on the order of 55-180 s [4, 5]. Here the CE separation conditions were further optimised to bring the SI-CE approach in line with the requirements for IC×CE. Under optimised conditions, fractions of the IC effluent were sampled by CE every 18.4 s for the entire duration of the ^{1}D analysis time.

The first 1.0 s of each modulation cycle is used to fill the sampling interface with IC effluent, followed by a 1.0 s electrokinetic injection by applying +5 kV. Next the 6-port valve was actuated and the modulator is flushed with BGE for 2.0 s. This step is very important to ensure complete elimination of IC effluent from the modulator prior to commencing the ^{2}D separation. A relatively high flow rate (2.400 mL/min) was needed during the flush step since considerable modulator-induced ^{2}D tailing occurred with insufficient flushing time or lower flow rates. The penultimate step involves reducing the BGE flow rate and applying the separation voltage of +30 kV 12.0 s. The last 2.4 s of each modulation cycle is occupied by Lab-VIEW for data storage. While these coupling parameters lead to discontinuous sampling whereby approximately 93% of the ^{1}D effluent is sent to waste, the sampling frequency is sufficient to provide highly satisfactory quantitative performance and adequate reconstruction of the ^{1}D chromatogram (see **Table 2-1**).

Partial transfer limits the ultimate sensitivity of any 2D approach, however since the SI-CE interface provides non-focusing modulation, there are no sensitivity gains to be made by simply sampling more frequently. It is however, important to avoid a $M_R < 3$ which would lead to poor representation of first dimension chromatogram and can reduce the precision of quantification [10]. A twelve second ^{2}D separation time is appropriate for the present investigation. While more rapid CE separations are possible, gains in ^{2}D separation speed would be obtained at the expense of loss in resolution of the second dimension. In order to minimise the total ^{2}D run time while maintaining acceptable resolution to prevent co-migration of co-eluting pairs, CE separation with field strength as high as +2 kV/cm was pursued in this work. In addition to speed and resolution, long-term stability of operation in the second dimension is vital. Consequently, BGE longevity becomes a key factor. With conductivity detection, large low-conductivity BGE co- and counter-ion result in stable background signal [11]. Therefore, nicotinic acid and HEPES were used as

BGE components. PVP was also added to the BGE to maintain a stable electroosmotic flow sufficient for backflushing and equilibrating of the capillary during the 2D separations.

Figure 2-3 shows the long-term stability of SI-CE operation for 130 sequential runs in a time frame of 48.5 min for a representative set of analytes consisting of chloride, MCAA and TBAA as fast, moderately slow and slow ions, respectively. This resulted in migration time RSDs of 0.7%, 0.8% and 0.9% along with 3.3%, 11.2% and 8.9% for peak areas for chloride, MCAA and TBAA, respectively, demonstrating that there is sufficient repeatability of the CE system to function as a ^{2}D separation.

The two-dimensional separation space for the IC×CE analysis of 100 ng/mL solution of 9 haloacetic acids along with bromate and dalapon in presence of 100 ng/mL inorganic ions such as chloride, nitrite, chlorate, bromide, nitrate and phosphate is presented in **Figure 2-4**. Importantly each of the peak pairs co-eluted from ^{1}D such as bromate-MBAA (peaks 3 and 2), dalapon-DCAA (peaks 6 and 5), nitrite-DBAA (peaks 9 and 10) and phosphate-TCAA (peaks 8 and 14) were fully resolved using the 2D approach. The unusual 2D peak shapes are caused by the non-focusing modulation approach as well as electromigration dispersion which results in movement of the peak maximum in CE. IC×CE peak shapes are directly affected by the changing first dimension peak profile as different parts of the first dimension peaks are sampled. This observation is consistent with previous discussion of non-focusing pulsed-flow

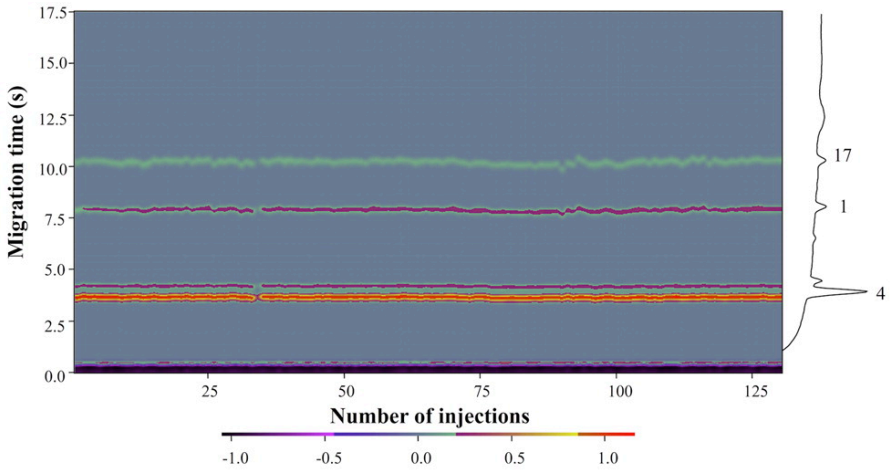

***Figure 2-3**: 130 sequential injections of standard solution con-taining chloride, MCAA and TBAA. Experimental conditions; BGE, 20 mM NA-HEPES containing 0.1% PVP (pH 4.4); sam-ple flow, 0.300 mL/min for 1.0 s; injection voltage, +5 kV for 1.0 s; cleaning time, 0.5 s at 2.400 mL/min; separation voltage, +30 kV for 17.5 s; and, capillary dimensions as specified in the experimental section. Peak identification: 4: chloride (100 ng/mL), 1: MCAA (200 ng/mL) and 17: TBAA (500 ng/mL). The colour intensity represents the peak height.*

modulation in multidimensional chromatography [12]. **Figure 2-5**B illustrates how the ^{1}D peak concentration profile is preserved in each of the ^{2}D separations.

Figure 2-5 also illustrates the modulation timing using the ^{1}D conductivity detector response for nitrate with vertices superimposed to indicate the time and frequency of CE injections. Preservation of the ^{1}D peak concentration profile leads to a shift in the peak maxima in ^{2}D separation as the concentration changes along the first dimension peak. Importantly the start of the peak occurs at exactly the same time irrespective of analyte concentration. This phenomenon is normal in electrophoresis and is a result of electrodispersion [13].

For the same run in **Figure 2-4**, with the average ^{1}D peak width of 0.89 min (4σ), peak capacity in IC was calculated to be 51 based on the method proposed by Neue [14]. Additionally, the peak capacity in CE was estimated to be 17 by dividing the separation window by the mean peak width of the widest fast and slow migrating analytes peaks. Multiplying peak capacities in both dimensions, indicates a maximum theoretical 2D peak capacity of 867 for IC×CE. Using the minimum convex hull approach [15], in which the peaks are surrounded by the smallest polygon having inner angles of ≤ 180°, the utilised fraction of separation space (*f*) was calculated to be 68%. Taking this as well as first dimension undersampling [16], the realised 2D peak

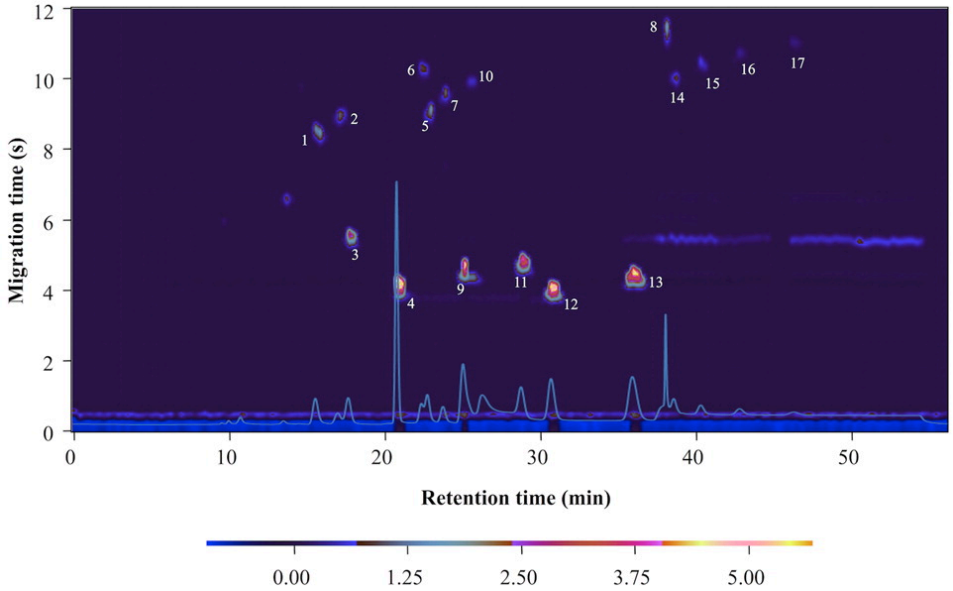

***Figure 2-4**: Experimental 2D plot for separation of 100 ng/mL of HAAs, dalapon and inorganic anions. First dimension eluent profile, 7 mM hydroxide for the first 16.8 min, 18 mM for 16.8 to 34.2 min, 60 mM for 34.4 to 51.2 min followed by 7 mM for 51.4 to 56 min; flow rate, 0.300 mL/min; suppressor current, 150 mA; injection volume, 1000 µL. Second dimension BGE, 20 mM NA-HEPES containing 0.1% PVP (pH 4.4); injection voltage, +5 kV; separation voltage, +30 kV. Other conditions as specified in the experimental section. Peak identifications as in **Table 2-1**.*

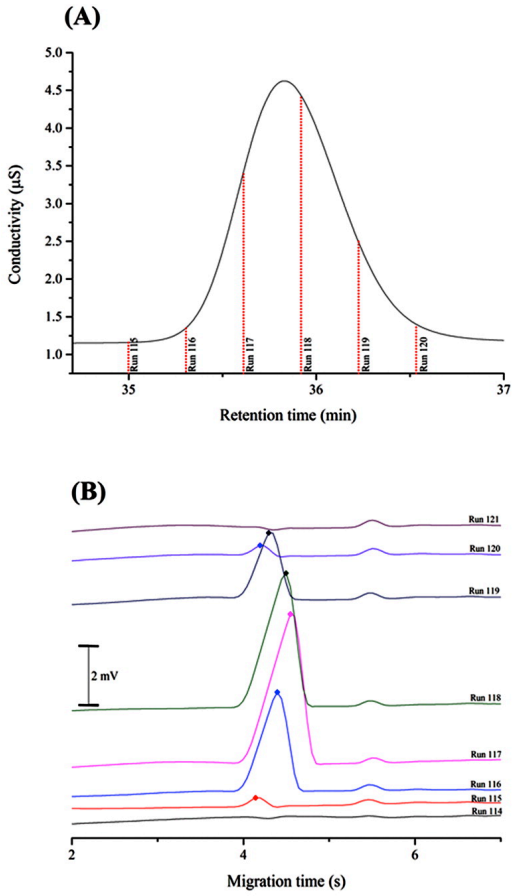

***Figure 2-5**: (A) First dimension peak for nitrate with retention time of 35.83 min and peak width (4σ) of 1.03 min. CE injection occurs every 18.4 s indicated by vertical lines (B) Consecutive second dimension runs at the indicated points.*

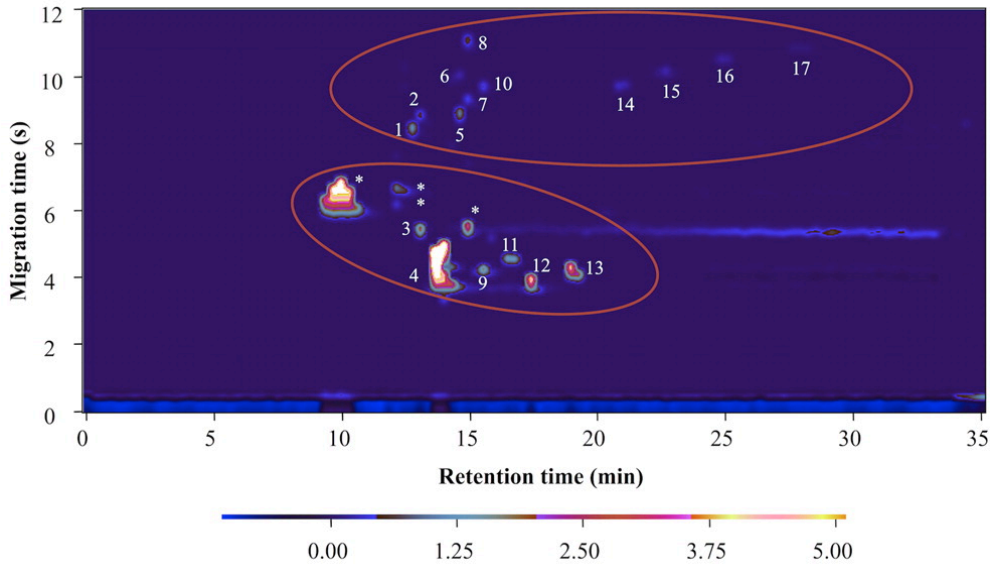

***Figure 2-6**: 2D plot for tap water spiked with 40 ng/mL of the analyte set. First dimension eluent profile, 7 mM hydroxide for the first 8 min, raising to 44 mM within 3 min, up to 83 mM from 10 to 30 min followed by 7 mM for 31 to 35 min; flow rate, 0.300 mL/min; suppressor current, 150 mA; injection volume, 1000 µL. Second dimension conditions as in **Figure 2-2**. Peak identifications as in **Table 2-1**. * Unknown compounds.*

capacity was calculated to be 498. This is equivalent to a peak production of 9 peaks/min, which represents close to 10-fold increase in peak capacity compared to IC.

As a result of enhanced peak capacity, a simpler single ramp gradient eluent profile can be employed in the first dimension instead of the finely tuned multi-step gradient profile. **Figure 2-6** demonstrates the IC×CE separation of a tap water sample spiked with 40 ng/mL of the analytes described in US-EPA method 557. Here, a one-step gradient ramp of 1.95 mM/min within a total run time of 35 min was applied, making a 37% time saving compared to US-EPA method 557. While IC×CE permits simplified gradient optimisation and faster analysis, these gains are accompanied by a loss in measured peak capacity (312 vs 498), however the target analytes are adequately resolved from one-another, and from the matrix ions.

Analytical figures of merit for the 2D IC×CE analysis of the analyte set are given in **Table 2-1**. Peak identification was performed by matching the position of spots. Worst-case relative standard deviations of peak positions were 0.9% and 1.4% for IC and CE respectively. The structured order of elution and migration simplifies peak identification; the 2D space can be divided into two distinct regions of more mobile inorganic and slow organic anions due to the sample dimensionality. With two independent time coordinates the chance of misidentification is greatly reduced compared to one-dimensional approaches. Higher RSD% value for the position of inorganic spots stems in more drastic movement of the peak maximum for these analytes as a result of increased electromigration dispersion (as in **Figure 2-5**B).

Compared to gradient × gradient 2DLC where the total dilution factor can be as high as 50 [17], non-focused transfer of 7% of the IC eluent to CE is an acceptable trade-off between sufficient sampling and detection. While detection limits are respectable compared to other multidimensional approaches, we recognise a need to improve solute transfer to ^{2}D. This will undoubtedly require a form of peak focusing, of which there are numerous well-known CE approaches worthy of investigation. Values of 1.0-17.8% deviation for peak areas as well as correlation coefficients in the range of 0.9229-0.9944 can also be explained by the fact that modulation occurs under non-focusing conditions and that integration is performed using chromatographic approaches, not those refined for electrophoresis.

2.5 Conclusion

In this work, feasibility of comprehensively coupling CE with IC was demonstrated to improve the peak capacity and decrease the analysis time for separation and quantification of haloacetic acids in a matrix of common inorganic anions. Employing SI-CE as the second dimension requires no instrumental modification for performing 2D separations and offers the great advantage of discrete operating of each dimension at any time.

However, the non-focusing modulation approach and low duty cycle sampling of the IC effluent to accommodate the CE injection volume and ensure efficient sampling frequency, has placed a great burden on detection and therefore sensitivity like any other LC-CE approaches where the sample is inevitably diluted in the eluent [18]. In this study, with water being the target matrix, the simplest solution for this problem was loading larger volume of the sample. This urges development of modulation approaches which incorporate preconcentration methods such as stacking and sweeping to improve the analyte transfer from the first dimension effluent.

Moreover, the IC×CE experimental parameters (i.e. choice of stationary phase, eluent profile and background electrolyte composition) were chosen based on existing methods and/or previous experience which underlines the need for systematic optimisation approaches for chromatographic × electrophoretic separations similar to the studies performed in the area of 2D liquid-phase separations [19-21].

While improving the transfer efficiency and systematic optimisation of the separation parameters are certainly the way forward to exploit the potentials of IC×CE, the chip-based SI-CE approach with in-plane detection previously introduced in our group [7] offers the possibility of integrating the second dimension as one of the components in IC detector compartment.

2.6 References

[1] S. Kar, P.K. Dasgupta, Direct coupling of ion chromatography with suppressed conductometric capillary electrophoresis, J. Micro. Sep., 8 (1996) 561-568.

[2] A. Beutner, S. Kochmann, J.J.P. Mark, F.-M. Matysik, Two-dimensional separation of ionic species by hyphenation of capillary ion chromatography x capillary electrophoresis - mass spectrometry, Anal. Chem., 87 (2015) 3134-3138.

[3] F.-M. Matysik, Capillary batch injection – A new approach for sample introduction into short-length capillary electrophoresis with electrochemical detection, Electrochem. Commun., 8 (2006) 1011-1015.

[4] G.A. Blanco, Y.H. Nai, E.F. Hilder, R.A. Shellie, G.W. Dicinoski, P.R. Haddad, M.C. Breadmore, Identification of Inorganic Improvised Explosive Devices Using Sequential Injection Capillary Electrophoresis and Contactless Conductivity Detection, Anal. Chem., 83 (2011) 9068-9075.

[5] A.J. Gaudry, R.M. Guijt, M. Macka, J.P. Hutchinson, C. Johns, E.F. Hilder, G.W. Dicinoski, P.N. Nesterenko, P.R. Haddad, M.C. Breadmore, On-line simultaneous and rapid separation of anions and cations from a single sample using dual-capillary sequential injection-capillary electrophoresis, Anal. Chim. Acta, 781 (2013) 80-87.

[6] B. US-EPA Method 557: Determination of Haloacetic Acids, and Dalapon in Drinking Water by Ion Chromatography Electrospray Ionization Tandem Mass Spectrometry (IC-ESI-MS/MS), (September 2009) EPA 815-B-809-012 (last accessed on 820 Feb 2015 from http://water.epa.gov/scitech/drinkingwater/labcert/upload/met2557.pdf).

[7] A.J. Gaudry, Y.H. Nai, R.M. Guijt, M.C. Breadmore, Polymeric Microchip for the Simultaneous Determination of Anions and Cations by Hydrodynamic Injection Using a Dual-Channel Sequential Injection Microchip Electrophoresis System, Anal. Chem., 86 (2014) 3380-3388.

[8] J.C. Giddings, Sample dimensionality: A predictor of order-disorder in component peak distribution in multidimensional separation, J. Chromatogr. A, 703 (1995) 3-15.

[9] W. Khummueng, J. Harynuk, P.J. Marriott, Modulation Ratio in Comprehensive Two-dimensional Gas Chromatography, Anal. Chem., 78 (2006) 4578-4587.

[10] A. Ghosh, C.T. Bates, S.K. Seeley, J.V. Seeley, High speed Deans switch for low duty cycle comprehensive two-dimensional gas chromatography, J. Chromatogr. A, 1291 (2013) 146-154.

[11] S.D. Noblitt, F.M. Schwandner, S.V. Hering, J.L. Collett Jr, C.S. Henry, High-sensitivity microchip electrophoresis determination of inorganic anions and oxalate in atmospheric aerosols with adjustable selectivity and conductivity detection, J. Chromatogr. A, 1216 (2009) 1503-1510.

[12] P.M. Harvey, R.A. Shellie, Factors affecting peak shape in comprehensive two-dimensional gas chromatography with non-focusing modulation, J. Chromatogr. A, 1218 (2011) 3153-3158.

[13] G.L. Erny, E.T. Bergström, D.M. Goodall, S. Grieb, Predicting Peak Shape in Capillary Zone Electrophoresis: a Generic Approach to Parametrizing Peaks Using the Haarhoff−Van der Linde (HVL) Function, Anal. Chem., 73 (2001) 4862-4872.

[14] U.D. Neue, Theory of peak capacity in gradient elution, J. Chromatogr. A, 1079 (2005) 153-161.

[15] G. Semard, V. Peulon-Agasse, A. Bruchet, J.-P. Bouillon, P. Cardinaël, Convex hull: A new method to determine the separation space used and to optimize operating conditions for comprehensive two-dimensional gas chromatography, J. Chromatogr. A, 1217 (2010) 5449-5454.

[16] X. Li, D.R. Stoll, P.W. Carr, Equation for Peak Capacity Estimation in Two-Dimensional Liquid Chromatography, Anal. Chem., 81 (2009) 845-850.

[17] F. Bedani, P.J. Schoenmakers, H.-G. Janssen, Theories to support method development in comprehensive two-dimensional liquid chromatography – A review, J. Sep. Sci., 35 (2012) 1697-1711.

[18] M.R. Schure, Limit of Detection, Dilution Factors, and Technique Compatibility in Multidimensional Separations Utilizing Chromatography, Capillary Electrophoresis, and Field-Flow Fractionation, Anal. Chem., 71 (1999) 1645-1657.

[19] P.J. Schoenmakers, G. Vivó-Truyols, W.M.C. Decrop, A protocol for designing comprehensive two-dimensional liquid chromatography separation systems, J. Chromatogr. A, 1120 (2006) 282-290.

[20] G. Vivó-Truyols, S. van der Wal, P.J. Schoenmakers, Comprehensive Study on the Optimization of Online Two-Dimensional Liquid Chromatographic Systems Considering Losses in Theoretical Peak Capacity in First- and Second-Dimensions: A Pareto-Optimality Approach, Anal. Chem., 82 (2010) 8525-8536.

[21] K.M. Kalili, A. de Villiers, Systematic optimisation and evaluation of on-line, off-line and stop-flow comprehensive hydrophilic interaction chromatography × reversed phase liquid chromatographic analysis of procyanidins, Part I: Theoretical considerations, J. Chromatogr. A, 1289 (2013) 58-68.

Part 2

Method development

3 Effect of background electrolyte pH on sample dimensionality and peak capacity in ion chromatography × capillary electrophoresis

"Everything should be as simple as possible, but not simpler."
—Albert Einstein

This chapter has been submitted for peer review as a research article. Herein, it is reproduced with minor modifications to avoid replication of overlapping content with Chapter 4.

3.1 Overview

Full utilisation of 2D peak capacity requires careful exploitation of sample attributes in order to maximise the area of separation space covered by sample components. Ionisation state of a multivalent acid is one of the most influential factors impacting its electrophoretic mobility and can be easily altered through the change of background electrolyte pH in capillary electrophoresis. This attribute was used as a sample dimension in the current chapter to enable resolution of low-molecular-mass organic acids (LMMOAs) using the online comprehensive ion chromatography × capillary electrophoresis system introduced in Chapter 2. Employing a systematic screening approach, which uses Euclidean distance as an indication of resolution between 2D peaks, it was demonstrated that the fractional surface coverage changed significantly with varying the background electrolyte pH as well as the eluent profile. Based on the obtained simulations, separation space coverage was increased from 44 %(using a separation pH of at least 2 units above the pK_a) to 59% resulting in a more ordered separation with a peak capacity of 1011 for separation of 23 LMMOAs.

3.2 Introduction

The key to full utilisation of the peak capacity offered by hyphenation of orthogonal separation mechanisms is selective exploitation of each sample attribute that can be used for separation purposes by individual separation dimensions - a concept referred to as the sample dimensionality [1]. While it is impractical to have one separation dimension for each sample dimension, it has been proved in various examples that even through exploiting only one sample attribute, a high degree of orthogonally is obtainable; for instance utilising the selective interaction of diastereomers with a carbon adsorption surface for a reversed-phase liquid chromatography × reversed-phase liquid chromatography (RPLC×RPLC) 2D separation of low-molecular-mass polystyrenes [2] or reaction with different fluorescent labels in case of nano liquid chromatography × micro free-flow electrophoresis (nLC×μFFE) separation of peptide and amino acid samples [3]. Hence, it is of immense importance to search for differences in separation selectivity prior to performing a 2D separation to ensure an ordered distribution of component peaks in the 2D space, which results in reduced peak overlapping and helps to achieve the maximum peak capacity of the 2D system [1].

Peak capacity of a perfectly ordered 2D separation equals the product of the peak capacities in ^{1}D and ^{2}D [4]. However, full coverage of the rectangular 2D separation plane by equally spaced peaks is almost impossible even when the most orthogonal separation mechanisms are coupled. Due to factors such as undersampling of the ^{1}D [5] and incomplete utilisation of the separation space [6], the achievable peak capacity of a 2D system often deviates from the product rule.

Providing quite different and complementary separation selectivities [7] has resulted in emerging powerful 2D technologies comprising of both IC and CE for separation of ionic and ionogenic compounds as discussed in Chapters 1 and 2 [8-10]. Despite a high degree of orthogonally, if the separation conditions are not chosen carefully, the separative behaviour of IC and CE can be correlated as shown further in the current chapter. In order to study the degree of dependence of surface coverage on sample dimensionality, low-molecular-mass organic acids (LMMOAs) were chosen as model compounds in this study.

LMMOAs are present in various metabolic pathways, such as the citrate and glyoxylate cycles. These compounds serve numerous functions in various areas: they

are of interest in clinical studies as biomarkers for diagnostic purposes [11, 12]; examples of their role in agriculture, environmental and biotechnological sciences include impacting the fertiliser release into soil [13], mobilisation of metals in the environment [14] and inhibition of microbial fermentation processes [15]; in food and beverages, LMMOAs contribute to flavour, colour and aroma and therefore are used as markers for product adulteration and quality [16, 17]; they are also added to food as preservatives due to their effects on bacteria[18]. Having closely similar structures, full profiling of these acids, especially in complex matrices, is not feasible in a single dimensional (1D) approach [19]. As a result, an additional degree of selectivity is required through the application of 2D separations. The main objectives of the work presented in this chapter are performing IC×CE for resolution of these acids and, demonstrating the impact of background electrolyte pH on sample dimensionality and peak capacity through a simplified approach based on maximising the Euclidean distance between 2D peaks while assessing the degree of separation space coverage using the minimum convex hull approach [20].

3.3 Theory/ background

3.3.1 Prediction of retention in IC

Retention of anion A^{x-} on a certain ion exchange stationary phase under gradient elution can be described by **Equation 3-1** [21]:

$$k_{eff} = \frac{t_D}{t_0} + \frac{1}{Bt_0}[10^a B(b+1)(t_0 - \frac{t_D}{k_0}) + C_i^{(b+1)}]^{1/b+1} - \frac{C_i}{Bt_0} \quad and \quad k_{eff} = \frac{t_R - t_0}{t_0}$$

Equation 3-1

Where t_R is the retention time of the analyte, k_{eff} and k_0 are the gradient retention factor and isocratic retention factor, respectively. And, t_0, t_D, C_i and B are the void time, dwell time, initial concentration of the eluent and gradient slope (mM/min), consecutively. Constants *a*- and *b*- are the intercept and slope of the linear solvent strength (LSS) model for IC which describes the retentive behaviour of an ion under isocratic elution concentration of C [22]:

$$\log k = a - b \log C$$

Equation 3-2

As described by Quarry et al. [23], constants *a*- and *b*- can be predicted precisely using the retention data for two or more gradient runs. Therefore, in principle, only

two sets of gradient retention times suffice for prediction of retention under any other gradient conditions.

3.3.2 Prediction of migration in CE

Migration of the conjugate base of the polyprotic acid H_xA at any given background electrolyte pH is described by **Equation 3-3** [24, 25]:

$$\mu_{eff} = \frac{\sum_{i=1}^{x} 10^{ipH - \sum_{j=1}^{i} pK_{aj}} \cdot \mu_{H_{x-i}A^{-i}}}{1 + \sum_{i=1}^{x} 10^{ipH - \sum_{j=1}^{i} pK_{aj}}}$$

Equation 3-3

$$\mu_{app} = \mu_{eff} + \mu_{eof}$$

Equation 3-4

$$\mu = \frac{Ll}{Vt}$$

Equation 3-5

Where μ_{eff} is the effective electrophoretic mobility of the acid, $\mu_{Hx\text{-}iA}{}^{-i}$ is the mobility at the i^{th} ionisation state, pK_a is the thermodynamic acidity constant. μ_{app} and μ_{eof} in **Equation 3-4** are the apparent and the electroosmotic mobilities, respectively. Mobility can be calculated from **Equation 3-5** using the migration time (t), separation voltage (V) and total capillary length (L) in addition to the effective length of the capillary (l).

Therefore, if $\mu_{Hx\text{-}iA}{}^{-i}$ and the pK_a are known, μ_{eff} can be predicted for any background electrolyte pH.

3.3.3 2D peak capacity

The maximum theoretical peak capacity ($n_{c,2D}$) in orthogonal 2D separations ideally equals the product of peak capacities in each dimension ($^1n_c \times {}^2n_c$). However, as a result of the degree of orthogonally being far from unity as well as due to undersampling of the ^{1}D effluent the 2D peak capacity derived from the product rule is usually an overestimation and therefore needs to be corrected as shown by Gilar et al. [6] and Li et al. [5] in **Equation 3-6** and **Equation 3-7**:

$$n_{c,2D}^{*} = \frac{{}^1n_c \times {}^2n_c \times f_c}{\beta}$$

Equation 3-6

$$\beta = \frac{1}{\sqrt{1 + 3.35(\frac{{}^{2}t_c \, {}^{1}n_c}{{}^{1}t_G})^2}}$$

Equation 3-7

Where β and f_c are the undersampling correction factor and fractional coverage, respectively. ${}^{2}t_c$ is the second dimension cycle time and ${}^{1}t_G$ represents the first dimension gradient time. The parameter fractional coverage in this equation is a measure of the utilised 2D separation space and reflects the degree of orthogonality as well. f can be calculated using the minimum convex hull approach [20], in which normalised 2D peak positions (values between 0-1 assigned to peak positions in each dimension as in [6]) are surrounded by a polygon with interior angles of $\leq 180^{\circ}$. The inner area of this convex polygon presents the fraction of separation plane theoretically occupied by peaks and can intuitively be related to the degree of 2D resolution.

3.4 Materials and methods

3.4.1 Chemicals and reagents

10 000 mg/L stock solutions of the anions were prepared by dissolving analytical grade 2-hydroxyisobutyric acid, citric acid tri-sodium dihydrate, sodium foramte, fumaric acid, glutaric acid, sodium DL-lactate, *trans*-aconitic acid, *cis*-aconitic acid, DL-malic acid, DL-isocitric acid tri-sodium salt and glycolic acid all from Sigma Aldrich (Sigma-Aldrich, St. Louis, MO, USA); soldium malonate, sodium oxalate, and sodium succinate hexahydrate from BDH (BDH, West Chester, PA, USA); sodium acetate and adipic acid from Ajax (Ajax Chemicals, Unilab, Auckland, New Zealand); and, sodium pyruvate, α-ketoglutaric acid di-sodium dihydrate salt, maleic acid, sodium D-gluconate acid and D-galacturonic acid, quinic acid from Fluka (Sigma-Aldrich, St. Louis, MO, USA) in Milli-Q water or basic aqueous solution of 0.1 M sodium hydroxide (in case of the acid having low water solubility).

Nicotinic acid (NA), 4-(2 hydroxyethyl)piperazine-1-ethanesulfonic acid (HEPES), tris(hydroxymethyl)aminomethane (Tris), 2-(cyclohexylamino)ethanesulfonic acid (CHES) and poly(vinylpolypyrrolidone) (PVP) used for preparation of background electrolyte were all purchased from Sigma-Aldrich.

Reagents used for conditioning new capillaries included sodium hydroxide (Sigma-Aldrich), hydrochloric acid, and methanol from Merck (Merck, Darmstadt, Germany).

Milli-Q water from a Millipore purifier system (Millipore, Bedford, MA, USA) was used for the IC eluent, external water for the suppressor and preparation of all solutions.

3.4.2 Instrumentation

Two-dimensional separations were performed using a similar set-up as described in Chapter 2. Briefly, first-dimension separations were performed on an IC-5000 ion chromatograph equipped with a ASRS Ultra II 2-mm suppressor operated in external water mode (Thermo Fisher Scientific, Sunnyvale, CA, USA) using IonPac–AS24 analytical column (250 mm × 2 mm ID) connected to AG24 guard column (50 mm×2 mm ID). Separation flow rate and temperature were maintained at 0.150 mL/min and 20 °C, respectively. Injection volume was 50 µL for all the analyses. Details of the eluent profiles can be found in figure captions. IC effluent was sequentially sampled by a capillary electrophoresis instrument equipped with a tee-piece connected to a six-port injection valve using Tracedec C^4D (Innovative Sensor Technologies, Strassahof, Austria) for detection [10, 26, 27]. The two dimension were connected using a 700 mm × 0.125 mm ID PEEK tubing (Thermo Fisher Scientific). Instrument control and data acquisition was achieved using a program written in LabVIEW (LabVIEW 2011, National Instruments, Austin, TX, USA). And, data processing was performed in Origin 9.0 (OriginLab, Northampton, MA, USA).

CE experiments were conducted at room temperature in an 82 mm × 0.025 mm ID bare fused-silica capillary connected to a 151 mm × 0.100 mm ID bare fused-silica capillary using a 7 mm × 0.250 mm ID piece of Teflon tubing at the detector outlet. The capillaries were finely cut and polished using a rotating sanding paper prior to connection. The cut capillaries were then immersed in a vial of acetone and sonicated for 30 minutes. Upon drying, the finely cut tips were carefully inserted into the piece of Teflon tubing under an optical microscope. The Teflon tubing ID was loosened to 0.360 mm through the use of an additional piece of fused silica capillary and a heat gun prior to the joining. **Figure 3-1** shows a 4x-enlarged image of the joint. The connection was glued for further insulation using Araldite 5 minutes epoxy glue (Selleys Pty Ltd, Padstow, NSW, Australia). All separations were performed at electric field strength of +3.28 kV/cm using this set-up.

3.5 Results and discussions

The charge state of functional groups within an ionogenic molecule as well as the separation media (e.g. stationary phase), are the two most important factors influencing ion chromatographic and/or electrophoretic behaviour of a compound. As ionisation state is directly determined by the acidity constants, pH of both IC eluent and CE background electrolyte play a crucial role in IC × CE separation of LMMOAs. Modern IC, however,

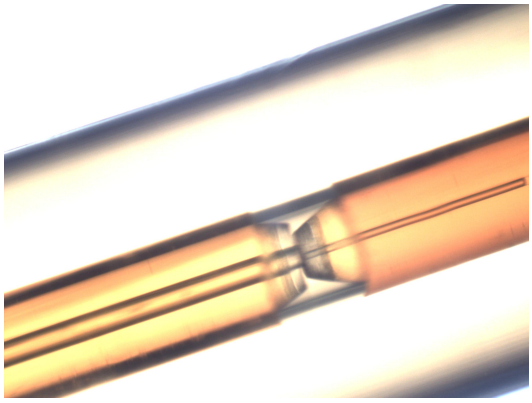

Figure 3-1*: Enlarged image of the joint separation capillary; the larger bore capillary (left) and the narrow separation capillary (right)*

uses high ionic strength eluents to facilitate analyte desorption as well as for supressed conductivity detection. Typically separated using hydroxide eluent, the eluent pH for IC separation of LMMOAs is in the range of 11-14, which is substantially higher than the pK_a of most LMMOAs. As a result, background electrolyte pH in CE can be utilised as a sample dimension for maximising the coverage of the 2D space. Additionally, peak positions and spacing can be altered through variation of the eluent composition performing gradient elution in IC.

Through systematic modelling of each separation dimension, it is possible to minimise the number of experiments required for finding the appropriate background electrolyte pH in CE and eluent profile in IC via rapid calculation of all possible combinations of experimental variables and ranking the 2D separations. Retention in IC can be modelled well by the LSS model, while migration in CE can be predicted by **Equation 3-3** as discussed in section 3.3.2. In order to use these models, it is necessary to determine the constants *a*- and *b*- for LSS model in IC as well as mobilities of the ionic species and pK_a values in CE. CE parameters were either sourced from Peakmaster simulation software [28] and literature [29-32] or measured

using a background electrolyte of 30 mM Tris-30 mM CHES containing 0.1% PVP. While the former were measured experimentally using two IC gradients of 1.25 mM/min and 0.625 mM/min run with initial and final eluent concentrations of 5 and 65 mM over a gradient time of 60 and 120 min, respectively.

Effective single dimensional IC separation of LMMOAs requires tandem mass spectrometry (MS/MS) detection due to the chromatographic separation being predominantly charge-based, so these acids display similar retentive behaviour due to similarities in their structure and/or charge [33]. In a similar manner, it can be concluded from the pH-μ_{eff} plots for mono-, di- and tri-valent LMMOAs in **Figure 3-2**, that there is no background electrolyte pH at which all compounds have different μ_{eff}, hence full resolution of LMMOAs through single-dimensional aqueous CE is challenging and there is a need to introduce additional selectivity through the use of an additional separation dimension. Moreover, **Figure 3-2** displays that even 0.1 unit change in pH would result in a substantial change in electrophoretic mobilities, which if optimised using a one-at-a-time approach would result in performing a large number of experiments.

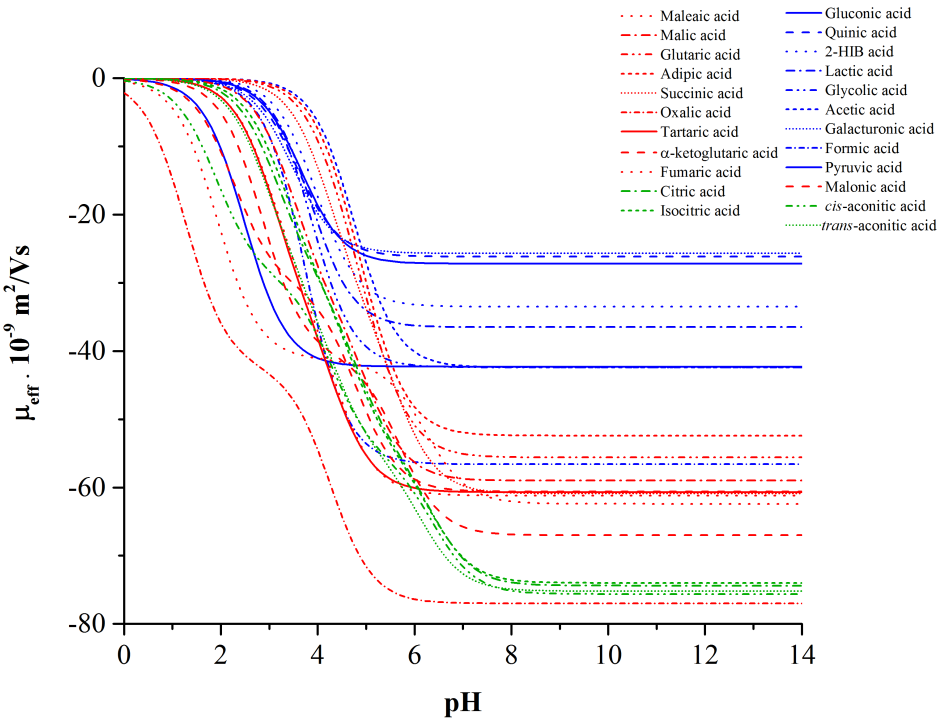

***Figure 3-2**: Change of effective electrophoretic mobility with background electrolyte pH for monovalent (blue), divalent (red) and trivalent (green) acids included in this study.*

While sophisticated prediction and simulation of 2D separations have been described previously [34], herein, a simplified screening approach was pursued using computer-assisted simulation performed in an in-house-written Matlab programme (Matlab2013b, Mathworks, Natick, MA, USA). A large number of ion chromatograms were generated using **Equation 3-1** for single ramp gradient profiles comprising of fixed starting and ending concentrations of 5 and 65 mM hydroxide while varying the gradient time in 1 min steps between 30 min to 120 min. The predicted 90 chromatograms were then paired with predicted 93 electropherograms derived through the use of **Equation 3-3** for 0.1 unit increments in background electrolyte pH. This resulted in a suite of *90×93* chromatoelectropherogrmas for each of which pairwise temporal Euclidean distances were calculated for every 2D analyte peak against all the other peaks (**Figure 3-3**). As shown previously by Schure [35], such a simplified approach is suitable for measuring 2D resolution in case of small to medium-sized molecules. In the next stage, the pairs with minimum Euclidean distance were identified for each predicted 2D plot and, combination of IC gradient × CE background electrolyte pH maximising these distances were chosen as optimal conditions for 2D separation.

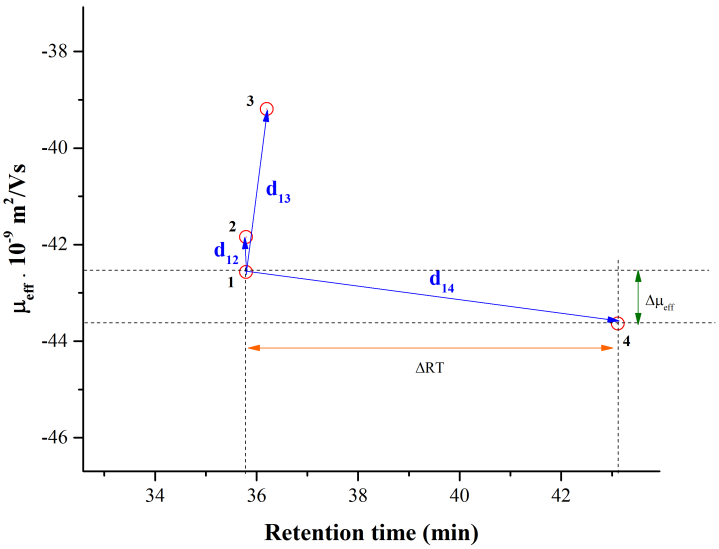

***Figure 3-3**: Calculation of Euclidean distance for identification of critical pairs.* $d = \sqrt{\Delta\mu_{eff}^2 + \Delta RT^2}$ *. Pairs 1 and 2 have the minimum distance from each other (critical pair) while 1 and 4 are furthest apart.*

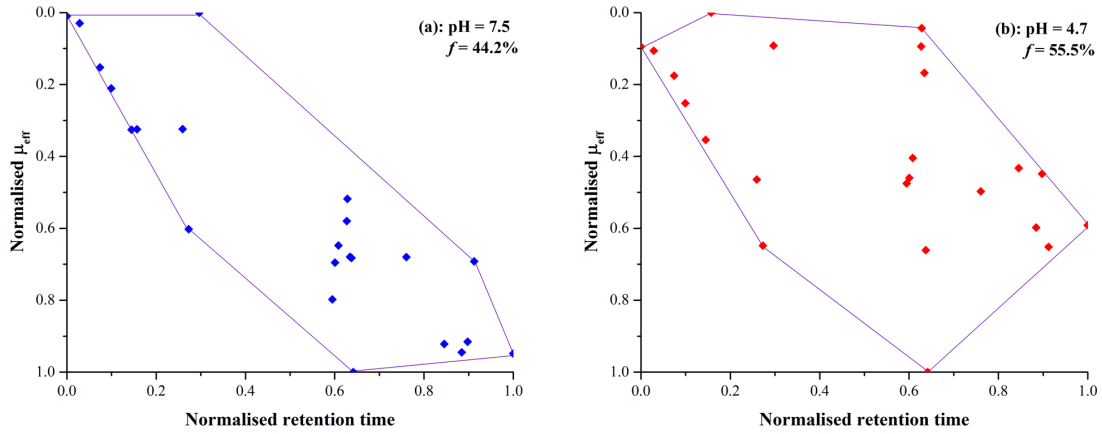

***Figure 3-4**: Predicted 2D chromatoelectropherograms and convex hull fractional coverage of 2D separation space for 1.67 mM/min single gradient ramp eluent profile in IC × background electrolyte pH of 7.5 (a) and 4.7 (b) in CE.*

Figure 3-4 shows example simulated chromatoelectropherograms for two various background electrolyte pH: one with a background electrolyte pH of 7.5 (**Figure 3-4**a) and the other with a background electrolyte pH 4.7 (**Figure 3-4**b). Both separations are based on the minimum IC gradient time of 30 min with a gradient slope of 1.67 mM/min hydroxide in the ^{1}D. **Figure 3-4**a demonstrates that choosing a high background electrolyte pH would fail due to indistinguishable electrophoretic behaviour even in a 2D set-up in which fully orthogonal separation mechanisms are coupled. While **Figure 3-4**b shows that selective exploitation of the ionisation state in ^{2}D even where a minimum degree of resolution is obtained in the ^{1}D separation, results in a substantial increase in the peak capacity. This sheds a light on the importance of taking sample dimensionality into account when optimising 2D separations. Moreover, it can be seen in this figure that the fractional coverage of 2D separation space and therefore peak capacity is greater in case of background electrolyte pH of 4.7 (55.5% against 44.2%). Additionally, a value of 0.66 for Kendall's correlation coefficient [36] between the peak positions in the ^{1}D and ^{2}D in **Figure 3-4**a versus 0.38 in **Figure 3-4**b confirms that orthogonality is reduced using a background electrolyte of pH 7.5 (calculation of Kendall's correlation was performed using the Wessa Free Statistics Software [37]). Although choosing a lower pH of 4.7 would result in substantially better resolution of the acids as seen in **Figure 3-4**b, there is further need for optimisation possibly through improving the eluent profile in order to attempt full resolution of the comigrating peaks.

Using the method described above, the optimal first and second dimension separation conditions were predicted to comprise of a gradient elution of 0.65 mM/min hydroxide over 92 minutes and a background electrolyte pH of 4.7, respectively. **Figure 3-5**a depicts the experimental 2D separation of LMMOAs under the optimal conditions. The predicted and experimental retention times and normalised electrophoretic mobilities of the optimised 2D separation along with error% values are shown in **Table 3-1**. Comparing the predicted versus experimental values, it can be seen that the highest retention time prediction error is 3%. In case of mobilities, however, due to a number of inherent systematic errors as well as selective interactions between the analytes and background electrolyte components it is not possible to directly compare the experimental and predicted values. The systematic errors affecting the accuracy of mobility measurements can be attributed to several factors which have been reviewed and studied in details previously [38].

***Table 3-1**: Experimental vs predicted retention time and normalised electrophoretic mobilities for the optimised 2D separation demonstrated in **Figure 3-5**.*

ID	Analyte	RT (min)			Normalised μ_{eff}		
		Experimental	Predicted	%Error	Experimental	Predicted	Correlation Coefficient
1	Gluconate	12.58	12.28	2.43	0.11	0.11	0.9604
2	Quinate	12.58	12.42	1.27	0.09	0.14	
3	2-HIB	14.22	13.79	3.00	0.18	0.25	
4	Lactate	14.61	14.26	2.42	0.25	0.36	
5	Glycolate	15.83	15.50	2.12	0.35	0.49	
6	Acetate	16.23	15.93	1.92	0.00	0.00	
7	Pyruvate	20.70	20.68	0.09	0.46	0.65	
8	Formate	21.10	20.84	1.26	0.65	0.85	
9	Galacturonate	22.72	22.23	2.21	0.09	0.10	
10	Malonate	44.84	44.03	1.38	0.48	0.66	
11	Maleate	45.45	44.81	1.43	0.46	0.61	
12	Malate	45.45	44.81	1.41	0.40	0.53	
13	Adipate	46.26	45.78	1.04	0.04	0.06	
14	Glutarate	46.67	45.98	1.49	0.09	0.17	
15	Tartrate	47.07	46.37	1.52	0.66	0.78	
16	Succcinate	47.48	46.76	1.53	0.17	0.27	
17	Oxalate	47.88	47.15	1.55	1.00	1.00	
18	α-ketoglutarate	56.00	55.34	1.18	0.50	0.58	

Table 3-1 *continued*

ID	Analyte	RT (min)			Normalised μ_{eff}		
		Experimental	Predicted	%Error	Experimental	Predicted	Correlation Coefficient
19	Fumarate	66.96	65.87	1.65	0.65	0.82	
20	Citrate	66.55	65.87	1.03	0.43	0.54	
21	*cis*-aconitate	70.61	69.76	1.21	0.60	0.81	
22	Isocitrate	70.61	69.76	1.21	0.45	0.54	
23	*trans*-aconitate	78.72	77.95	1.00	0.59	0.69	

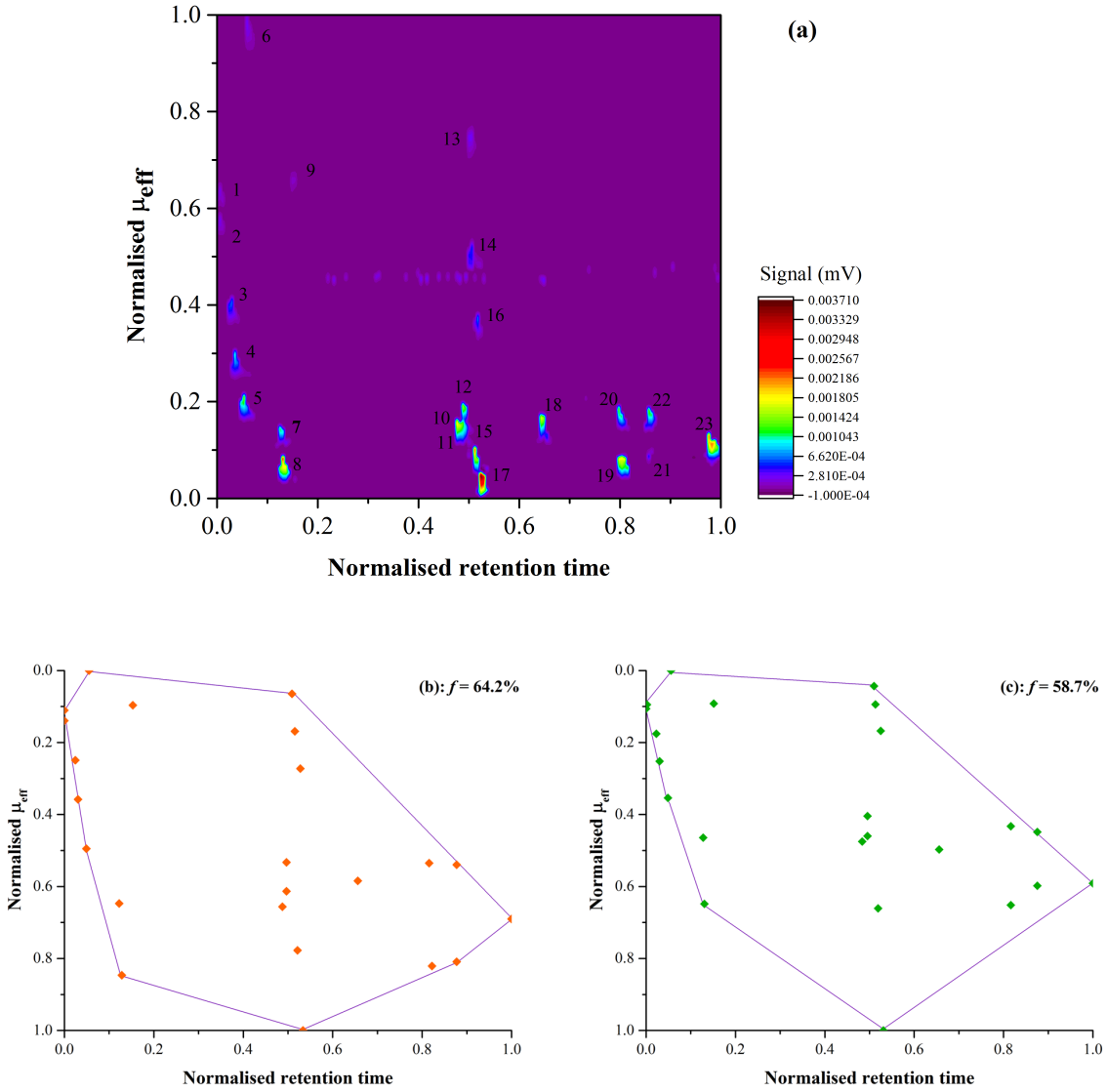

***Figure 3-5**: Upper panel (a), experimental optimised 2D separation of LMMOAs. IC conditions: IonPac AS24 separation column at 20 °C, separation flow rate of 0.150 mL/min, eluent profile: 5 mM hydroxide from 0-10 min followed by an increase to 65 mM by 102 min. CE conditions: fused silica separation capillary of 82 mm × 0.025 mm ID, +30 kV separation voltage, 10 mM NA titrated to pH 4.7 using HEPES, separations performed at room temperature. Peak IDs are the same as in **Table 3-1**. Bottom panel, experimental (b) versus predicted (c) fractional coverage for the optimised 2D separation.*

Firstly, high electric field strength (≥ +3 kV/cm) results in excessive Joule heating and therefore an inevitable rise of temperature inside the capillary which, leads to a change in the viscosity of the background electrolyte as well as in some cases variations in the pK_a of the acids and/or the background electrolyte components. Secondly, ramping increase of the separation voltage in the initial few seconds of the separation has proven to show quite a significant impact on measurement of mobility

in fast CE separations especially in case of the present work where a short detection length was utilised. Additionally, due to inclusion of PVP in background electrolyte, in order to suppress the electroosmotic flow, the obtained electrophoretic mobilities are considerably lower than the predicted values both as a result of increased viscosity of the background electrolyte as well as due to potential interactions between the anions and PVP and/or HEPES [39-41]. While it is possible to attempt to eliminate these systematic errors which are also reflected in the good correlation (0.9604) between the predicted and experimental electrophoretic mobilities, use of the uncorrected values for prediction of the optimal background electrolyte pH is still valid due to normalisation of the mobilities. These results imply that using the simplified approach proposed in this work, it is possible to define and optimise several objective functions such as 2D separation factor (in form of the Euclidean distance), analysis time and fractional space coverage.

As shown in the bottom panel of **Figure 3-5**, predicted (64.2%) *vs* experimental (58.7%) fractional space coverage values are also comparable and the deviation between the two can be explained through (i) presence of a subtle counter-EOF, although the EOF has been supressed using PVP, has resulted in increased gaps between the migration times as well as (ii) interaction of oxalate with pierazine-moiety containing background electrolyte cation, HEPES, similar to the effect previously noted by Noblitt et al. [42], has resulted in reduced electrophoretic mobility for this analyte and therefore more utilisation of the separation space as shown in **Figure 3-5**. This degree of coverage of the separation space resulted in a peak capacity of 1011 and a peak production rate of 11 peaks/min.

A closer look at **Figure 3-6**, which demonstrates the 2D plots for separation of yoghurt and mandarine juice, reveals that peaks 10 and 11 were not fully resolved. In order to overcome this shortcoming, mono-, di- and tri- valent ions were placed into three different clusters and attempts were made to optimise the background electrolyte pH for each individual cluster given the fact that the IC separation is largely charge-based and, there is a gap between the three elution clusters which would allow change of the background electrolyte pH throughout the first dimension run time, accordingly. However, there was no gain in selectivity using such an approach. Alternatively, simaltaneous tuning of the separation selectivity in both dimensions was necessary. This topic has been further covered in Chapter 4 of this thesis.

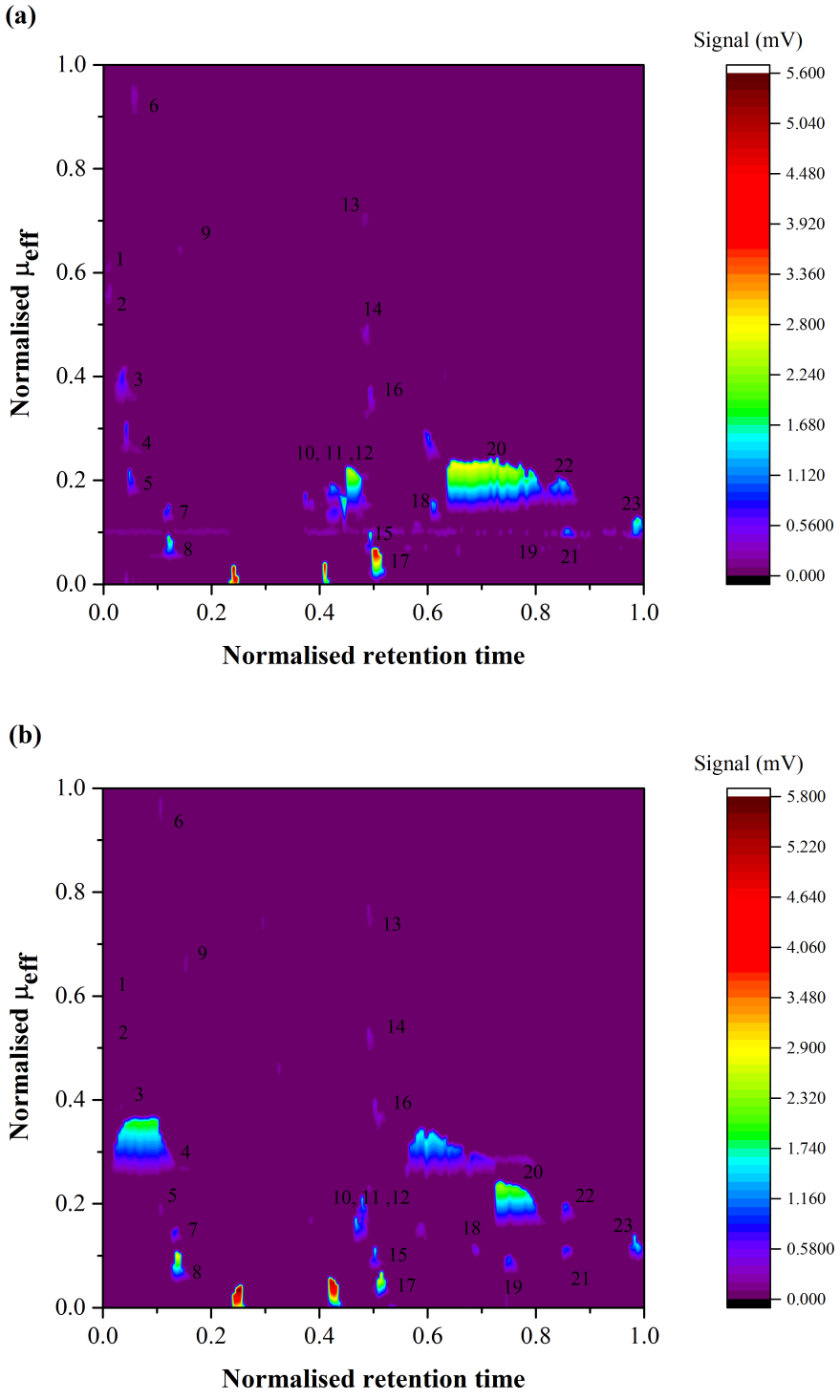

***Figure 3-6**: Chromatoelectropheorgrams for diluted mandarine juice (a) and yoghurt extract (b) samples both spiked with 10 mg/L of the acids. Peak IDs are the same as in **Table 3-1**.*

3.6 Conclusions

As noted in a review article by Haddad [7], separation selectivity in CE is mainly dictated by the analyte and can be changed through changing the composition of the background electrolyte. In contrast to IC where, apart from analyte-dependent parameters, the stationary phase imposes a huge influence on selectivity. With the role of background electrolyte pH on separation selectivity in ^{2}D for IC×CE separation of LMMOAs discussed in the current chapter, the impact of ^{1}D selectivity will be covered further in Chapter 4.

In brief, the present study demonstrates the effectiveness of using Euclidean distance between 2D peaks as a rapid approach for identifying the optimal background electrolyte pH as well as optimisation of the IC eluent profile. Additionally, prediction of IC×CE peak positions was achieved through the use of LSS model for IC and the fundamental equation relating the electrophoretic mobility of polyprotic ions to the background electrolyte pH in CE. While further optimisation of the eluent profile and minimising the gaps in between the mon-, di- and tri- valent clusters through designing multi-step gradients with the aim of reducing the analysis time is possible [21], there is undoubtedly a need for systematic selection of the selectivity parameters in IC or more precisely optimisation of *2D separation selectivity* in order to achieve full resolution of the target analytes prior to focusing on efficiency and analysis time.

3.7 References

[1] J.C. Giddings, Sample dimensionality: A predictor of order-disorder in component peak distribution in multidimensional separation, J. Chromatogr. A, 703 (1995) 3-15.

[2] M.J. Gray, G.R. Dennis, P.J. Slonecker, R.A. Shalliker, Evaluation of the two-dimensional reversed-phase–reversed-phase separations of low-molecular mass polystyrenes, J. Chromatogr. A, 1015 (2003) 89-98.

[3] M. Geiger, M.T. Bowser, Effect of Fluorescent Labels on Peptide and Amino Acid Sample Dimensionality in Two Dimensional nLC × µFFE Separations, Anal. Chem., 88 (2016) 2177-2187.

[4] J.C. Giddings, Two-dimensional separations: concept and promise, Anal. Chem., 56 (1984) 1258A-1270A.

[5] X. Li, D.R. Stoll, P.W. Carr, Equation for Peak Capacity Estimation in Two-Dimensional Liquid Chromatography, Anal. Chem., 81 (2009) 845-850.

[6] M. Gilar, J. Fridrich, M.R. Schure, A. Jaworski, Comparison of Orthogonality Estimation Methods for the Two-Dimensional Separations of Peptides, Anal. Chem., 84 (2012) 8722-8732.

[7] P.R. Haddad, Comparison of ion chromatography and capillary electrophoresis for the determination of inorganic ions, J. Chromatogr. A, 770 (1997) 281-290.

[8] S. Kar, P.K. Dasgupta, Direct coupling of ion chromatography with suppressed conductometric capillary electrophoresis, J. Micro. Sep., 8 (1996) 561-568.

[9] A. Beutner, S. Kochmann, J.J.P. Mark, F.-M. Matysik, Two-dimensional separation of ionic species by hyphenation of capillary ion chromatography x capillary electrophoresis - mass spectrometry, Anal. Chem., 87 (2015) 3134-3138.

[10] L. Ranjbar, A.J. Gaudry, M.C. Breadmore, R.A. Shellie, Online comprehensive two-dimensional ion chromatography × capillary electrophoresis, Anal. Chem., 87 (2015) 8673–8678.

[11] J. Kałużna-Czaplińska, E. Żurawicz, W. Struck, M. Markuszewski, Identification of organic acids as potential biomarkers in the urine of autistic children using gas chromatography/mass spectrometry, J. Chromatogr. B, 966 (2014) 70-76.

[12] P. Tůma, E. Samcová, K. Štulík, Determination of the spectrum of low molecular mass organic acids in urine by capillary electrophoresis with contactless conductivity and ultraviolet photometric detection—An efficient tool for monitoring of inborn metabolic disorders, Anal. Chim. Acta, 685 (2011) 84-90.

[13] Y. Wang, X. Chen, J.K. Whalen, Y. Cao, Z. Quan, C. Lu, Y. Shi, Kinetics of inorganic and organic phosphorus release influenced by low molecular weight organic acids in calcareous, neutral and acidic soils, J. Plant Nutr. Soil Sci., 178 (2015) 555-566.

[14] A.P. Schwab, D.S. Zhu, M.K. Banks, Influence of organic acids on the transport of heavy metals in soil, Chemosphere, 72 (2008) 986-994.

[15] H.B. Klinke, A.B. Thomsen, B.K. Ahring, Inhibition of ethanol-producing yeast and bacteria by degradation products produced during pre-treatment of biomass, Appl. Microbiol. Biotechnol., 66 (2004).

[16] L. Saavedra, A. García, C. Barbas, Development and validation of a capillary electrophoresis method for direct measurement of isocitric, citric, tartaric and malic acids as adulteration markers in orange juice, J. Chromatogr. A, 881 (2000) 395-401.

[17] S. Ehling, S. Cole, Analysis of Organic Acids in Fruit Juices by Liquid Chromatography−Mass Spectrometry: An Enhanced Tool for Authenticity Testing, J. Agric. Food. Chem., 59 (2011) 2229-2234.

[18] M. Stratford, T. Eklund, Organic acids and esters, in: N.J. Russell, G.W. Gould (Eds.) Food Preservatives, Springer US, Boston, MA, 2003, pp. 48-84.

[19] S.S. Brudin, R.A. Shellie, P.R. Haddad, P.J. Schoenmakers, Comprehensive two-dimensional liquid chromatography: Ion chromatography × reversed-phase liquid chromatography for separation of low-molar-mass organic acids, J. Chromatogr. A, 1217 (2010) 6742-6746.

[20] G. Semard, V. Peulon-Agasse, A. Bruchet, J.-P. Bouillon, P. Cardinaël, Convex hull: A new method to determine the separation space used and to optimize operating conditions for comprehensive two-dimensional gas chromatography, J. Chromatogr. A, 1217 (2010) 5449-5454.

[21] E. Tyteca, S.H. Park, R.A. Shellie, P.R. Haddad, G. Desmet, Computer-assisted multi-segment gradient optimization in ion chromatography, J. Chromatogr. A, 1381 (2015) 101-109.

[22] Chapter 5 Retention Models for Ion-Exchange, in: R.H. Paul, R.H. Paul (Eds.) Journal of Chromatography Library, Elsevier, 1990, pp. 133-162.

[23] M.A. Quarry, R.L. Grob, L.R. Snyder, Prediction of precise isocratic retention data from two or more gradient elution runs. Analysis of some associated errors, Anal. Chem., 58 (1986) 907-917.

[24] S.J. Gluck, K.P. Steele, M.H. Benkö, Determination of acidity constants of monoprotic and diprotic acids by capillary electrophoresis, J. Chromatogr. A, 745 (1996) 117-125.

[25] J.M. Cabot, E. Fuguet, C. Ràfols, M. Rosés, Determination of acidity constants by the capillary electrophoresis internal standard method. IV. Polyprotic compounds, J. Chromatogr. A, 1279 (2013) 108-116.

[26] G.A. Blanco, Y.H. Nai, E.F. Hilder, R.A. Shellie, G.W. Dicinoski, P.R. Haddad, M.C. Breadmore, Identification of Inorganic Improvised Explosive Devices Using Sequential Injection Capillary Electrophoresis and Contactless Conductivity Detection, Anal. Chem., 83 (2011) 9068-9075.

[27] A.J. Gaudry, R.M. Guijt, M. Macka, J.P. Hutchinson, C. Johns, E.F. Hilder, G.W. Dicinoski, P.N. Nesterenko, P.R. Haddad, M.C. Breadmore, On-line simultaneous and rapid separation of anions and cations from a single sample using dual-capillary sequential injection-capillary electrophoresis, Anal. Chim. Acta, 781 (2013) 80-87.

[28] M. Jaroš, K. Včeláková, I. Zusková, B. Gaš, Optimization of background electrolytes for capillary electrophoresis: II. Computer simulation and comparison with experiments, Electrophoresis, 23 (2002) 2667-2677.

[29] H. Holvik, H. Høiland, Acidity constants of galacturonic and glucuronic acids in water at 298.15 K from conductance and e.m.f. measurements, The Journal of Chemical Thermodynamics, 9 (1977) 345-348.

[30] C. Klofutar, N. Šegatin, Electrical Conductivity Studies of Quinic Acid and its Sodium Salt in Aqueous Solutions, J. Solution Chem., 36 (2007) 879-889.

[31] L. Pfendt, Z. Vitnik, Determination of all pKa values of some di- and tri-carboxylic unsaturated and epoxy acids and their polylinear correlation with the carboxylic group atomic charges, Journal of Chemical Research, 2003 (2003) 247-248.

[32] S.L. Miller, D. Smith-Magowan, The Thermodynamics of the Krebs Cycle and Related Compounds, J. Phys. Chem. Ref. Data, 19 (1990) 1049-1073.

[33] L.J. Wang, S. Henday, B. Ogren, W. Schnute, D. Hazlebeck, A. Roberts, J. Zhang, R. Corpuz, Determination of 32 Low Molecular Mass Organic Acids in Biomass Using IC/MS, Dionex Corporation Application Note, (2009) (http://www.thermofisher.com/).

[34] B.W.J. Pirok, S. Pous-Torres, C. Ortiz-Bolsico, G. Vivó-Truyols, P.J. Schoenmakers, Program for the interpretive optimization of two-dimensional resolution, J. Chromatogr. A, 1450 (2016) 29-37.

[35] M.R. Schure, Quantification of Resolution for Two-Dimensional Separations, J. Micro. Sep., 9 (1997) 169-176.

[36] R. Al Bakain, I. Rivals, P. Sassiat, D. Thiébaut, M.-C. Hennion, G. Euvrard, J. Vial, Comparison of different statistical approaches to evaluate the orthogonality of chromatographic separations: Application to reverse phase systems, J. Chromatogr. A, 1218 (2011) 2963-2975.

[37] Wessa, Kendall tau Rank Correlation (v1.0.11) in Free Statistics Software (v1.1.23-r7), Office for Research Development and Education, URL http://www.wessa.net/rwasp_kendall.wasp/.

[38] P.M. Nowak, M. Woźniakiewicz, P. Kościelniak, Seven Approaches to Elimination of the Inherent Systematic Errors in Determination of Electrophoretic Mobility by Capillary Electrophoresis, Anal. Chem., (2017).

[39] T. Kaneta, T. Ueda, K. Hata, T. Imasaka, Suppression of electroosmotic flow and its application to determination of electrophoretic mobilities in a poly(vinylpyrrolidone)-coated capillary, J. Chromatogr. A, 1106 (2006) 52-55.

[40] V. Madajová, E. Turcelová, D. Kaniansky, Influence of poly(vinylpyrrolidone) on isotachophoretic separations of inorganic anions in aqueous electrolyte systems, J. Chromatogr. A, 589 (1992) 329-332.

[41] S.D. Noblitt, L.R. Mazzoleni, S.V. Hering, J.L. Collett Jr, C.S. Henry, Separation of common organic and inorganic anions in atmospheric aerosols using a piperazine buffer and capillary electrophoresis, J. Chromatogr. A, 1154 (2007) 400-406.

[42] S.D. Noblitt, F.M. Schwandner, S.V. Hering, J.L. Collett Jr, C.S. Henry, High-sensitivity microchip electrophoresis determination of inorganic anions and oxalate in atmospheric aerosols with adjustable selectivity and conductivity detection, J. Chromatogr. A, 1216 (2009) 1503-1510.

4 In silico screening of two-dimensional separation selectivity for ion chromatography × capillary electrophoresis

"Somewhere there is a map of how it can be done."
— Ben Stein

This chapter has been submitted for peer review as a research article. Herein, it is reproduced with minor modifications to avoid replication of overlapping content with the preceding chapters.

4.1 Overview

A prerequisite for ordered two-dimensional (2D) separations and full utilisation of the enhanced 2D peak capacity is selective exploitation of the sample attributes as described in Chapter 3. In order to take sample dimensionality into account prior to optimisation of a 2D separation, a new approach based on construction of 2D separation selectivity maps is proposed and demonstrated for IC×CE separation of low-molecular-mass organic acids as test analytes. For this purpose, 1D separation selectivity maps were constructed based on calculation of pairwise separation factors and identification of critical pairs for four IC stationary phases and 28 levels of background electrolyte pH in CE. The derived maps were then superimposed and the effectiveness of the respective 2D separations were assessed using an *in silico* approach, followed by testing examples of one successful and one unsuccessful 2D combinations experimentally. The results confirmed the efficacy of the predictions, which require a minimal number of experiments compared to the traditional one-at-a-time approach. Following the same principles, the proposed framework can also be adapted for optimisation of separation selectivity in various 2D combinations and for other applications.

4.2 Introduction

Traditionally, prior to performing a 2D separation, the 1D separation selectivity in each dimension is adjusted through a number of trial-and-error experiments. However, in cases where sample dimensionality changes notably with changing the separation conditions, pursuing a trial-and-error approach would result in performing a large number of experiments which is far from practical, especially with increasing the number of sample components or the selectivity parameters that need to be considered in the search. In addition, such a strategy would not necessarily guarantee an ordered 2D separation since selectivity in each dimension is considered independently. An example of significant changes in selectivity caused by changing separation conditions can be seen in CE separation of low-molecular-mass organic acids (LMMOAs) as shown in Chapter 3, where even a 0.1 unit change in the background electrolyte pH results in very different electrophoretic mobilities due to the change in ionisation state [1].

In the present study a proof-of-concept approach for simultaneous screening of 2D separation selectivity performing a minimum number or even no experiments is demonstrated and evaluated for ion chromatography × capillary electrophoresis (IC×CE) separation of LMMOAs as test analytes. In order to find the most orthogonal separation conditions with regard to the sample dimensionality amongst numerous combinations of stationary phases in IC and background electrolyte pH in CE, pairwise separation factors for each analyte against all the other analytes were calculated and separation selectivity maps highlighting the critical pairs which were difficult to separate were plotted for each separation dimension. 1D selectivity maps were then superimposed for all possible IC column and CE pH combinations. Those combinations demonstrating no overlapping critical pairs were deemed to be the best for achieving full resolution of all analytes.

4.3 Theory/ background

Prediction of resolution (*Rs*) for two neighbouring chromatographic peaks *A* and *B* is only possible when all the three contributors, namely efficiency (*N*), selectivity (α) and retention (*k*) are known as shown in **Equation 4-1** [2]:

$$Rs = \frac{\sqrt{N}}{4}(\alpha - 1)(\frac{k_A}{1+\bar{k}}) \quad and \quad \bar{k} = \frac{k_A + k_B}{2}$$

Equation 4-1

The retention mechanism in IC is well understood and modelled [3] and this enables precise prediction of the selectivity and retention terms in **Equation 4-1**. It is also generally possible to predict the peak width and therefore the separation efficiency, however, predictions for individual peak widths using a single isocratic plate number (N) are prone to errors, especially in case of asymmetrical peaks which are quite common in IC [4-6].

Although the separation factor ($\alpha = k_A/k_B; k_A \geq k_B$) is not an adequate measure for describing the separation quality, it can be easily predicted and utilised for screening purposes. As a rule of thumb, a value of $\alpha \geq 1.2$ indicates adequate separation and suffices for baseline resolution of neighbouring peaks.

4.3.1 Prediction of retention in IC

Retention of an anion A^{x-} on an ion exchange stationary phase using an hydroxide eluent can be described by **Equation 4-2** [3]:

$$\log k_{A^{x-}} = \log K_{A^{x-},OH^-} + x\log Q + \log\frac{w}{V_m} - x\log[OH^-]$$

Equation 4-2

Where k_A^{x-} is the retention factor, $[OH^-]$ is the concentration of the eluent, K_{A^{x-},OH^-} is the selectivity coefficient between the analyte and the hydroxide eluent competing for ion-exchange sites on the ion-exchanger stationary phase, and Q, V_m and w are the ion-exchange capacity, dead volume and weight of the stationary phase, respectively. For a certain stationary phase, **Equation 4-2** also known as the linear solvent strength (LSS) model in IC, can be simplified to:

$$\log k_{A^{x-}} = a_{A^{x-}} - b_{A^{x-}}\log[OH^-]$$

Equation 4-3

where the intercept, a-, includes the first three terms in **Equation 4-2** and the slope, b-, is ideally equal to the ratio of the charges of the analyte and the eluent competing ion.

Equation 4-2 also demonstrates that for analytes of the same charge, separation selectivity (α) is independent of the size and capacity of the column as well as the composition of the eluent as shown in **Equation 4-4** [7, 8]:

$$\log\alpha_{A^{x-},B^{x-}} = \log\frac{k_{A^{x-}}}{k_{B^{x-}}} = \log K_{A^{x-},OH^-} - \log K_{B^{x-},OH^-}$$

Equation 4-4

Combination of **Equation 4-3** and **Equation 4-4** suggests that in order to predict α for analytes of the same charge, one simply needs to subtract the intercepts of the ideally parallel correlation lines of LSS model for the two analytes:

$$\log \alpha_{A^{x-},B^{x-}} = a_{A^{x-}} - a_{B^{x-}}$$ ***Equation 4-5***

However in practice, the LSS correlation lines for the analytes of the same charge are not necessarily parallel since both *a*- and *b*- can deviate from theory to some extent and, therefore, are calculated through experimental measurement of retention factor for at least three isocratic eluent compositions [9]. As a result, to predict the separation selectivity from the LSS model, the distance between LSS correlation lines for analytes *A* and *B* needs to be calculated. Regardless of the eluent concentration, if the maximum distance between the lines is less than 0.08 ($0 \leq \log \alpha < 0.08$), the analyte pair is considered as critical suggesting that the utilised stationary phase is unlikely to offer sufficient selectivity for baseline resolution of the two ions.

4.3.2 Prediction of migration in CE

As described previously in Chapter 3, migration of a polyprotic acid H_xA in capillary electrophoresis is dependent on various factors, most significantly on its ionisation state. With the ionisation degree being determined by the thermodynamic acidity constant (pK_a), the effective mobility of a polyprotic acid (μ_{eff}) can be related to the pH of the background electrolyte using **Equation 4-6** [10, 11]:

$$\mu_{eff} = \frac{\sum_{i=1}^{x} 10^{ipH - \sum_{j=1}^{i} pK_{aj}} \cdot \mu_{H_{x-i}A^{-i}}}{1 + \sum_{i=1}^{x} 10^{ipH - \sum_{j=1}^{i} pK_{aj}}}$$

Equation 4-6

$$\mu_{app} = \mu_{eff} + \mu_{eof}$$

Equation 4-7

$$\mu = \frac{Ll}{Vt}$$

Equation 4-8

Where $\mu_{Hx\text{-}iA}^{-i}$ is the mobility of the intermediate specie at the i^{th} ionisation state with μ_A^{-x} being the mobility of the most deprotonated form. μ_{app} and μ_{eof} are the analyte apparent electrophoretic mobility and the mobility for the electroosmotic flow, respectively. Electrophoretic mobility can be calculated using the migration time (*t*),

separation voltage (V) and total capillary length (L) in addition to the effective length of the capillary (l) as shown in **Equation 4-8**.

Through the use of **Equation 4-6**, if the mobility of the intermediate species and the acidity constants are known, μ_{eff} can be predicted at any pH of the background electrolyte.

As shown by Terabe et al. [12], in a similar manner to chromatography, dependence of resolution of analyte peaks A and B to electrophoretic separation selectivity can be expressed by:

$$Rs = \left(\frac{Vl}{32L}\right)^{1/2}\left(\frac{\bar{\mu}_{eff}}{D}\right)^{1/2}\left(\frac{\alpha-1}{\alpha}\right)\left(1+\frac{\mu_{eof}}{\bar{\mu}_{eff}}\right)^{-1/2} \quad ;\alpha = \frac{\mu_{eff,B}}{\mu_{eff,A}} \geq 1$$

Equation 4-9

Equation 4-9 shows that once μ_{eff} is known, separation selectivity can be predicted for any given background electrolyte pH as an indicative parameter rather than an exact measure for predicting resolution, since it excludes any efficiency term as mentioned earlier. CE separation selectivity values greater than 1.02 are required to achieve baseline resolution in absence of electroosmotic flow [12].

4.4 Materials and methods

4.4.1 Chemicals and reagents

The chemicals used in all experiments were of analytical grade. 10,000 mg/L stock solutions of the anions were prepared by dissolving 2-hydroxyisobutyric acid, citric acid tri-sodium dihydrate, sodium foramte, fumaric acid, glutaric acid, sodium DL-lactate, *trans*-aconitic acid, *cis*-aconitic acid, DL-malic acid, DL-isocitric acid tri-sodium salt and glycolic acid, all from Sigma Aldrich (Sigma-Aldrich, St. Louis, MO, USA); sodium acetate and adipic acid from Ajax (Ajax Chemicals, Unilab, Auckland, New Zealand); soldium malonate, sodium oxalate, and sodium succinate hexahydrate from BDH (BDH, West Chester, PA, USA); and, sodium pyruvate, α-ketoglutaric acid di-sodium dihydrate salt, maleic acid, sodium D-gluconate acid and D-galacturonic acid, quinic acid from Fluka (Sigma-Aldrich, St. Louis, MO, USA) in either Milli-Q water or basic aqueous solution (in case of the acid having low water solubility) through the addition of 0.1 M sodium hydroxide solution.

Background electrolyte components, nicotinic acid (NA), 4-(2 hydroxyethyl)piperazine-1-ethanesulfonic acid (HEPES), tris(hydroxymethyl)aminomethane (Tris), 2-(cyclohexylamino)ethanesulfonic acid

(CHES) and poly(vinylpolypyrrolidone) (PVP), were all purchased from Sigma-Aldrich.

Reagents used for conditioning new capillaries included sodium hydroxide (Sigma-Aldrich), hydrochloric acid, and methanol, all purchased from Merck (Merck, Darmstadt, Germany). Araldite 5 minutes epoxy glue (Selleys Pty Ltd, Padstow, NSW, Australia) was used for electrical isolation of the joint capillaries.

Milli-Q water from a Millipore water purifier (Millipore, Bedford, MA, USA) was used as input for the IC eluent generator, external water feeding of the suppressor, and preparation of all solutions.

4.4.2 Instrumentation

2D separations were achieved in the same manner described in Chapters 2 and 3 [13]. In brief, first-dimension separations were performed using either an IonPac AS11-HC or AS19 column (250 mm × 2 mm ID) with the respective guard columns namely IonPac AG11-HC and IonPac AG19 (50 mm×2 mm ID) on an IC-5000 ion chromatograph equipped with a ASRS Ultra II 2-mm suppressor operated in external water mode (Thermo Fisher Scientific, Sunnyvale, CA, USA). All analyses were performed at a flow-rate of 0.150 mL/min while the separation temperature was maintained at 30°C. Details of the eluent profiles can be found in figure captions. An injection volume of 50 µL was used in all the experiments. The IC effluent was sampled by a sequential injection capillary electrophoresis (SI-CE) instrument equipped with a Tracedec capacitively coupled conductivity detector (C^4D) from Innovative Sensor Technologies, Strassahof, Austria [13-15]. A 700 mm × 0.125 mm ID PEEK tubing (Thermo Fisher Scientific) was used for connecting the two dimensions. Instrument control and data acquisition was performed using a program written in LabVIEW (LabVIEW 2011, National Instruments, Austin, TX, USA). Data processing was performed in Origin 9.0 (OriginLab, Northampton, MA, USA).

All CE experiments were conducted at room temperature in an 86 mm × 0.025 mm ID bare fused-silica capillary which was jointed to a 152 mm × 0.100 mm ID bare fused-silica capillary using a 7 mm × 0.250 mm ID piece of Teflon tubing. Through the use of a short separation capillary all separations were performed at an electrical field strength of +3.14 kV/cm. Details of the procedure used for cutting, connecting and insulating the joint capillaries, together with a microscope image of the joint, can be found in Chapter 3.

4.4.3 QSRR modelling

In order to optimise the separation selectivity in IC a fully *in silico* approach was followed using the retention data embedded in Virtual Column software (Thermo Fisher Scientific, Sunnyvale, CA, USA). Isocratic *a*- and *b*- values for 18 analytes were derived by fitting their respective embedded gradient retention times to **Equation 4-10**, which describes gradient elution retention in IC [16, 17]:

$$t_g = (\frac{1}{u})\{(\frac{1}{B})[(10^b+1)10^a Bt_0u + C_i^{(10^b+1)}]^{1/(10^b+1)} - \frac{C_i}{B}\} + t_0$$

Equation 4-10

Where t_g is the retention time of the analyte under gradient elution, u and C_i are the flow-rate and initial concentration of the eluent, respectively, and B is the normalised gradient ramp derived through dividing the gradient ramp (R) by the separation flow-rate (R/u). The fittings were performed using the Solver function in Microsoft Excel 2011 for the two most different gradients (having different starting concentrations and gradient ramps) as previously reported by Quary et al. [18].

Virtual Column contains data for 18 out of the 23 target analytes. For the remaining analytes, namely 2-hydroxyisobutyrate, gluconate, galacturonate, adipate and α-ketoglutarate, quantitative structure-retention relationship (QSRR) modelling was employed to predict *a*- and *b*- values based solely on their chemical structures in an approach previously described by Park et al. [19]. In brief, QSRR models for *a*- and *b*- values in the LSS retention model (**Equation 4-3**) were generated by partial least square (PLS) regression using the most relevant molecular descriptors selected by a genetic algorithm (GA). The dataset used for this purpose consisted of fitted isocratic *a*- and *b*- values (as described earlier in this section) for 43 anions on four columns (250 mm × 4 mm ID Thermo Fisher IonPac AS11-HC, AS11, AS19, and AS16) under the following conditions: eluent flow-rate of 1.0 mL/min, a column temperature of 30°C, and suppressed conductivity detection. To derive molecular descriptors, molecular structures of the respective ions were drawn using MarvinSketch version 6.2.1 (ChemAxon, Budapest, Hungary) and subjected to initial conformational searches. The geometry of the 50 lowest energy structures, found by using the Merck Molecular Force Field (MMFF94) [20-23] (implemented in Balloon [24, 25]), were then optimised in water by the semi-empirical Parametric Method 7 (PM7) [26] carried out in Molecular Orbital PACkage (MOPAC) (Stewart Computational Chemistry, Colorado Springs, CO, USA). Optimised 3D structures were then imported into Dragon 6.0 software (Talete, Milano, Italy) to calculate molecular

descriptors. 4885 descriptors were initially calculated, from which descriptors containing constant values, those with at least one missing value, those having a standard deviation ≤ 0.0001, or those with an absolute pair-wise correlation ≥0.9 were excluded. In the next step, the most relevant descriptors were selected from the remaining 489 descriptors using a GA with the following parameters: original population size.- 50; the maximum selection probability - 20 variables per chromosome; the average selection probability - 10 variables per chromosome; cross-over probability - 50%; mutation - 1%; the number of assessments prior to a backward elimination – 100 [27]. Prior to descriptor selection and modelling, ions of the same charge in the dataset were ranked according to their pairwise Tanimoto similarity (TS) scores to each target ion. Subsequently, training sets for modelling *a*- and *b*- values were derived by including only the top 5 most similar ions to each target ion. These training sets were then employed to build individual QSRR models for prediction of *a*- and *b*- values for the corresponding target ions. For this purpose, the GA was run using each training set and PLS models were built by correlating the *a*- and *b*- values with the descriptors chosen by the GA. This procedure was repeated 5 times and the mean values of predicted *a*- and *b*- values were used for prediction of separation selectivity. The GA-PLS algorithm used was a customised version of the original Matlab (MathWorks, Natick, MA, USA) routines written by Leardi and González[28]. TS calculations were performed using JChem for Excel (ChemAxon, Budapest, Hungary).

4.5 Results and discussions

4.5.1 General approach

Effective single dimensional IC separation of LMMOAs is only feasible while using tandem mass spectrometry (MS/MS) detection due to similar retentive behaviour of the acids as a result of similarities in their structure and/or charge. Although offering a substantial degree of resolution, use of MS/MS is unsuitable for the detection of lower molecular-mass acids e.g. formic acid, acetic acid and oxalic acid, due to volatility issues or weak response [29]. As a result, to address the deficiencies of single dimensional IC for separation of these acids, two-dimensional separations using IC as one of the dimensions have emerged [30]. However, none of these studies provides details of insights into the basis of column selection and choice of separation

selectivity in either of dimensions. Using IC×CE separation of LMMOAs as an example, the current Chapter aims to introduce a framework for adjusting the separation selectivity via systematic screening of separation conditions as a critical initial stage in optimisation of 2D separations.

With several factors, such as stationary phase composition, type and structure of ion-exchange resin, type, concentration and pH of the eluent, eluent modifiers and temperature affecting the separation selectivity in IC [31] and, pH, ionic strength and composition of the background electrolyte, surface/electroosmotic flow modifiers, separation voltage and temperature impacting the separation selectivity in CE, optimisation of separation selectivity for IC×CE separation of LMMOAs in a one-at-a-time approach would result in an exceedingly large number of experiments if all parameters are included in the study. Fortunately, in the case of both techniques, computer software packages such as Virtual Column [9] and Peakmaster [32] which include a database of an extensive number of ions and separation parameters can be utilised to facilitate faster method development.

4.5.2 Separation selectivity in IC

Virtual Column software, developed by Madden et al. in 2002 [9] and commercialised by Thermo Fischer Scientific later, offers the possibility of choosing the most suitable stationary phase and elution profile, as well as prediction of retention time and subsequent simulation of IC chromatograms for the separation of 122 ions (including 78 anions on 11 commercially available columns [4]). Although a considerable number of LMMOAs are included in its database (18 out of the 23 compounds of interest in this work), Virtual Column does not predict any separation conditions which would provide full resolution of these acids. Use of an orthogonal second dimension is therefore essential to achieve full resolution, however, even this approach does not necessarily guarantee full resolution of LMMOAs if separation conditions in each dimension are chosen independently. As an example, choosing the separation column based on the minimum resolution (R_s min) criterion defined in Virtual Column would lead to the assumption that the AS19 column with an R_s min value of 0.254 (against 0.113 for AS11, 0.068 for AS11-HC and, 0.083 for AS16) offers the best performance for the 2D separation of the acids, however, this is not the case as demonstrated further in this section. Therefore a simultaneous rather than subsequent approach for the selection of separation selectivity in both dimensions,

implemented by taking the often-ignored sample dimensionality into consideration, is favoured to ensure full exploitation of the peak capacity of a 2D system [33].

The stationary phase in IC and the background electrolyte pH in CE can be considered as the two main parameters affecting the selectivity in a typical IC×CE separation and therefore these were studied in detail as described below. In order to minimise the number of experiments, the data embedded in both Virtual Column and Peakmaster were used for identifying the *critical pairs* where available. The term critical pair refers to a pair of analytes that cannot be baseline-resolved when using a certain IC column or CE background electrolyte pH. Critical pairs in each dimension were identified by prediction of the separation factor for each analyte against all the other LMMOAs, as described below.

Critical pairs in IC ($1.0 \leq \alpha < 1.2$) were identified after considering the fact that the likelihood of co-elutions occurring for LMMOAs of different charge is extremely low. This arises because all analytes under consideration are quite similar in overall structure and their separation is therefore based predominantly on charge. Analytes of the same charge were compared against each other within mono-, di- and tri-valent clusters. In such a manner, as shown earlier, the separation selectivity is independent of eluent concentration, which implies that any pair of analytes with $1.0 \leq \alpha < 1.2$ will not be fully resolvable on the respective stationary phase even through optimisation of the hydroxide eluent concentration/profile.

In order to calculate the pairwise separation factors, the distances ($\log\alpha$) between the correlation lines in LSS plots, based on the fitted and predicted isocratic *a*- and *b*-values for the given compounds, were calculated. This process was performed for the 18 compounds present in the Virtual Column database and the 2 additional acids (2-hydroxyisobutyrate, and adipate) for which isocratic *a*- and *b*- values were predicted using QSRR. Galacturonate, gluconate and α-ketoglutarate were excluded from the predictions due to the lack of a sufficient number of structurally similar compounds in the dataset which hinders the accurate prediction of their *a*- and *b*- values. The best training sets for these three compounds all showed similarity indices <0.40, as seen in the similarity ranking **Table 4-1** in the supporting information. Previous studies have suggested that a training set of at least 5 compounds having average similarities greater than 0.5 compared to the test compound is a requirement for reliable predictions [19, 27]. The exclusion of galacturonate, gluconate and α-ketoglutarate from predicition of *a*- and *b*- values is a direct result of the small dataset available on

***Table 4-1**: Similarity ranking table for QSRR modelling*

Target analyte:	**2-hydroxyisobutyrate**		**ketoglutarte**		**adipate**		**galacturonate**		**gluconate**	
	Top 5 similar compounds	TS index	Top 5 similar compounds	TS index	Top 5 similar compounds	TS index	Top 5 similar compounds	TS index	Top 5 similar compounds	TS index
	lactate	0.86	glutarate	0.67	glutarate	0.64	quinate	0.71	quinate	0.74
	propionate	0.59	succinate	0.49	succinate	0.52	valerate	0.42	valerate	0.42
	glycolate	0.55	malate	0.41	malonate	0.41	lactate	0.38	lactate	0.38
	pyruvate	0.52	tartrate	0.41	malate	0.39	butyrate	0.34	butyrate	0.34
	butyrate	0.50	malonate	0.30	tartrate	0.39	propionate	0.26	propionate	0.26

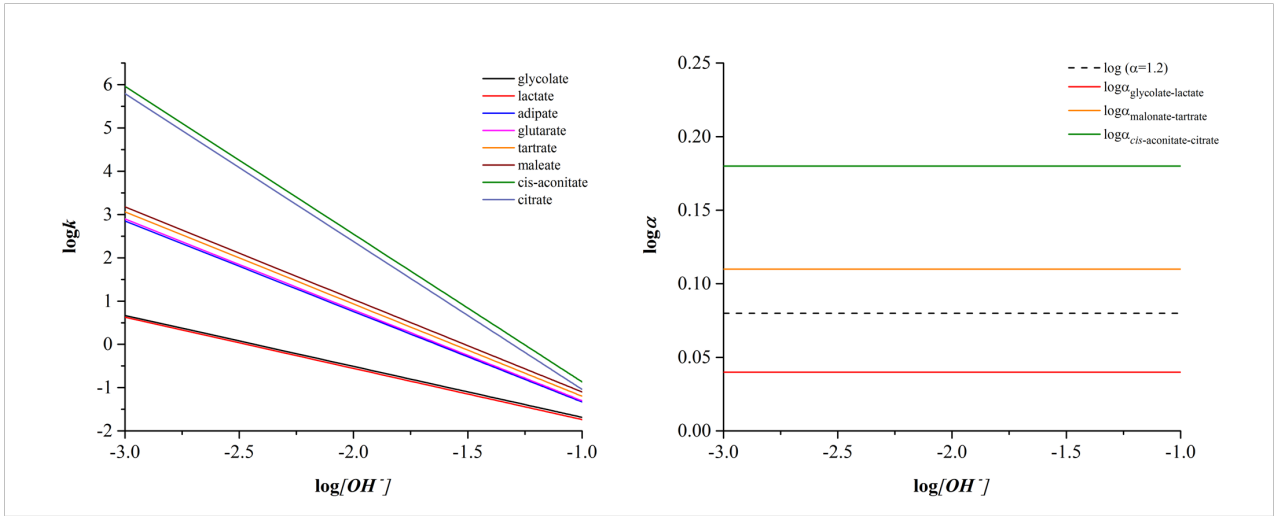

(a) **(b)**

***Figure 4-1**: (a): log[OH]-logk (LSS) correlations for a representative number of mono-, di- and tri-valent ions and (b): pairwise log[OH]-logα for the same analytes presented in (a).*

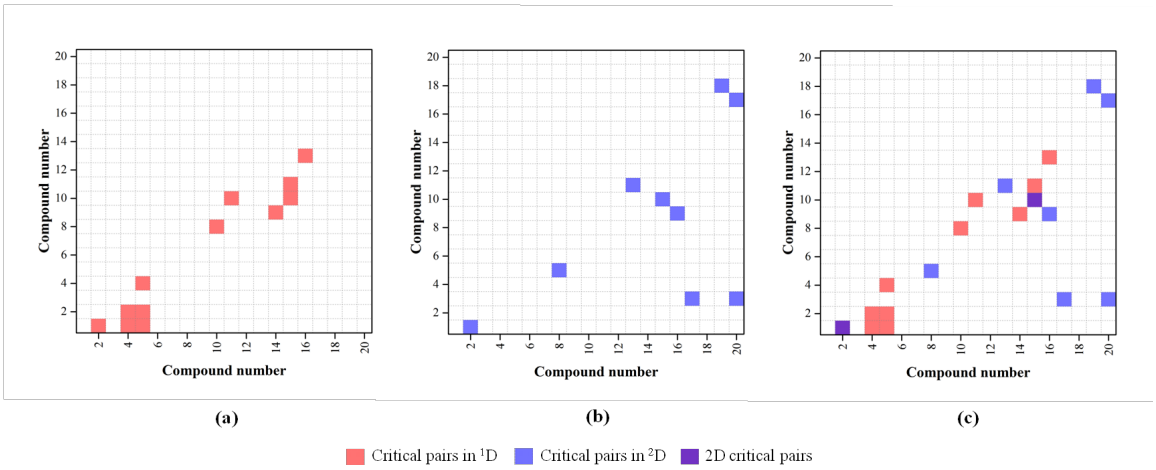

***Figure 4-2**: (a): pairwise IC selectivity map for AS11-HC column; (b): pairwise CE selectivity map for background electrolyte pH 5.2; (c): pairwise 2D selectivity map for combination of AS11-HC column in ^{1}D and background electrolyte pH 5.2 in ^{2}D. 2D critical pairs (in purple) are 1-2 as well as 13-18. Compound IDs (in alphabetical order for separate clusters): 1, 2-hidroxyisobutyrate; 2, acetate; 3, formate; 4, glycolate; 5, lactate; 6, pyruvate; 7, quinate; 8, adipate;; 9, fumarate; 10, glutarate; 11, malate; 12, maleate; 13, malonate; 14, oxalate; 15, succinate; 16, tartrate; 17, cis-aconitate; 18, citrate; 19, isocitrate and 20, trans-aconitate.*

Virtual Column and shows the potential value of larger datasets. The primary purpose of the current work is to provide proof-of-concept for the proposed selectivity screening methodology, rather than precise optimisation of the 2D separation for all analytes in a particular application.

Figure 4-1 shows LSS correlations along with their calculated pairwise $\log\alpha$ graphs for a selected number of analyte pairs. Any pairs lying below the threshold line of $\log(\alpha = 1.2)$ (e.g. lactate-glycolate on AS11-HC as shown in **Figure 4-1**b) were deemed to be critical pairs in IC. In cases where the line stood above the threshold (e.g. maleate-tartrate and *cis*-aconitate-citrate), co-elution was regarded as unlikely implying that the retention of these compounds was substantially different.

The identified critical pairs were then illustrated for individual columns as *selectivity maps*. As an example, **Figure 4-2**a depicts the IC selectivity map for separation of the LMMOAs on AS11-HC. Each red square on the map represents a chromatographic critical pair corresponding to compound IDs on the vertical and horizontal axes. This selectivity map also confirms that full single-dimensional resolution of the acids using this particular column is impossible.

4.5.3 Separation selectivity in CE

In the next step, the critical pairs in CE were identified following the discussion in theory/background section. Briefly, effective mobility was calculated for each analyte at increments of 0.1 units of background electrolyte pH (from pH 4.7 to pH 7.5) based on **Equation 4-6** using the pK_a values, and the mobility of intermediate and totally ionised species embedded in Peakmaster 5.3 for 18 out of 23 analytes [32]. Thermodynamic acidity constants for the remaining 5 analytes (galacturonate, quinate, α-ketoglutarate, *cis*-aconitate and *trans*-aconitate) were extracted from the literature [34-37], while the mobilities of the fully ionised species for these acids were experimentally measured using a background electrolyte of pH 8.80 with an ionic strength of 4.95 mM (30 mM Tris-30 mM CHES containing 0.1% PVP). The obtained mobilities were further extrapolated against the Peakmaster data in order to construct a uniform dataset. Similar to our previous findings, the use of relative effective mobilities (separation factor) eliminates the need for accurate prediction of apparent mobilities in CE in the same manner as relative retention factors in IC.

Selectivity maps were plotted for each pH level in CE. An example of a CE selectivity map for pH 5.2 can be seen in **Figure 4-2**b, where each blue square represents an electrophoretic critical pair ($\alpha_{CE} < 1.02$). Once again, this selectivity map clearly demonstrates that 1D electrophoretic separation of the current analyte set with a background electrolyte pH of 5.2 is not feasible and thus a 2D separation is necessary.

4.5.4 2D selectivity maps

Figure 4-2c depicts the 2D selectivity map, which was constructed by superimposing 1D selectivity maps. The purple squares on this map depict 2D critical pairs which are analyte pairs (1 and 2 as well as 10 and 15 in this case) that cannot be resolved even through an orthogonal coupling of IC with CE due to an inappropriate choice of pairing an IonPac AS11-HC column in the ^{1}D with a background electrolyte pH 5.2 in the ^{2}D.

A representative number of 2D selectivity maps for four IC columns and three background electrolyte pH levels have been included in **Figure 4-3**. It is worthy to mention that AS24, which was used as the ^{1}D column in Chapter 3, was excluded from this study as its lack of efficacy for separation of the LMMOAs was proved in our previous experiments. A selected number of selectivity maps for this column have

been included in Appendix 1. It can be inferred from **Figure 4-3** that amongst all the included columns and pH levels, hyphenation of AS11 or AS11-HC in IC and pH level of 4.7 in CE is a potentially successful 2D combination while using either AS 19 or AS16 in ^{1}D with the same pH level would not result in full resolution. In the same way, **Figure 4-3** indicates that use of a background electrolyte pH of 5.2 resulting in fewer critical pairs in 1D CE, does not necessarily guarantee a successful 2D separation even when used with the IC column which offers the highest degree of resolution. This clearly justifies the necessity of simultaneous rather than subsequent selectivity screening as described earlier.

Figure 4-4 depicts experimental 2D chromatoelectropherograms of AS11-HC × pH 4.7 and AS19 × pH 4.7 combinations and verifies the predictions made from the overlapping selectivity maps. Furthermore, it demonstrates that choosing the IC column based solely on the ranking suggested by Virtual Column, or choosing the background electrolyte pH based only on the total lowest number of critical pairs/co-migrations, does not guarantee full 2D resolution of the peaks. A simultaneous optimisation approach, such as that proposed here, is required for optimisation of selectivity in both dimensions.

Other important noticeable features in the 2D chromatoelectropherograms are the presence of electrodispersion which results in asymmetrical peak shapes, along with wider than normal peaks in case of galacturonate and adipate which might be due to potential interactions with HEPES as the background electrolyte counter-ion or the PVP coating on the capillary surface in the CE dimension [38, 39]. While these interactions and peak widths were not taken into account when performing the calculations, **Figure 4-4** confirms that 2D separation selectivity can be predicted through the combination of 1D separation factors in an initial screening step. Additionally, in cases where accurate predictions and optimal eluent profiles are required, further optimisation can be conducted using various approaches described previously in Chapter 3 in addition to the literature [40-42] in conjunction with *a*- and *b*- values either measured through two scanning gradient runs [18] or ported against the embedded data [43] in IC as well as by using measured mobilities and pK_a values in CE [11].

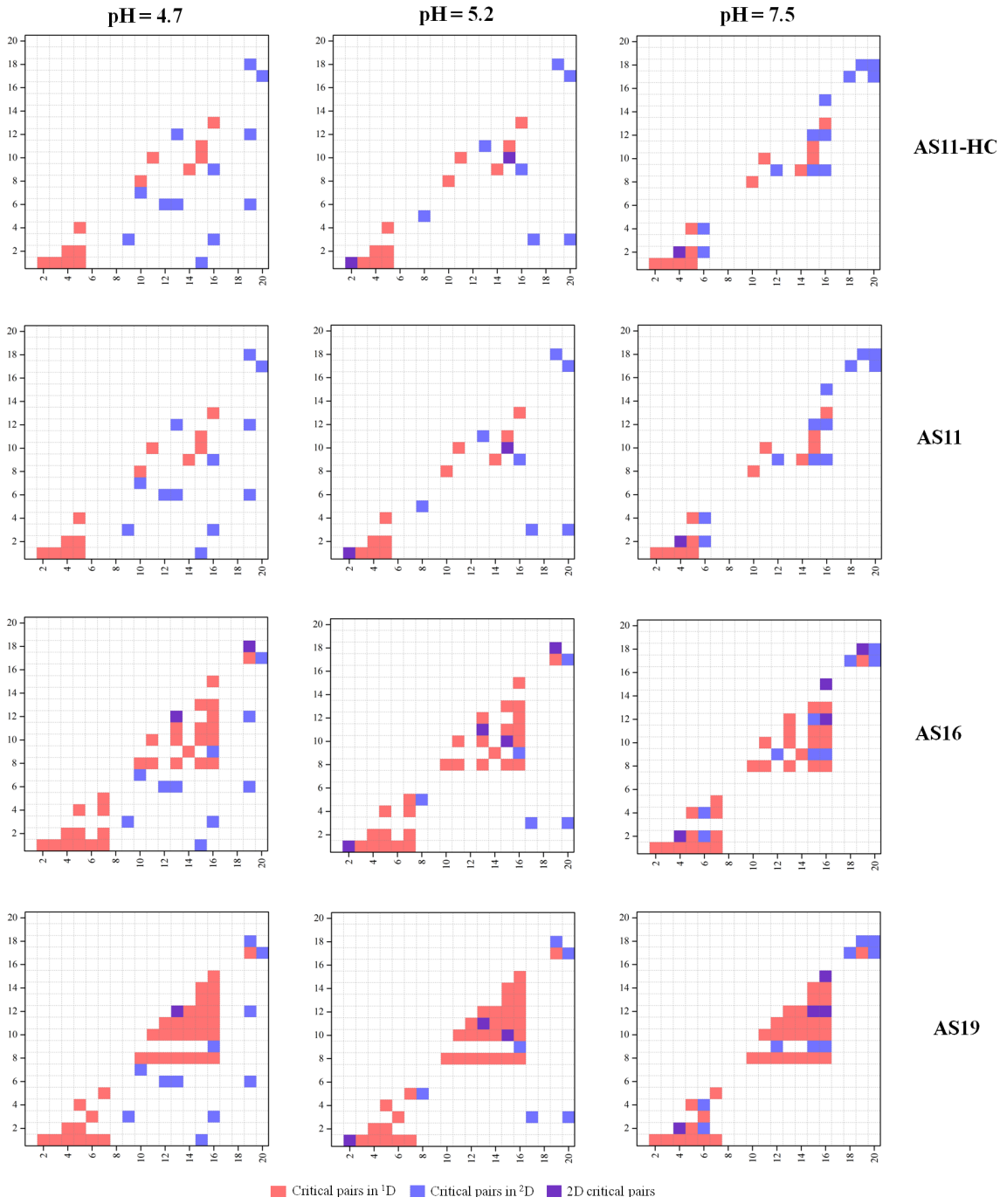

***Figure 4-3**: Representative pairwise 2D selectivity maps for combination of four stationary phases and three background electrolyte pH. Compound IDs are the same as in **Figure 4-2**.*

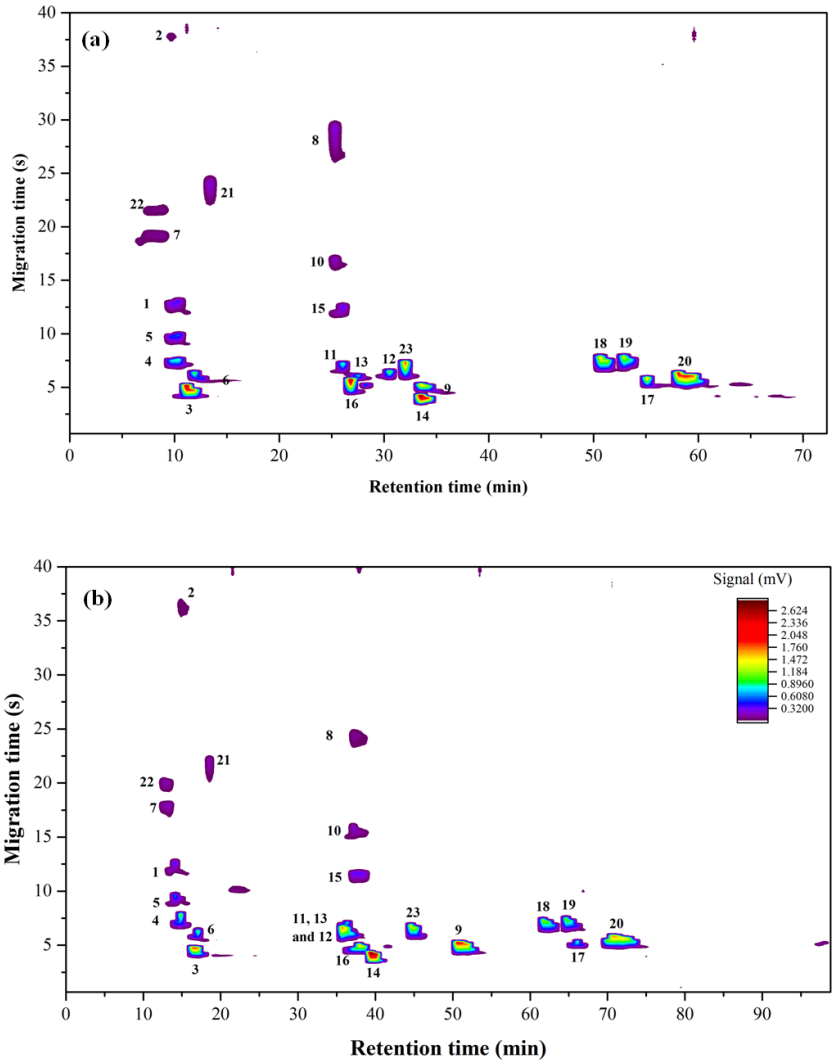

***Figure 4-4**: 2D chromatoelectropherograms for separation of 20 mg/L solution of 23 LMMOAs using (a): AS11-HC column in IC × BGE pH 4.7 in CE (b): AS-19 column in IC × BGE pH 4.7; hydroxide eluent gradient in both cases: starting concentration of 1 mM with a gradient ramp of 0.58 mM/min and flow-rate of 0.150 mL/min with a separation temperature of 30°C. CE conditions: in both cases a background electrolyte of 10 mM NA containing 0.1% PVP titrated with HEPES to pH 4.7 was used. The remaining experimental conditions are the same as in the Materials and methods section.*

4.6 Conclusions

While IC and CE are deemed highly orthogonal separation mechanisms, the current study demonstrates that taking the sample dimensionality into account is vital to achieve complete resolution. Through the introduction of superimposed 2D separation selectivity maps for LMMOAs, we have successfully presented and validated a systematic approach for *in silico* screening of separation selectivity for IC×CE.

In a similar manner, 2D separation selectivity in RPLC×CE as well as RPLC×RPLC and RPLC×IC can be optimised utilising relevant models. For example, the hydrophobic subtraction model proposed by Snyder. et al. for the description of column selectivity in RPLC [44] has the potential to be utilised for *in silico* screening of nearly 700 commercially available columns, albeit under a single isocratic condition [45]. In comparison, the LSS model for IC provides the possibility for retention prediction over a wide range of eluent concentration for a given IC column. This concept becomes of great importance especially when utilising separation mechanisms which are not fundamentally orthogonal, for example in RPLC×RPLC couplings where there is a need for introducing some degree of orthogonally through the use of separation columns and/or mobile phases of different selectivity in order to achieve effective 2D separations. Last but not least, it is possible to include more parameters in the selectivity studies and plot multi-layered maps rather than the double-layered ones presented in this work. Also, in the case of separations with substantially higher number of target analytes with various layers in the selectivity maps, it is possible to computerise the processing step through the use of block detection algorithms rather than visual recognition of the critical pairs.

4.7 References

[1] S.K. Poole, S. Patel, K. Dehring, H. Workman, C.F. Poole, Determination of acid dissociation constants by capillary electrophoresis, J. Chromatogr. A, 1037 (2004) 445-454.

[2] J.P. Foley, Resolution equations for column chromatography, Analyst, 116 (1991) 1275-1279.

[3] Chapter 5 Retention Models for Ion-Exchange, in: R.H. Paul, R.H. Paul (Eds.) Journal of Chromatography Library, Elsevier, 1990, pp. 133-162.

[4] R.A. Shellie, B.K. Ng, G.W. Dicinoski, S.D.H. Poynter, J.W. O'Reilly, C.A. Pohl, P.R. Haddad, Prediction of Analyte Retention for Ion Chromatography Separations Performed Using Elution Profiles Comprising Multiple Isocratic and Gradient Steps, Anal. Chem., 80 (2008) 2474-2482.

[5] P. Zakaria, G.W. Dicinoski, B.K. Ng, R.A. Shellie, M. Hanna-Brown, P.R. Haddad, Application of retention modelling to the simulation of separation of organic anions in suppressed ion chromatography, J. Chromatogr. A, 1216 (2009) 6600-6610.

[6] E. Tyteca, S.H. Park, R.A. Shellie, P.R. Haddad, G. Desmet, Computer-assisted multi-segment gradient optimization in ion chromatography, J. Chromatogr. A, 1381 (2015) 101-109.

[7] C. Liang, C.A. Lucy, Characterization of ion chromatography columns based on hydrophobicity and hydroxide eluent strength, J. Chromatogr. A, 1217 (2010) 8154-8160.

[8] M.C. Bruzzoniti, E. Mentasti, C.A. Pohl, J.M. Riviello, C. Sarzanini, Effect of ion-exchange site and eluent modifiers on the anion-exchange of carboxylic acids, J. Chromatogr. A, 925 (2001) 99-108.

[9] J.E. Madden, M.J. Shaw, G.W. Dicinoski, N. Avdalovic, P.R. Haddad, Simulation and Optimization of Retention in Ion Chromatography Using Virtual Column 2 Software, Anal. Chem., 74 (2002) 6023-6030.

[10] S.J. Gluck, K.P. Steele, M.H. Benkö, Determination of acidity constants of monoprotic and diprotic acids by capillary electrophoresis, J. Chromatogr. A, 745 (1996) 117-125.

[11] J.M. Cabot, E. Fuguet, C. Râfols, M. Rosés, Determination of acidity constants by the capillary electrophoresis internal standard method. IV. Polyprotic compounds, J. Chromatogr. A, 1279 (2013) 108-116.

[12] S. Terabe, K. Otsuka, H. Nishi, Separation of enantiomers by capillary electrophoretic techniques, J. Chromatogr. A, 666 (1994) 295-319.

[13] L. Ranjbar, A.J. Gaudry, M.C. Breadmore, R.A. Shellie, Online comprehensive two-dimensional ion chromatography × capillary electrophoresis, Anal. Chem., 87 (2015) 8673–8678.

[14] G.A. Blanco, Y.H. Nai, E.F. Hilder, R.A. Shellie, G.W. Dicinoski, P.R. Haddad, M.C. Breadmore, Identification of Inorganic Improvised Explosive Devices Using Sequential Injection Capillary Electrophoresis and Contactless Conductivity Detection, Anal. Chem., 83 (2011) 9068-9075.

[15] A.J. Gaudry, R.M. Guijt, M. Macka, J.P. Hutchinson, C. Johns, E.F. Hilder, G.W. Dicinoski, P.N. Nesterenko, P.R. Haddad, M.C. Breadmore, On-line simultaneous and rapid separation of anions and cations from a single sample using dual-capillary sequential injection-capillary electrophoresis, Anal. Chim. Acta, 781 (2013) 80-87.

[16] P. Jandera, J. Churáček, Gradient elution in liquid chromatography, J. Chromatogr. A, 91 (1974) 223-235.

[17] Y. Baba, N. Yoza, S. Ohashi, Computer-assisted prediction of retention times for inorganic polyphosphates in gradient ion-exchange chromatography, J. Chromatogr. A, 350 (1985) 461-467.

[18] M.A. Quarry, R.L. Grob, L.R. Snyder, Prediction of precise isocratic retention data from two or more gradient elution runs. Analysis of some associated errors, Anal. Chem., 58 (1986) 907-917.

[19] S.H. Park, M. Talebi, R.I.J. Amos, E. Tyteca, P.R. Haddad, R. Szucs, C.A. Pohl, J.W. Dolan, Towards a chromatographic similarity index to establish localised Quantitative Structure-Retention Relationships for retention prediction. II Use of Tanimoto similarity index in ion chromatography, J. Chromatogr. A, (2017) http://dx.doi.org/10.1016/j.chroma.2017.1002.1054.

[20] T.A. Halgren, Merck molecular force field. I. Basis, form, scope, parameterization, and performance of MMFF94, J. Comput. Chem., 17 (1996) 490-519.

[21] T.A. Halgren, Merck molecular force field. II. MMFF94 van der Waals and electrostatic parameters for intermolecular interactions, J. Comput. Chem., 17 (1996) 520-552.

[22] T.A. Halgren, Merck molecular force field. III. Molecular geometries and vibrational frequencies for MMFF94, J. Comput. Chem., 17 (1996) 553-586.

[23] T.A. Halgren, R.B. Nachbar, Merck molecular force field. IV. conformational energies and geometries for MMFF94, J. Comput. Chem., 17 (1996) 587-615.

[24] M.J. Vainio, M.S. Johnson, Generating Conformer Ensembles Using a Multiobjective Genetic Algorithm, Journal of Chemical Information and Modeling, 47 (2007) 2462-2474.

[25] J.S. Puranen, M.J. Vainio, M.S. Johnson, Accurate conformation-dependent molecular electrostatic potentials for high-throughput in silico drug discovery, J. Comput. Chem., 31 (2010) 1722-1732.

[26] J.J.P. Stewart, Optimization of parameters for semiempirical methods VI: more modifications to the NDDO approximations and re-optimization of parameters, J. Mol. Model., 19 (2013) 1-32.

[27] E. Tyteca, M. Talebi, R. Amos, S.H. Park, M. Taraji, Y. Wen, R. Szucs, C.A. Pohl, J.W. Dolan, P.R. Haddad, Towards a chromatographic similarity index to establish localized quantitative structure-retention models for retention prediction: Use of retention factor ratio, J. Chromatogr. A, 1486 (2017) 50-58.

[28] R. Leardi, A. Lupiáñez González, Genetic algorithms applied to feature selection in PLS regression: how and when to use them, Chemometrics Intellig. Lab. Syst., 41 (1998) 195-207.

[29] L.J. Wang, S. Henday, B. Ogren, W. Schnute, D. Hazlebeck, A. Roberts, J. Zhang, R. Corpuz, Determination of 32 Low Molecular Mass Organic Acids in Biomass Using IC/MS, Dionex Corporation Application Note, (2009) (http://www.thermofisher.com/).

[30] S.S. Brudin, R.A. Shellie, P.R. Haddad, P.J. Schoenmakers, Comprehensive two-dimensional liquid chromatography: Ion chromatography × reversed-phase liquid chromatography for separation of low-molar-mass organic acids, J. Chromatogr. A, 1217 (2010) 6742-6746.

[31] C.A. Pohl, J.R. Stillian, P.E. Jackson, Factors controlling ion-exchange selectivity in suppressed ion chromatography, J. Chromatogr. A, 789 (1997) 29-41.

[32] M. Jaroš, K. Včeláková, I. Zusková, B. Gaš, Optimization of background electrolytes for capillary electrophoresis: II. Computer simulation and comparison with experiments, Electrophoresis, 23 (2002) 2667-2677.

[33] J.C. Giddings, Sample dimensionality: A predictor of order-disorder in component peak distribution in multidimensional separation, J. Chromatogr. A, 703 (1995) 3-15.

[34] H. Holvik, H. Høiland, Acidity constants of galacturonic and glucuronic acids in water at 298.15 K from conductance and e.m.f. measurements, The Journal of Chemical Thermodynamics, 9 (1977) 345-348.

[35] C. Klofutar, N. Šegatin, Electrical Conductivity Studies of Quinic Acid and its Sodium Salt in Aqueous Solutions, J. Solution Chem., 36 (2007) 879-889.

[36] L. Pfendt, Z. Vitnik, Determination of all pKa values of some di- and tri-carboxylic unsaturated and epoxy acids and their polylinear correlation with the carboxylic group atomic charges, Journal of Chemical Research, 2003 (2003) 247-248.

[37] S.L. Miller, D. Smith-Magowan, The Thermodynamics of the Krebs Cycle and Related Compounds, J. Phys. Chem. Ref. Data, 19 (1990) 1049-1073.

[38] S.D. Noblitt, L.R. Mazzoleni, S.V. Hering, J.L. Collett Jr, C.S. Henry, Separation of common organic and inorganic anions in atmospheric aerosols using a piperazine buffer and capillary electrophoresis, J. Chromatogr. A, 1154 (2007) 400-406.

[39] T. Kaneta, T. Ueda, K. Hata, T. Imasaka, Suppression of electroosmotic flow and its application to determination of electrophoretic mobilities in a poly(vinylpyrrolidone)-coated capillary, J. Chromatogr. A, 1106 (2006) 52-55.

[40] B.W.J. Pirok, S. Pous-Torres, C. Ortiz-Bolsico, G. Vivó-Truyols, P.J. Schoenmakers, Program for the interpretive optimization of two-dimensional resolution, J. Chromatogr. A, 1450 (2016) 29-37.

[41] G. Vivó-Truyols, S. van der Wal, P.J. Schoenmakers, Comprehensive Study on the Optimization of Online Two-Dimensional Liquid Chromatographic Systems Considering Losses in Theoretical Peak Capacity in First- and Second-Dimensions: A Pareto-Optimality Approach, Anal. Chem., 82 (2010) 8525-8536.

[42] K.M. Kalili, A. de Villiers, Systematic optimisation and evaluation of on-line, off-line and stop-flow comprehensive hydrophilic interaction chromatography × reversed phase liquid chromatographic analysis of procyanidins, Part I: Theoretical considerations, J. Chromatogr. A, 1289 (2013) 58-68.

[43] S.H. Park, R.A. Shellie, G.W. Dicinoski, G. Schuster, M. Talebi, P.R. Haddad, R. Szucs, J.W. Dolan, C.A. Pohl, Enhanced methodology for porting ion chromatography retention data, J. Chromatogr. A, 1436 (2016) 59-63.

[44] L.R. Snyder, A New Look at the Selectivity of RPC Columns, Anal. Chem., 79 (2007) 3254-3262.

[45] L.R. Snyder, J.W. Dolan, P.W. Carr, The hydrophobic-subtraction model of reversed-phase column selectivity, J. Chromatogr. A, 1060 (2004) 77-116.

5 Concluding remarks and future perspectives

"The important thing is not to stop questioning."
—Albert Einstein

An alternative online interfacing/modulation approach for comprehensive two-dimensional ion chromatography × capillary electrophoresis (IC×CE) has been introduced in this thesis. Adapting the previously designed sequential injection-capillary electrophoresis system towards faster CE separation speed and long-term stability of operation, high electric field strength separations (+2.0-3.3 kV/cm) were performed through the use of a short separation capillary (8-15 cm). High-speed CE separations allowed for comprehensive sampling of the ion chromatographic effluent.

In the first example of performing IC×CE for separation of haloacetic acids and inorganic anions, presented in Chapter 2, the separation conditions were chosen based on previous knowledge and experience. However, despite a high degree of orthogonality between the two separation mechanisms, a correlation of 0.66 was observed between the IC and CE separations of low-molecular-mass organic acids using a background electrolyte pH of 7.5 for CE dimension. This shed a light on the necessity of selective exploitation of sample attributes in order to make full resolution of the acids possible. Due to the presence of multiple acidic functional groups in the structure of the acids, ionisation state was chosen as the sample dimension and was varied through changing the background electrolyte pH. However, significant changes in electrophoretic mobility occurred even with 0.1 unit change in the pH. In such a manner, following a one-at-a-time optimisation approach would result in an exceedingly large number of experiments. Therefore, a simplified optimisation approach based on maximising the Euclidean distance between the 2D peak positions was proposed to enable finding the optimal separation pH, which is described in Chapter 3.

It was further noticed that full resolution was not possible without tuning the eluent profile in IC. Even with an optimised IC elution, the stationary phase was shown to impose a great influence on two-dimensional separation selectivity. As a result the direction of the optimisation was shifted towards performing an initial screening step prior to optimisation of the resolution as proposed in Chapter 4. The work presented

in this chapter was based on *in sillico* calculation of pairwise separation factors in each dimension and constructing selectivity maps highlighting the critical pairs. Critical pairs were identified as the analyte pairs that cannot be separated using either a certain stationary phase or a certain background electrolyte pH. The selectivity maps were then superimposed to reveal the most effective combinations of first and second dimension selectivity. As concluded in Chapter 4, this approach was proposed as a universal framework for performing a selectivity screening step prior to optimisation of various 2D liquid-phase separation approaches through the use of the respective retentive models or design of experiments in cases where the separation mechanism is not well-modelled.

Although through this approach full resolution of the acids was achieved using AS11-HC×pH 4.7 hyphenation without any further need for optimisation of the eluent profile, it is generally necessary to perform an eluent profile optimisation step in cases where the separation selectivity of an ion is affected due to the change in the polarisability as a result of changing the eluent profile (as shown in Chapter 3 for fumaric acid and *cis*-aconitate) or in order to minimise the analysis time.

While we have attempted to address a number of shortcomings in the area of two-dimensional ion analysis of low-molecular-mass species, the need for improving the transfer efficiency between the chromatographic and electrophoretic dimensions still remains unmet and thus hyphenation continues to suffer from a higher degree of diminished sensitivity when compared to other liquid-phase coupled technologies. Moreover, with the majority of liquid chromatographic approaches having either a varying eluent composition of high ionic strength or high organic solvent content, in contrast to suppressed IC which has an outflow of essentially water, the chromatographic × electrophoretic approaches are susceptible to matrix affects in the second dimension. Therefore, to exploit the complementary separation selectivity offered by alternative ion separation technologies such as ion exclusion chromatography which uses acidic eluent for separation of anionogenic compounds (Please see Appendix 2), it is necessary to design coupling approaches which would minimise such interferences. Additionally, hyphenation of chromatographic ion analysis technologies offering potentially higher degree of orthogonality i.e. ion exclusion chromatography × ion chromatography can be a way forward in separation of low-molecular-mass ionogenic species as demonstrated in Appendix 3.

Appendices

1. Selectivity maps for IC×CE separation presented in Chapter 3

Selected number of 2D selectivity maps for separation of LMMOAS using IonPac AS24 stationary phase in ^{1}D. The plots are constructed based on *a*- and *b*- values derived in Chapter 3. Peak IDs are as follows: 1, 2-hydroxyisobutyrate; 2, acetate; 3, formate; 4, galacturonate, 5, gluconate, 6, glycolate; 7, lactate; 8, pyruvate; 9, quinate; 10, α-ketoglutaric; 11, adipate; 12, fumarate; 13, glutarate; 14, malate; 15, maleate; 16, malonate; 17, oxalate; 18, succinate; 19, tartrate; 20, *cis*-aconitate; 21, citrate; 22, isocitrate and 23, *trans*-aconitate.

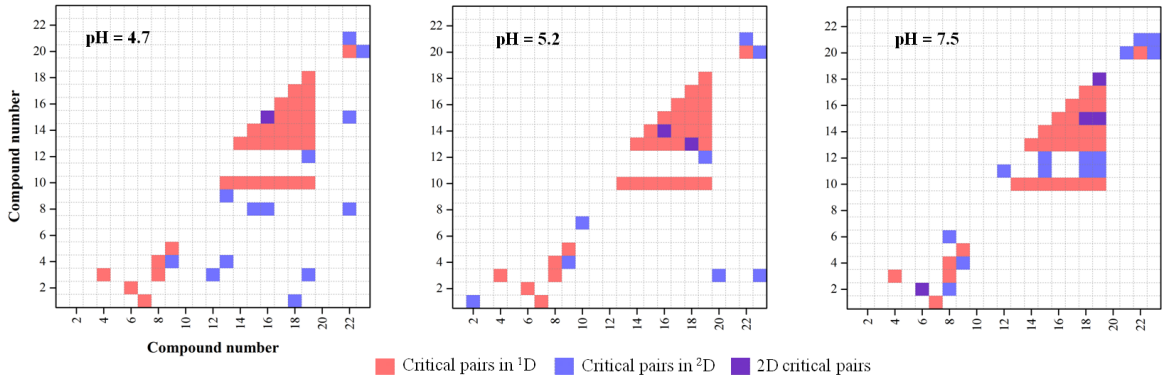

2. Hypothetical ion exclusion × capillary electrophoresis separation of low-molecular-mass organic acids

Selectivity maps for hypothetical ion exclusion × capillary electrophoresis (ICE×CE) separation of LMMOAs using the retention times obtained from isocratic elution of the acids on IonPac ICE-AS1 (9 mm × 250 mm) at a flow rate of 0.700 mL/min of 0.4 mM HCl paired with predicted effective electrophoretic mobilities for a selected number of background electrolyte pH values. Peak IDs are as follows: 1, 2-hydroxyisobutyrate; 2, acetate; 3, formate; 4, galacturonate, 5, gluconate, 6, glycolate; 7, lactate; 8, pyruvate; 9, quinate; 10, α-ketoglutaric; 11, adipate; 12, fumarate; 13, glutarate; 14, malate; 15, maleate; 16, malonate; 17, oxalate; 18, succinate; 19, tartrate; 20, *cis*-aconitate; 21, citrate; 22, isocitrate and 23, *trans*-aconitate.

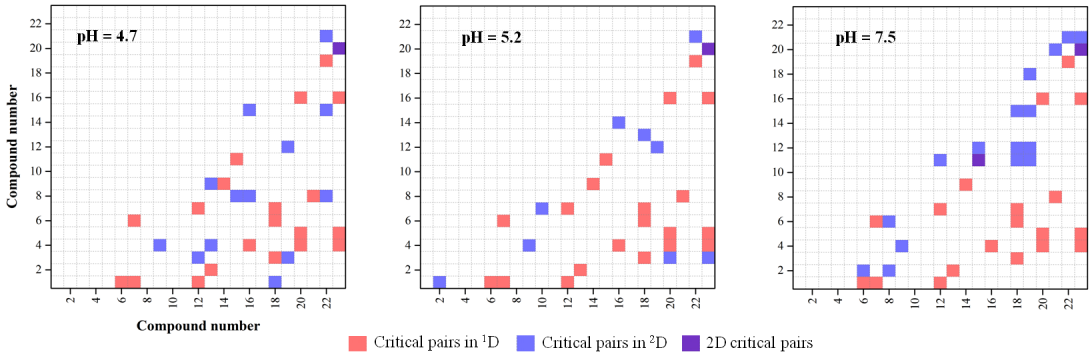

It can be concluded from this figure that full resolution of LMMOAs using ICE×CE requires further optimisation of the separation selectivity potentially through changing the stationary phase as well as eluent composition and profile.

Fractional space coverage plot and Kendall correlation for hypothetical ICE×CE separation of low-molecular-mass organic acids for the separate conditions presented above.

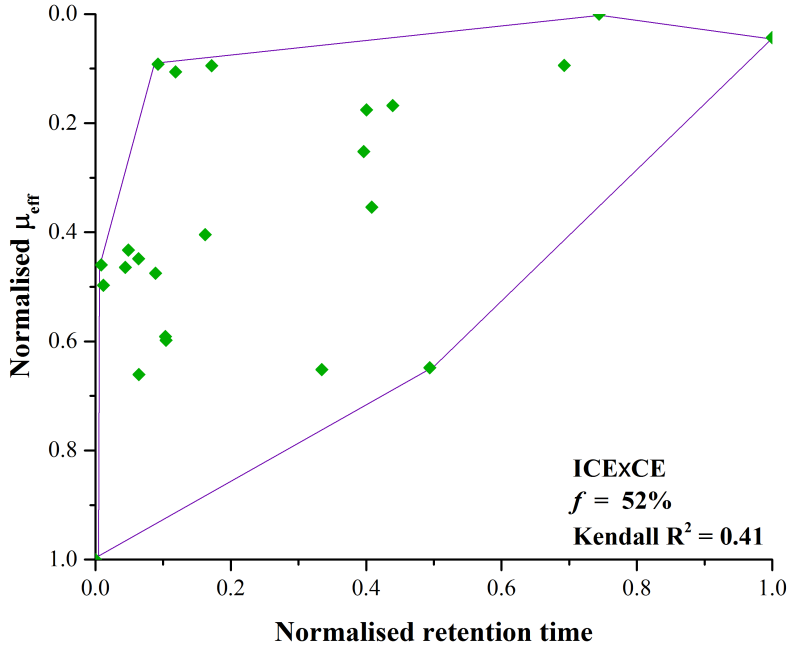

3. Alternative hyphenations: ion exclusion chromatography × ion chromatography

Fractional space coverage for hypothetical ion exclusion × ion chromatography (ICE×IC) separation of LMMOAs using the retention times obtained from isocratic elution of the acids on IonPac ICE-AS1 (9 mm × 250 mm) at a flow rate of 0.700 mL/min of 0.4 mM HCl paired with predicted retention times for optimised separation of LMMOAs in Chapter 3 using IonPac AS24.